ÉCOLE POLYTECHNIQUE
FÉDÉRALE DE LAUSANNE

Master Thesis

Optimization of drip irrigation using a sensor network in Sahel Region (Burkina Faso) - Analysis of soil water and plant dynamics in the framework of project Info4Dourou 2.0

Author:
Tom Müller
EPFL

Supervisor:
Clémence Bouleau
CODEV - EPFL, Switzerland

Thesis director:
Professor **Paolo Perona**
AHEAD - EPFL, Switzerland

EPFL - SWITZERLAND
-
Spring 2015

Acknowledgments

My special thanks go to my supervisor Mrs. Clémence Bouleau from the *Cooperation and development center (CODEV) at the EPFL* who allowed me to participate to *Info4Dourou 2.0*, an exciting and innovating project, as well as Professor Paolo Perona for his scientific support and warm encouragements and for the trust they put in me during the whole project duration.
I would like to thank all the people I collaborated with in Burkina Faso, starting with Mr. Seydou Kabore, director of ACERD and local coordinator of the project in Burkina Faso, for his logistic support and continuous encouragement. I specially thank my college Mr. Daniel Nikiema for his technical support, his collaboration and help during the whole project and for the time he spent with me. I would like to thank also Mr. René Ouedraogo for his constant availability, his support during the experiments and his friendship. I also thank the other members of the ACERD office, Mr. Eric Ahmed Karantao, Mr. Sidiki Kabore and Mrs. Nadine. A special thank also goes to Dr. Moussa Sanon from the *Environmental and Agricultural Research Institute (INERA)* for his scientific support and his precious advice in Burkina Faso. I am also very thankful to the NGO *International Development Enterprises (iDE)*, who lent their crops for my experiments. I thank the director of iDE Burkina Faso, Mr. Laurent Stravato, who approved and encouraged my work and collaboration with them. I particularly thank Mrs. Aïda Ganaba, agronomist at iDE, for her collaboration and flexibility with my experiments. I am very thankful to Mr. Bukare and Mr. Simeon without whom I would not have been able to manage the crops, for their daily labor in the fields and their rigorous application of the irrigation schedules. I thank the (*National Meteorological Institute (DGM)* for their collaboration with the project and the *Swiss Agency for Development and Cooperation (DDC)* in Burkina Faso who co-financed the research project *Info4Dourou 2.0* together with private foundations (*Velux Stiftung* and *Stiftung Drittes Millennium*). Finally, I thank all the friends I made in Ouagadougou who participated in making those three months as exciting from a professional and personal perspective.

In Switzerland, I warmly thank the *Sensorscope* team who designed the wireless sensor network, in particular Davis Daidie for his technical support, his advice about the project and his help with the equipments. From the *CODEV*, I also thank Mr. Matthieu Gani for his help in the project and my fellow student and engineer, Mr. Theo Baracchini who also worked on the project and was very helpful in the development of the numerical model and in the analysis of the project's results. He also coordinated many students who performed an interesting synthesis of previous results. From the research group of Pr. Paolo Perona at EPFL, *Applied HydroEconomics and Alpine environmental Dynamics (AHEAD)*, I also thank Mr. Lorenzo Gorla who helped me preparing the research equipments and provided important support and my fellow student, Mr. Pierre Razurel, who collaborated with Theo Baracchini on the students project. I thank all the students from Mr. Perona's lecture on *Soil Water Resource Manaement*, who made interesting analyses of the data. I finally thank the students association *Ingénieur Du Monde (IDM)* who gave a financial support to my project and allowed me to share my experience with other EPFL students.

Abstract

The research project *Info4Dourou 2.0*'s main goal is to improve agriculture in semi-arid regions by developing a support system that optimizes agricultural production and water consumption based on continuous soil humidity measurements using a sensor network. In this context, the main purpose of the study was to give more scientific support to the agronomic model on which the sensor network is based. In particular the research aims at understanding the soil water and plant dynamics in order to give recommendations on the system design. The main feature of the system is to indicate when irrigation must be triggered and in which soil moisture conditions. The thesis developed a numerical model based on the software HYDRUS 2D to acquire a precise knowledge on the soil water dynamics and was calibrated and coupled with field experiments on two vegetable crops of eggplant and cabbage in Burkina Faso using drip kit irrigation systems. A great focus was given on the plant response to different irrigation schedules and to water stress, considering aerial biomass development, root distribution and final yields. Water stress was linked to continuous measurements of the soil matrix potential at different depth and locations. The field experiments showed that a daily irrigation frequency resulted to better canopy development during the first part of the growth but that great water savings are possible by optimizing the schedule. Water stress was difficult to track precisely by following daily sap flow behavior which suggested that plant stress occurs before transpiration reduction, especially when biomass is building up. The adaptability of the root distribution was demonstrated and was clearly correlated with the wetted zone which depended on the irrigation schedule. From the numerical model, it was shown that using one sensor at a depth of about 10 cm was most appropriate in order to pilot irrigation during the whole crop growth. The analysis showed that most of the water savings could be achieved at relatively high threshold values and that low thresholds mainly resulted to transpiration reduction which was not advisable. A threshold of -20 kPa was proposed for the beginning of the growth stage which then decreases to a value of -50 kPa at full canopy development. These thresholds are believed to be adequate for most vegetable crops since they allow to keep the soil matrix potential in the root zone at values that are tolerated by most plants. An analysis of the influence of the soil texture also showed that similar values seem to perform well for most soils, if assuming an adaptation of the root distribution to the wetted zone. The study focused mainly on water stress but more research could be done on the impact of the irrigation system on nutrients availability for example.

Table of contents

1 Introduction

1.1 Irrigation in Burkina Faso

Burkina Faso is one of the poorest country in the world, with a gross domestic product (GDP) per capita of about 1528 US $ in 2012 and ranking 181 over 187 countries in the world [1]. Its Inequality-adjusted Human Development Index (IHDI) of 0.252 is also one of the lowest in the world ranking 181 over 187 [1]. In 2011 in Burkina Faso, 92% of the active population worked in the agricultural sector and agriculture represented 33.8% of the total GDP [2]. Agriculture is thus of paramount importance to promote economic growth and food security.

Agriculture takes place mainly during the rainy season (May-September) and irrigation is necessary during the dry months. While the production from irrigated surfaces represents only 1% of the total surface of arable lands, its share in the total production was estimated to be as high as 10% in 2012 [2]. Nevertheless, the potential to increase irrigation surfaces is important as only about 18% of the potential irrigated lands are equipped with irrigation systems. Improved irrigation practices are required where water is a scarce resource and good yields are difficult to obtain. Adapted technologies and knowledge are therefore essential to develop a sustainable and economically viable agricultural activity. The first project results have shown that estimating water needs is not straightforward and a better water management could improve agriculture by securing and/or improving yields, avoiding over-irrigation, and thus limiting water consumption (avoid pumping costs or manual labour) and avoiding soil degradation.

Several technologies were introduced in the past decades to promote dryland irrigation, such as adapted pumps (manual pumps, wells or drills, motor pumps and recently solar pumps), water tanks, as well as adapted irrigation systems [3].
In this context, drip irrigation systems have been introduced in sub-saharian regions. Drip irrigation systems have a much higher water delivery efficiency, reducing water losses by evaporation and deep leakages. Drip irrigation has shown an efficiency of about 70 to 95% while traditional gravitation agriculture only reaches about 40 to 75% [4].

Drip irrigation is still a marginal activity in Burkina Faso, representing about 1.5% of the irrigated surfaces [2], but new technologies are being developed to respond to the local context and environment of these regions and the market share is expected to grow in the near future. It was estimated in 2011, that small-scale private irrigation (smaller than 20 ha) represented 46% of the total irrigated surfaces in Burkina Faso [2]. A large potential to promote drip irrigation lies therefore in the promotion of family drip-kits that can be installed on small surfaces at affordable prices. For example the NGO *International Development Enterprises (iDE)*, has developed affordable drip kits that are adapted to small-scale producers and sold about 4460 kits in Burkina Faso in the past four years.

While those technologies improve greatly the labor work of the producers and improve water allocation, estimating adequate water needs and timing to maximize yields is still assessed by the producers. Irrigation is therefore usually done on a visual appreciation of the soil and plant state and producers mostly rely on their own experience. Precise irrigation based on hydro-meteorological and field data has the potential to further optimize the situation. However environmental data are scarce and modern automatic weather stations are costly and local maintenance is limited. Scientific support, data interpretation and communication to rural areas are also limited.

1.2 The research project Info4Dourou 2.0

In this context, the research project Info4Dourou 2.0 managed by the *Cooperation and Development center* (CODEV), from the *Ecole Polytechnique Fédérale de Lausanne* (EPFL), first aims at improving environmental data collection using technologies that are adapted to the local context and user. In particular, the project has developed in collaboration with the swiss EPFL start-up *Sensorscope* a Wireless Sensor Network (WSN) that is affordable, adapted to harsh weather conditions, simple to install and requiring low maintenance. These completely automatic weather stations allow real-time hydro-meteorological data acquisition which can be used to give a simple information to the local producer (via SMS), or used for scientific or research purposes by remote access via the web.

Info4Dourou 2.0 has been launched in 2012, and field experiments with local producers have been tested in several locations in Burkina Faso since then. It is supported by a team of local engineers in Burkina Faso who are in charge of the local coordination of the project and the installation and maintenance of the system. The system has been tested for its capacity to directly improve water consumption and yields (dryland irrigation support) and from a more scientific aspect as a tool for improving the understanding of the local hydro-meteorological processes. Eventually, the hydro-meteorological stations may be manufactured, assembled, maintained and commercialized locally.

1.3 The WSN and water management system

The wireless sensing network consists of adaptable base stations that transmit environmental data to a master station, that relay the data to a server. Each station consists of a small plastic box powered through four standard AA batteries that are charged by a small 1.2W solar panel and thus requires no external power supply. Many different sensors (temperature, soil moisture, wind speed, etc.) can be easily connected to the base station, thanks to a dedicated module. Each station possesses three such modules plots, while each module can connect up to six sensors, depending on their type and power requirements. The base stations use wireless communication and are self-organized into a multi-hop wireless network that eventually transmits the information to a master station. The master station then communicates the data to a database server via a GPRS connection. The base station can be easily transformed into a master station by adding a GPRS module to it [5].
This system allows a very wide deployment of the network and is especially adapted to data collection in harsh environments such as in high-mountains or drylands.

The research project Info4Dourou 2.0 focuses on optimizing the irrigation schedule and thus avoiding over-irrigation, water stress during the dry season and drought pockets during the rainy season. The WSN is used to monitor in real time the soil water status in the crop. In particular, a base station connects three Watermark sensors that record the soil matrix potential, an alternative measure of the water content in the soil, that directly represents the pressure needed to extract water from the soil. Below a certain threshold defined by the technician, the soil is considered too dry and further water depletion would result in water stress for the plant and in reduced yields. When the threshold is reached an information is sent to the producer, indicating that the irrigation should be triggered. The information is sent via text message (SMS) and additionally a LED embedded in the base station turns red. All measurements can also be accessed on-line via the real-time web interface "Climaps". The functioning of the system is illustrated in figure 1.1.

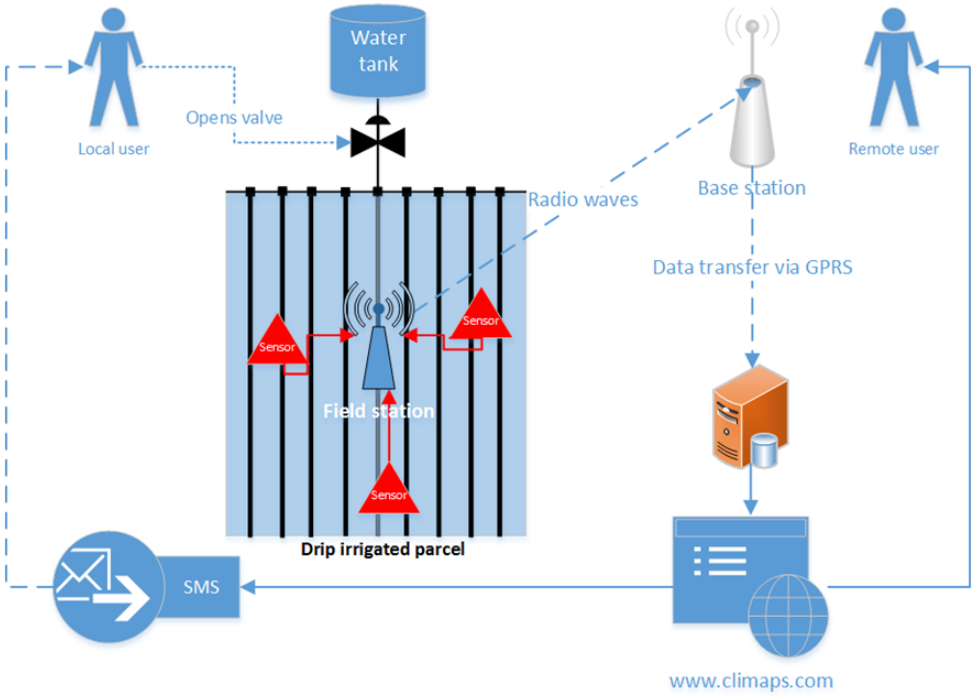

Figure 1.1: Illustration of the functioning of the Wireless Sensor Network.

The system deployed in Burkina Faso was only installed on vegetable crops where drip irrigation systems where already installed. Though the WSN would work for any irrigation practices (surface irrigation, californian system, etc.), it was only tested on drip irrigation systems that already help reducing water losses and where water consumption was easy to measure.
In order to have a representative measure of the soil water status, three Watermark sensors are placed in the field at different location and the median value is used for interpretation. Using the median allows to avoid problems due to heterogeneity in the water delivery (inherent to the drip kit) and heterogeneity in the crop growth. All sensors are placed 10 to 20 cm away from a dripper and at a depth of 10 to 15 cm. The project has been tested in 8 locations in Burkina Faso since 2012. In all locations, one experimental crop where irrigation was triggered using the WSN was grown in parallel with one control crop where irrigation was applied following the usual practice. Both crops were prepared similarly and at the same date in order to allow comparison in terms of final water consumption and harvest. The analysis of the results are promising and are summarized in figure 1.2. The graph on the left shows the ratio of total crop harvest over the water consumption (called Water Use Efficiency) for both control experiment and experimental crops. It appears clearly that the ratio is always higher for the experimental crop using the WSN. The graph on the right shows the median percentage of water savings and increased harvest in comparison with the control experiment. Negative values mean an additional water consumption for the experimental crop (blue bar) or a decrease in total harvest (green bar).

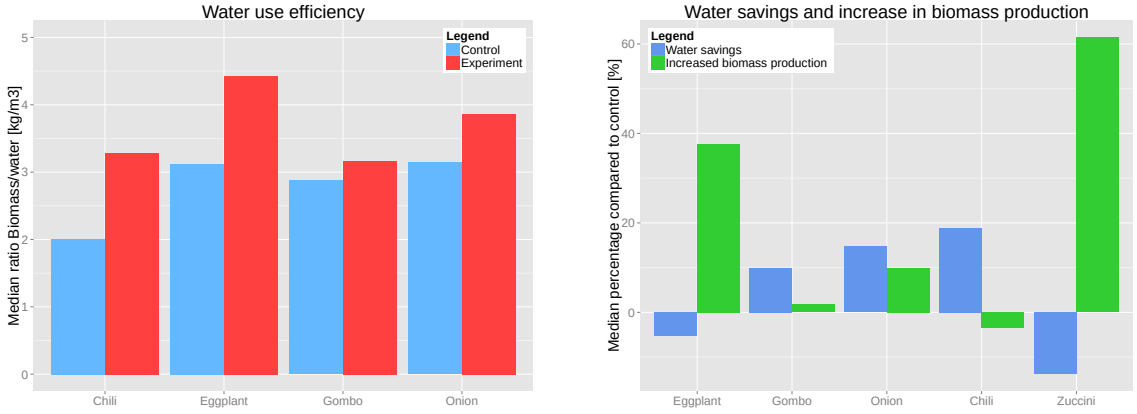

Figure 1.2: Summary of the results obtained in 8 locations in Burkina Faso since 2012 for different crops. Comparison between the control crops (standard irrigation practice) and experimental crops (using the sensor network).

1.4 Scope and objectives of the thesis

While the project Info4Dourou 2.0 has been launched in 2012 and the system has been tested on different locations, additional research still needs to be done on improving the current system, as the project focused more on the technical aspects of WSN, on the social acceptance of the technology and on the potential to improve irrigation scheduling, by comparing water consumption, yields, costs and revenues in the experimental sites. The ultimate goal of this thesis is to optimize the design of the current WSN used in Burkina Faso in order to propose an irrigation support system that assures the best yields given the water consumption. To achieve this goal, a good understanding of the water-soil-plant-atmosphere dynamics is essential.

The main focus of this study will be to understand the water dynamics in the soil and the plant response to different irrigation schedules. The irrigation schedule is characterized by the irrigation depth brought to the crop and the frequency of irrigation. The maximal irrigation depth is determined by the capacity of the water reservoir for drip-irrigation. If the irrigation depth is fixed, the irrigation frequency will be optimized to avoid water stress. Specifically, the study will assess the impact of different irrigation schedules (depth and frequency) on the water distribution in the soil and the plant response in terms of both root and aerial biomass developments. The main goals are the followings:

- Determining the best irrigation regime (depth and frequency of irrigation);
- Finding a proper location of the sensors, which is representative of the soil matrix potential in the whole root zone;

- Given the depth of the sensor, defining a threshold based on the soil matrix potential to trigger irrigation to avoid water stress and yield losses but to optimize water needs as well;
- Determining a system that is adapted to different vegetable crops;
- Designing a system that works for the whole crop growth;
- Understanding the impact of the soil texture on the system;
- Proposing different systems given a class of soil texture or crop type;
- Designing an efficient and affordable system adapted to Burkina Faso.

To acquire robust results we propose here to use two complementary approaches. On the one hand, two experimental crops were grown in Burkina Faso, with specific irrigation schedules on which soil, plant and meteorological data were collected. The influence of the irrigation frequency and irrigation depth on water stress and transpiration reduction as well as on plant yield was evaluated. Based on the field measurements, a numerical model using the software HYDRUS 2D was developed and calibrated by matching the measured and modeled soil moisture at different locations. The software will specifically be used to allow a better understanding of the soil water dynamics but did not include a plant growth model. Once the model has been properly calibrated, different irrigation schedules and thresholds will be tested and the corresponding total water needs and water stress will be quantified and compared with field measurements. Finally, the impact of the soil texture will also be assessed.

2 Theoretical background

2.1 Climate and soils in Burkina Faso

Burkina Faso is separated in three climatic zones. The Northern part of the country has a dry sahelian climate, while the western southern part is a soudaninan zone, with higher relative humidity and rainfalls. The general climate is shown in figure 2.1.

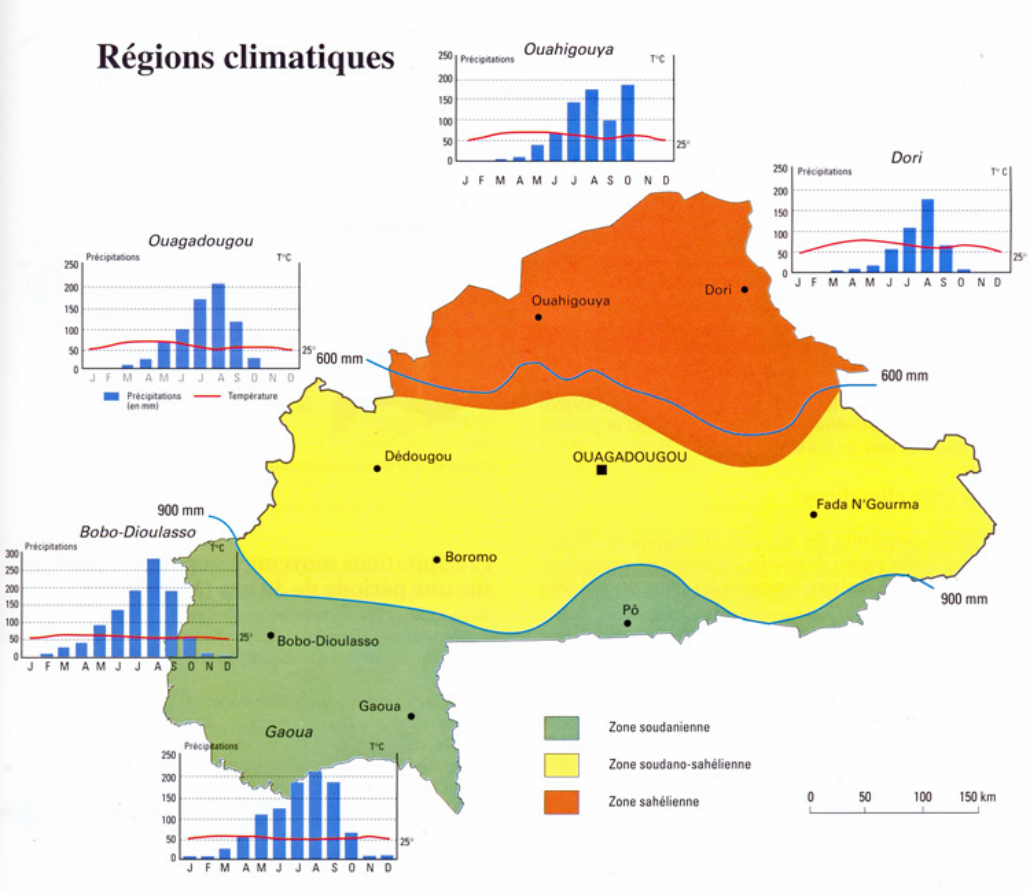

Figure 2.1: Overview of the climate in Burkina Faso [6].

In average, the rainy season occurs from May to October, while precipitation is inexistent during the rest of the year. During the wet months, irrigation may be required as short drought periods may occur between two rainfall events. The dry season is usually divided in two cultural periods. The dry "fresh" season, from November to March, is characterized by somewhat colder temperature but higher advective conditions, due to strong, dry, winds. It has been reported a maximal evapotranspiration rate 1.6 times higher than the reference evapotranspiration in such conditions (see chapter 2.4.3 for evapotranspiration definition). The growing cycle is longer but the vegetative development is usually higher. The dry "hot" season, from March to May is characterized by higher temperature and lower winds, resulting to a shorter growing season. Total water needs are lower but lower yields were also recorded for the onion [7].

In general, the soils in Burkina Faso are poor in organic matter and nutrients [8]. They are usually sandy and shallow with a ferralitic cuirasse situated near the surface. Eight main soil types were defined in Burkina Faso which are: (1) ferruginous tropical soils (39%); (2) poorly evolved soils (26%); (3) hydromorphic soils (13%); (4) brown eutrophic soils (6%); (5) vertisols (6%); (6) halomorphic soils (5%); (7) raw mineral soils (3%) and ferralitic soils (2%) [8]. Figure 2.2 shows their distribution. All textures are characterized by a sandy surface horizon on top of a somewhat more clayey one. The density increases with depth and drainage is usually reduced due to fine clay particles and fine sands. They have poor nutrients content and low organic matter [8]. We summarized the average physical properties of the main soil types in table 2.1 for the top 20 cm, where most of the crop roots are usually concentrated.

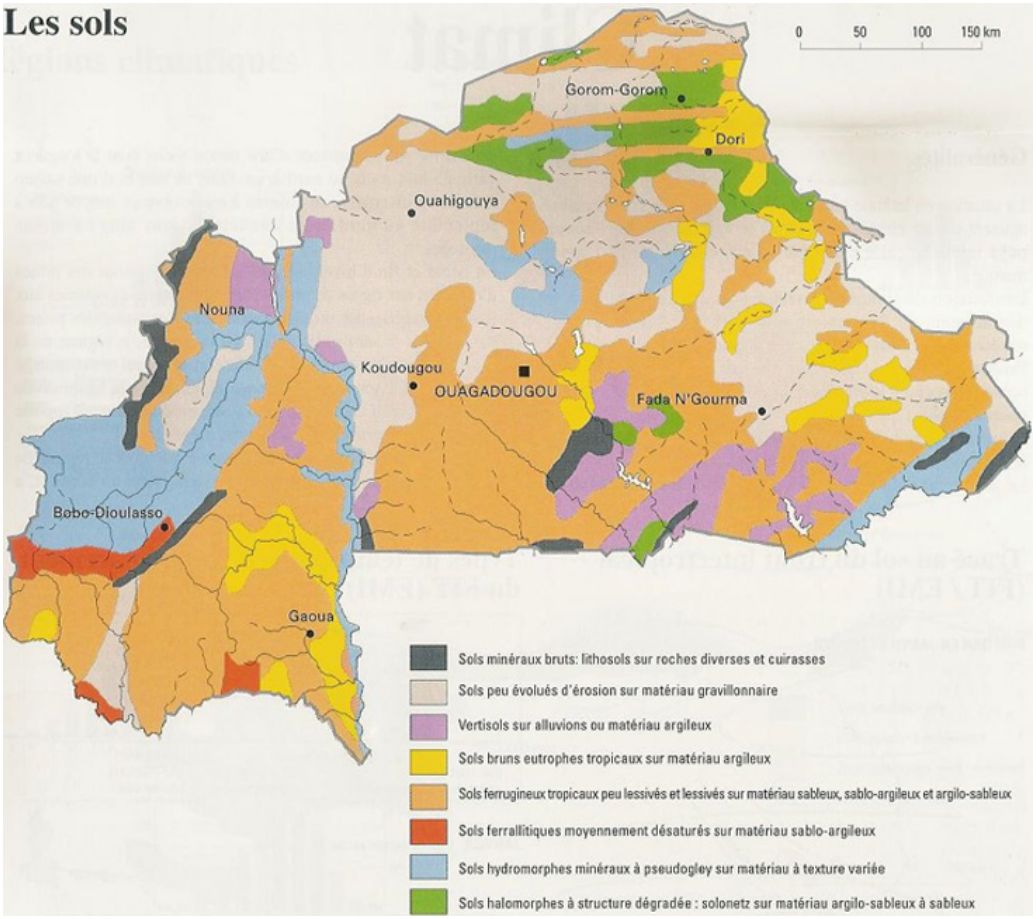

Figure 2.2: Overview of the main soil types in Burkina Faso [6].

	Particle size distribution			**Density**	**Soil moisture at field capacity**	**Soil moisture at wilting point**
	Clay %	Silt %	Sand %	[kg/m^3]	[%]	[%]
Ferruginous tropical soils	10.7	7.1	82.1	1.7	13.5	6.5
Poorly evolved soils	28.9	10.5	60.6	1.3	19.8	8.6
Hydromorphic soils	24.5	40.5	34.9	1.6	18.2	11.0
Brown eutrophic soils	22.3	8.5	69.1	1.4	15.78	8.2
Vertisols	3.1	6.5	90.4	1.7	5.8	1.4
Ferralitic soils	6.6	11.5	84.6	1.6	8.5	2.8

Table 2.1: Overview of the physical property of the top 20 cm of main soil types in Burkina Faso (from Dembele et al., 1991 [8])

Following the widely adopted USDA textural triangle [9], the textures can be classified as sandy loam, sandy clay loam or loam textures, except vertisols soils which corresponds to a loamy sand.

2.2 Plant and water dynamics

2.2.1 Water fluxes

Crop water management is complex and requires a good understanding of the interaction between the plant, the soil and the atmosphere. In particular, each water fluxes entering and leaving the continuum must be assessed. Those main fluxes are shown in figure 2.3 and are the precipitation; the runoff from the soil surface; the net irrigation depth; the capillary rise from shallow groundwater; the water losses due to deep percolation; the subsurface water movements and the crop evapotranspiration. The evapotranspiration can be further divided between the evaporation flux and the transpiration flux. Evaporation is the physical process of water evaporation at the soil surface due to the combined effect of radiation, temperature, wind and air humidity and only applies to the first centimeters of soils when soil is well wetted and can expand its effect to about 15 to 30 cm depending on the soil texture when the soil surface is drier [10]. Transpiration is the process of water uptake from the plants roots, through the stem, towards the leaves and its vaporization through the leaves stomata mainly. Transpiration is also influenced by meteorological conditions so that soil evaporation and plant transpiration are usually brought together to form the term evapotranspiration.

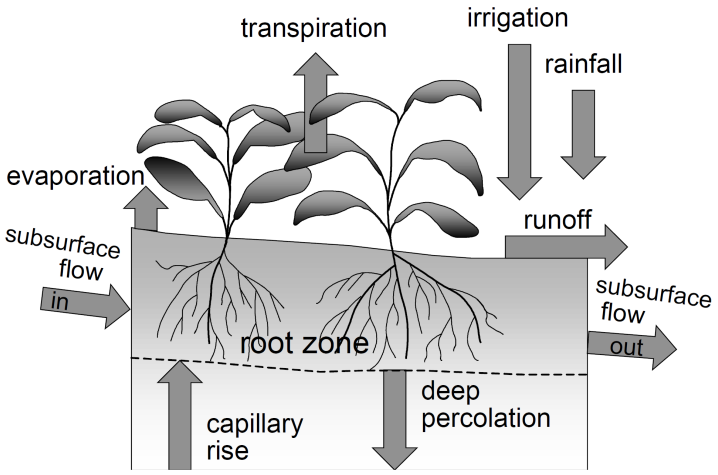

Figure 2.3: Main water fluxes involved in the soil water dynamics (from FAO, 1998 [11]).

2.2.2 Plant growth

During its growth, the plant will have different interactions with the atmosphere and the soil will react differently to water deficit and stress conditions. In order to determine a good water management, some stages of plant development must be defined.
A general definition of plant growth for annual crops is used by the FAO, 1998 [11]. The development is divided in four main growth stages:

- **Initial growth**: This is the first stage of growth just after transplanting, also called the vegetative state. During this stage, biomass and leaf area development is limited and ends when ground cover is about 10%. Evaporation from the ground is predominant compared to transpiration, especially when the soil is wetted frequently.
- **Crop development**: This is the stage of root and shoot biomass building and leaf area development. It ends at full leaf cover, which corresponds to the beginning of flowering for many crops.
- **Mid-season**: This stage is characterized by the flowering and production of fruits and it ends with the start of maturity, the beginning of ageing, the start of leaves senescence and the browning of fruits. This is generally the longest growth period for many vegetable crops and corresponds to the period of maximal water consumption.
- **Late season**: This last stage ends with the end of harvests or full senescence of the plant. During this stage crop water needs slowly decrease.

During each phases, some general parameters are used to characterize plant water needs, tolerance to stress, biomass growth, etc. The FAO possesses a wide database summing up reference values for these parameters [11]. The duration of crop growth stages as well as the growth parameters are however influenced by the hydro-meteorological conditions and are specific to each crop. Corrections to account for the local climate are therefore essential to build a realistic model.

2.2.3 Soil water dynamics

Different processes are dependent on the soil physical and chemical properties and will determine the water movements in the soil and its availability for the plant. Those processes are moreover spatially inhomogeneous in three dimensions. A good understanding of the water dynamics is essential to optimize the sensor network.

In unsaturated soils, the main soil physical properties are the hydraulic conductivity, the soil volumetric water content (called soil moisture) and the soil matrix potential (also called water potential). Those properties are linked to each other given the soil characteristics and different theoretical models exist to describe them.

The soil matrix potential represents the force that binds the water droplets to the thin soil pores. When the soil dries out only the water bound to the smaller pores, where the forces (capillarity and van der Walls) are greater, is retained. Its value is maximal at saturation and amounts to 0, and then decreases below zero when the soil dries out. The soil matrix potential is linked to the volumetric water content of the soil, but their relationship depends on the soil texture and their pore distribution. The hydraulic conductivity describes the speed of water infiltration through pore spaces. The hydraulic conductivity is maximal at saturation and decreases with increasing negative soil matrix potential. The equations characterizing the soil water dynamics are detailed in chapter 2.5.2.

Each soil type posses its own physical proprieties. The soil moisture retention curve (see figure 2.4) shows the relationship between the above mentioned parameters for different soil types. It is interesting to note in particular that coarse soils (such as sandy soils) have already very low soil moisture at relatively high soil matrix potential (around -30 kPa), while fine texture soils have a more constant decrease (note that the x-axis has a logarithmic scale). Due to this effect, coarse soils are characterized by the highest hydraulic conductivities at saturation but have a very steep decrease, so that the conductivity becomes much lower below -10 kPa.

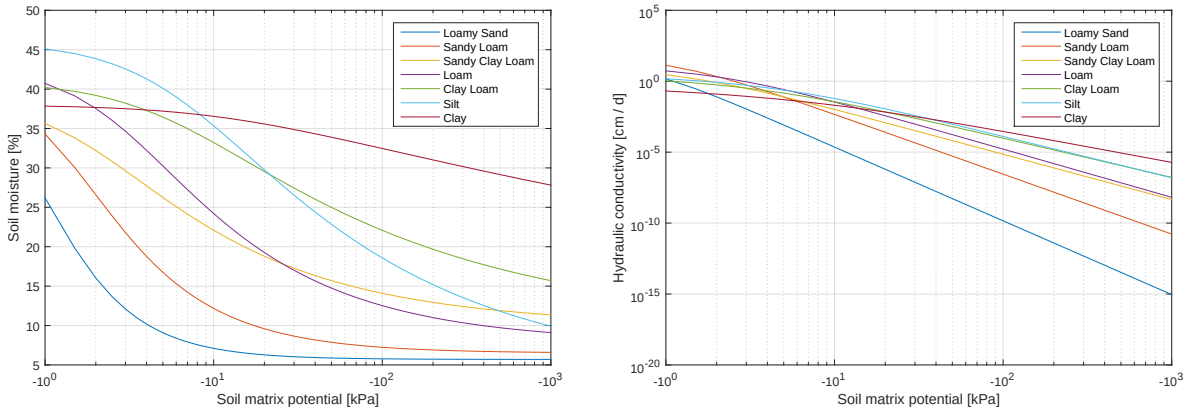

Figure 2.4: Relationship between soil matrix potential and soil moisture (right) and between soil matrix potential and hydraulic conductivity (left) for different soil texture. The curves were calculated based on the texture parameters proposed by Carsel et al., 1988 [29].

2.2.4 Water stress

The definition of water stress itself is not straightforward as different levels of water stress will have different effects on the plant. Water stress is usually linked to stomatal closure, which is a physiological response of the plant to a low water potential in its tissue. Water potential is a measure of the pressure in the plant tissue. Its value is negative which illustrates the succion of water, so that increasing negative values represent a greater force required to "pump" water. Stomatal closure limits water losses from the leaves to prevent damages of water stress (cell growth, photosynthesis, etc.) which in turn reduces the potential transpiration of the plant. It is therefore usually assumed that there is a direct link between transpiration reduction and a decrease in biomass production and yields [12]. Under no water stress condition, the xylem water potential ranges from about -0.1 to -1 MPa [13].
Some studies also suggest that some damages can occur before stomatal closure, at higher tissue water potential, such as cell growth reduction [14], and in particular at young stages during plant growth and biomass formation [15]. In AquaCrop, the new model from the FAO [15] & [10], different effects of water stress are defined. The first effect of water stress is the reduction of the canopy expansion, leading to an

suboptimal canopy cover at the end of the crop development stage. This in turn will have an effect on the potential transpiration (due to lower leaf area) and finally on the yields. Then occurs canopy senescence which decreases the canopy cover and transpiration rate, even after the end of the development stage, during the mid-season. More or less simultaneously to senescence, stomatal closure occurs when relatively severe water stress is applied. Stomatal closure will have a direct effect on transpiration reduction and will also decrease the photosynthesis leading to reduced fruits growth during yield formation. The AquaCrop model suggests that at early stage, plants are exposed to water stress relatively early leading to reduced canopy development and that transpiration reduction is not a good indicator of water stress at early growth stage, as it appears only for more severe stress. At mid-season, once canopy development is maximal, water stress can be more severe and is more linked to transpiration reduction and early canopy senescence. Finally, even though plants are tolerant to a higher soil water depletion level after early stages, the effect of water stress will be more severe as it will directly affect the growth and quality of the fruits [15].

Since the water availability in the soil directly influences the ability of the plant root to extract water, water stress is also linked to the soil water deficit. The soil water enters the roots due to a difference in water potential between the plant and the soil. The plant water potential must remain lower to some degree to the soil matrix potential so that the pressure difference overcomes the soil-root resistance [12]. The soil matrix potential is thus directly linked to plant water potential and water stress. Below a certain value of soil matrix potential, the roots will no longer be able to extract the water at maximal rate which will result in lower tissue water potential and water stress. Typical values of limiting soil matrix potential range from about -30 to -100 kPa, depending on the plant type [16].

2.2.5 Salinity stress

Water stress is not the only factor influencing plant growth. As soil moisture decreases after an irrigation event, the soil water salinity increases due to evaporation of the water at the soil surface and water and selective ion uptake by the roots. Some ions with limited mobility may accumulate in the root zone to levels that are critical for plant growth. The first effect of salinity stress is a decrease in the root water uptake capacity, followed by an osmotic stress due to high salts accumulation in the plant. Usually salinity stress is due to the accumulation in the soil and consequently in the plant tissues of Na^+ and Cl^- ions. There are various physiological effects of osmotic stress such as interruption of membranes, reduced photosynthetic activity, water loss from the leaves, nutrient imbalance, inhibition of essential nutrients uptake such as K^+ [17].

Salinity stress is a major concern for any irrigation technologies (surface, sprinkler, drip irrigation) when using irrigation water that contains a certain level of dissolved ions, given its source. Frequent irrigation therefore causes an increase in the salt concentration over the long term in the soil and leaching of the salts may be required. Leaching of the salts consists in the application of a higher irrigation amount than the actual evapotranspiration rate (above water consumption), in order to drain some water and part of the ions below the active root zone [18]. Usually salt leaching can be done intermittently when critical levels are reached in order to "flush" the salts out of the root zone. In the case of drip irrigation when applying frequent irrigation depths and keeping the soil in a medium-wet state, leaching is done continuously and the salts tend to accumulate at the edge of the wet zone, limiting salinity stress in the root zone [18]. The irrigation schedule has therefore an influence on the salinity concentration as it influences hydraulic conductivity and osmotic potential. Assouline et al., 2006 [19] showed for instance that a daily irrigation frequency resulted in the lowest salt concentration for drip irrigation of a bell pepper crop and was better than higher irrigation frequency.

Soil salinity is usually assessed by measuring the electrical conductivity of the pore water (EC_e). This was done historically by extracting the solution of a saturated soil paste but new in-situ methods rely on measuring the bulk soil electrical conductivity (EC_b) and converting it using a theoretical equation [20]. An extensive database on plant tolerance to soil salinity was summed up by Maas, 1993 [21],[22].

2.3 Irrigation technologies

Dryland irrigation still needs development, with only 18% of the potential surfaces being irrigated in Burkina Faso in 2012. Surface irrigation is the major practice in Burkina Faso, as it represents 85.4% of the total surface in 2011, against 13 % for sprinkler irrigation and 1.6% for drip-irrigation. Water supply is also a critical activity, since 75.3 % of the producers carry the water manually, while 15.2 % use motor-pumps and 6.3% use manual treadle pumps [2].

More advanced irrigation practices have therefore a great potential to reduce physical labor and time dedicated to irrigation, to save precious water amounts reducing pumping costs or allowing greater irrigation surfaces and to increase or stabilize yields.
Among the existing technologies, interests for drip-irrigation increased quickly in the past years, because of its potential to improve the water delivery from the water reservoir to the active root zone of the plants. The water delivery efficiency of drip irrigation is about 70-95%, against 55-85% for sprinkler irrigation and 40-75% for surface irrigation [4].

The figure 2.5 illustrates the different irrigation practices. The soil water availability is here illustrated by the mean root zone soil moisture (s). Irrigation is characterized by three main parameters. The intervention point ($\tilde{s}$) corresponds to the soil moisture at which irrigation is triggered and the target level $\hat{s}$ corresponds to the soil moisture level to which the soil is replenished after an irrigation application. Water stress occurs when the soil moisture falls below a certain level (s^*) so that in order to avoid stress, the intervention point must be equal or higher than s^*. The practice of letting $\tilde{s}$ fall below s^* is called deficit irrigation, as a mild water stress is applied to the crop. In the case of surface irrigation, high irrigation depths are applied at lower frequency so that the soil is almost saturated s^*. On the opposite, the goal of micro irrigation is to keep the soil moisture to a relatively constant value that is optimal for the plant so that the target level s^* is practically identical to the intervention point $\tilde{s}$. This is achieved by applying frequent (or even continuous) small irrigation depths during the day. This practice is different from classic irrigation schemes where the soil is almost brought to saturation, or at least to high soil moisture level after an irrigation event and then slowly dries out. Keeping a relatively constant soil moisture avoid over-irrigation and water stress situation [23].
In practice however, the drip irrigation systems available in Burkina Faso have a relatively high discharge rate, so that it is difficult to assure a constant soil moisture and irrigation is triggered once or twice a day, so that the target level is higher than the intervention point.

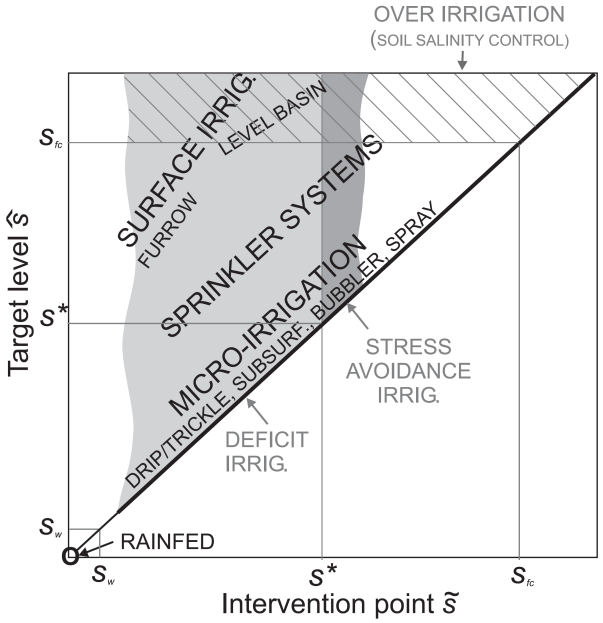

Figure 2.5: Illustration of the different irrigation practices. The white area corresponds to parameters combinations that do not occur in reality (from Vico et al., 2011 [24]).

2.3.1 Drip irrigation

Drip irrigation is an advanced irrigation system, consisting of a dense pipe network connected to a water reservoir that delivers the water directly near the plant stem. Usually PVC pipes are used and drippers are placed along them, which slowly delivers the water to the plants. Subsurface drip irrigation consists of an underground pipe network that directly delivers the water into the root zone, while surface drip irrigation systems are laid on the ground.
Drip irrigation can optimize water management greatly. It avoids water losses from tank to plants with its pipe network and the irrigated surfaces are limited to the plant zone, limiting surface evaporation. Since soil moisture in the root zone can be kept at a stabilized level, it can optimize plant growth and physical labor is simplified as only a main gage needs to be open to irrigate the whole field.

Drip irrigation systems were first constructed for advanced irrigation management in more developed countries but new systems are developed to match the needs of the producers and the technical specificities of the Sahel region. The first constrains concerning drip-irrigation in developing countries is the relatively high capital costs, which limit their promotion for small-scale producers with little savings. New technologies are in research to reduce the costs. Those new systems are efficient but some drawbacks can be noted. There is a risk of clogging of the drippers, due to the dirt from the irrigation water and a regular check of the drippers is therefore required, even though a filter is placed directly after the water reservoir. Another difficulty is to assure a relatively constant dripper discharge rate and an acceptable distribution uniformity of the water in whole field given the low pressure in the pipes. Different technologies of drippers have therefore been developed. The dripper can either consist of a simple hole made in the pipe, but irrigation uniformity is very bad. The NGO *iDE* has developed micro-tubes which are small tubes simply plugged in the pipe, they are relatively cheap, maintenance is easy and distribution uniformity is improved, the discharge is however directly linked to the pressure head in the pipe. More advanced emitters contain a device inside the pipe that creates a turbulent flow inside this device before the water exits the pipe. This allows to disconnect the water pressure inside drippers from the pipe and therefore to allow a lower and more constant discharge rate. Consequently, this type of technology allows a more uniform water distribution over the crop.

2.3.2 Irrigation schedule

While the irrigation systems cited above improve the water delivery efficiency and thus allow great water savings, those technologies do not manage the irrigation schedule. Many producers trigger irrigation following there own experience, without any calculations, or rely on general information from the national meteorological institute or NGOs.
The goal of developing a good irrigation schedule is to predict the crop water needs, and delivering the corresponding water amount and thus avoiding water losses mainly by percolation below the root zone and maximizing yields. There are different methods to achieve this goal.

Basic irrigation schedule

The classic method is based on a soil water balance approach. It consists of estimating the water needs by calculating the crop evapotranspiration (ET_c) based on historical meteorological and plant data adapted to the local context. This method is detailed in chapter 2.4.2. This is the most commonly used approach with a lot of data available. This method draws a fixed irrigation schedule.

Triggered irrigation

Other new approaches rely on direct measurements on the field to assess the plant state and to detect when to trigger irrigation [14]. It aims to detect a certain level of water depletion in the soil below which plant growth would be reduced, which indicates that irrigation should be triggered.

Measurements can be done directly on the plant, by assessing the plant water tissue by measuring the stem water potential with a pressure chamber or using a psychrometer, for example. The stomatal conductance can also be measured with a porometer or using thermal sensing on the plant leaves. Finally, the sap flow within the stem can be measured to detect transpiration reduction [14].

Alternatively, water stress can be assessed by measuring the soil water deficit. The irrigation can be triggered by using soil matrix potential sensors, that are placed in the soil. The difficulty resides in finding a location that is representative of the averaged soil moisture. The advantage of using soil matrix potential sensors is that there are not dependent on the soil type and are directly linked to the plant capacity to uptake water. Soil moisture sensors can also be used, but knowledges on the soil type are needed to express the critical value of soil matrix potential in soil moisture value.

Those methods do not assess the daily water needs but directly monitor water stress. They avoid irrigating too often and allow the soil to dry until a critical threshold is passed. It has therefore the potential to optimize plant growth by avoiding water stress and to avoid over-irrigation by optimizing the timing of irrigation. The system can be further automatized so that the irrigation is triggered directly when the threshold is detected, which save time for the producer.

Some limitations should however be noted. First, the system can only limit stress due to water deficit, but other phenomenon can limit growth such as heat, radiation or saline stress, diseases or lack of nutri-

ents, etc. The system is therefore not completely autonomous and the expertise of the producer is still required on the field. Secondly, the sensing system is usually only placed on a few plants or location in the soil, which assumes an homogeneous crop, with homogeneous soil texture, soil moisture and plant state. This may however not be the case, especially with low-cost drip kits which distribution uniformity is not assured. Finally, there is still a risk of irrigating too much at once, by applying a too important irrigation depth that would recharge the soil below the effective rooting depth.

2.4 Estimation of water needs

2.4.1 The water balance

The commonly used approach to estimate plant water needs aims at quantifying the different fluxes entering and leaving the soil-plant-atmosphere continuum in a given time interval, in order to assess the daily water losses and the soil water storage. The main fluxes of this system were discussed in chapter 2.2.1. They are the precipitation (P); the runoff (RO); the net irrigation depth (I); the capillary rise (CR); the crop evapotranspiration (ET_c) and deep percolation (DP) (figure 2.6).

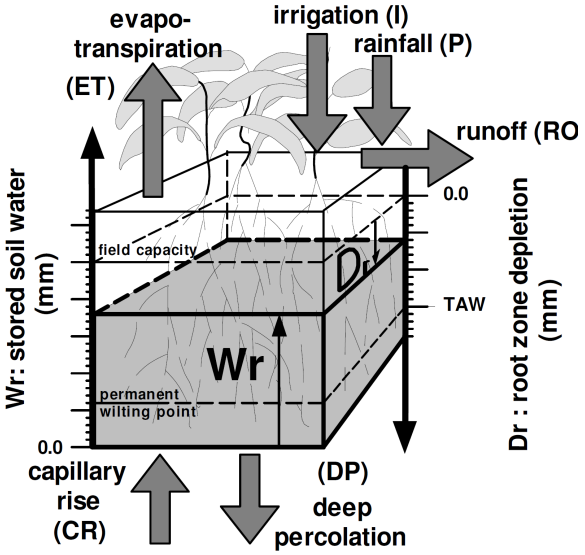

Figure 2.6: Water balance fluxes and root zone water reservoir (from FAO, 1998 [11]).

The balance of all those fluxes determine the quantity of water stored in the soil. The soil has moreover an upper and lower water storage capacity. The upper limit is reached when the soil moisture is at field capacity (θ_{fc}). Field capacity is usually defined as the water content corresponding to a soil matrix potential of -33 kPa, below which drainage flux is considered negligible. This definition is however not exact and is only relevant for medium soils. We prefer the definition used by Twarakavi et al., 2009 [25] and in HYDRUS 2D, defining field capacity as the soil matrix potential corresponding to an unsaturated hydraulic conductivity (K) of 0.01 cm/d. The lower limit is reached when roots can no longer extract water from the soil and is called the permanent wilting point (θ_{pwp}). The water content at permanent wilting point is normally defined as the water content at -1500 kPa. The total available water (TAW) in the root zone (z_r) can be then calculated via eq. (2.3). Using the water balance approach the goal is to calculate the water deficit (D_r), representing which part of the TAW is depleted. If using a daily interval, the water deficit at day i is defined by eq. (2.3) [11].
The plant will suffer from water stress when only a fraction of the TAW is depleted. A value corresponding to the average fraction of TAW that can be depleted (p) has been estimated for many crops at different growth stages and summed up by the FAO, 1998 [11]. The Readily Available Water (RAW) expresses therefore which soil moisture amount can be depleted before water stress occurs and is defined in eq. (2.3).

$$TAW = (\theta_{fc} - \theta_{pwp}) \cdot z_r \tag{2.1}$$

$$Dr_i = Dr_{i-1} - (P_i - RO_i) - I_i - CR_i + ET_i + DP_i \tag{2.2}$$

$$RAW = p \cdot TAW \tag{2.3}$$

In the case of drip irrigation during the dry season, many fluxes can be neglected. There is no precipitation during this season, drip irrigation avoids runoff and capillary rise is usually low due to deep water table and due to the sandy soil texture, so that the only important fluxes are the evapotranspiration, the deep percolation and the irrigation. By only considering those fluxes, the average soil moisture in the root zone can be estimated similarly to the water deficit and is detailed in eq. (2.4) and (2.5) [26].

$$nz\frac{\partial s(t)}{\partial t} = I(s,t) - ET(s,t) - L(s,t) \tag{2.4}$$

$$s(t) = \frac{\theta(t)}{\theta_{sat}} \tag{2.5}$$

Where n is the soil porosity; z is the root depth; $s(t)$ is the relative soil moisture at time t; θ_{sat} is the soil moisture at saturation; $I(s,t)$ is the rate of infiltration from the irrigation; $ET(s,t)$ is the evapotranspiration rate and $L(s,t)$ is the rate of deep infiltration (or leakage).

All these fluxes are dependent on the time t and the soil moisture s, as those fluxes can be limited when soil moisture falls below a certain point.

2.4.2 Irrigation schedule

The irrigation schedule is characterized by the irrigation depth brought to the crop and the frequency of irrigation. The irrigation depth corresponds to a water volume applied on a certain crop area. Its units are therefore expressed in liters/m^2 but more commonly in millimeters $[mm]$ like precipitations.
The best irrigation schedule should aim at avoiding water losses out of the root zone by optimizing the soil water availability. The main water losses are due to evaporation, transpiration and deep percolation in our system. The schedule should aim at avoiding deep percolation by applying an adapted irrigation depth and optimizing the plant transpiration. Moreover it is possible to reduce the soil evaporation from the top soil surface by reducing the irrigation frequency, letting the soil dry at the surface and promoting a deep root zone. Finding the best compromise between water savings and optimized transpiration is not straightforward and will be assessed in more detailed using the software HYDRUS 2D.

In general, with an appropriate water management, it is possible to avoid deep percolation so that the water needs are directly linked to the crop evapotranspiration. The basic irrigation schedule consists of matching the irrigation depth with the crop evapotranspiration, so that 100% of ET_c is brought to the field at a certain frequency. Eq. (2.6) and (2.7), illustrate the calculation of the frequency and the irrigation volume to apply to the crop given a chosen irrigation depth (Irr_n).
The irrigation depth can be as high as the RAW, with a low frequency, so that the water deficit increases until the RAW is almost reached and irrigation is triggered just before water stress occurs.

$$Irrigation\ frequency\ [day^{-1}] = \frac{ET_c \cdot f_{leaf}}{Irr_n \cdot f_w} \tag{2.6}$$

$$Actual\ irrigation\ volume\ [Liters] = \frac{Irr_n \cdot A_{dripkit} \cdot f_w}{e_t} \tag{2.7}$$

Where Irr_n is the net irrigation depth $[L/m^2/day]$ or $[mm]$; ET_c is the crop evapotranspiration $[L/m^2/day]$ or $[mm/day]$; $A_{dripkit}$ is the area of the drip kit $[m^2]$; e_t is the overall efficiency of water delivery to the plant (assumed to be 0.9) [-]; f_{leaf} is the fraction of soil covered by vegetation (at full development stage) $[m^2 \cdot m^{-2}]$ and f_w is the fraction of soil wetted by irrigation $[m^2 \cdot m^{-2}]$.

With the use of drip kits, irrigation occurs only at specific locations, near the plant, so that the crop is only partially irrigated. If the drippers have a high spacing (0.5m x 1m, for example), each irrigated area are disconnected, leading to very inhomogeneous water availability in the soil, with areas with reduced evaporation. In this context, it becomes critical to estimate the fraction of the soil that is effectively irrigated (f_w), in order to accurately calculate the irrigation volumes required. Moreover, the crop canopy may not cover the whole drip-kit area so that ET_c must be reduced to the fraction of soil covered by vegetation (f_{leaf}).

We used the software HYDRUS 2D to acquire a better understanding of these processes and to adjust our calculations. The calculated standard potential evaporation and transpiration were input parameters of the model. The modeling procedure with HYDRUS 2D is detailed in chapter 3.2.

2.4.3 Evapotranspiration calculation

A considerable amount of literature details the standard procedure to estimate water needs in the case of well watered, large and homogeneous fields. Estimation of water needs become however more complex in the case of partially covered crops with partially irrigated surface such as it is usually the case for drip irrigation. In such inhomogeneous cases, some locally specific parameters have to be calibrated to obtain realistic estimation. We detail here the calculation procedure for standard conditions (well watered and homogeneous crop) as it is the basis for any irrigation planning.
Evapotranspiration from a specific crop in its environment is calculated based on the evapotranspiration of a standard reference crop (ET_0) and adjusted with a crop coefficient (K_c), specific to each crop, and an environmental coefficient (K_s) as summarized in figure 2.7.

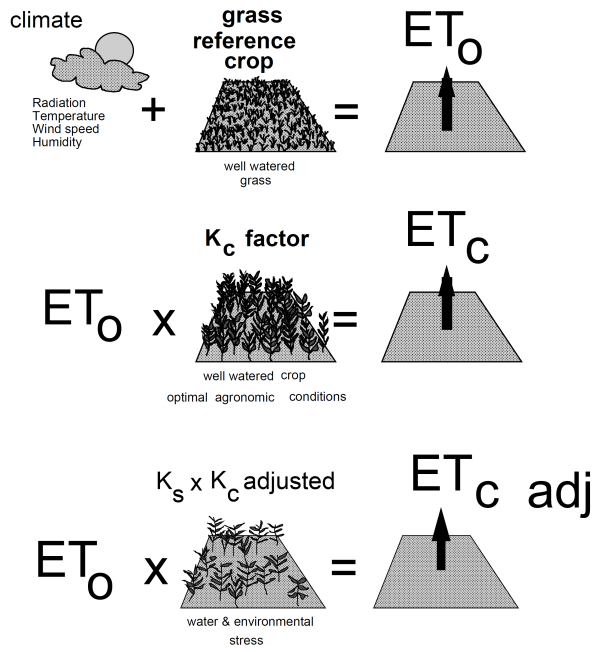

Figure 2.7: Standard procedure to calculate ET_c (from FAO, 1998 [11]).

Reference Evapotranspiration ET_0

The most widely accepted method to calculate the reference evapotranspiration ET_0 is based on the Penman-Monteith equations, detailed by the FAO, 1998 [11]. ET_0 for a grass reference surface is determined by the eq. (2.8).

$$ET_0 = \frac{0.408\Delta(R_n - G) + \gamma\frac{900}{T+273}u_2(e_s - e_a)}{\Delta + \gamma(1 + 0.34u_2)} \tag{2.8}$$

Where $ET_0$is the reference evapotranspiration $[mm \cdot day^{-1}]$; Rn the net radiation at the crop surface $[MJ \cdot m^{-2} \cdot day^{-1}]$; G the soil heat flux density $[MJ \cdot m^{-2} \cdot day^{-1}]$; T the air temperature at 2 m height $[°C]$; $u2$ the wind speed at 2 m height $[m \cdot s^{-1}]$; es the saturation vapour pressure $[kPa]$; ea the actual vapour pressure $[kPa]$; $es - ea$ the saturation vapour pressure deficit $[kPa]$; Δ the slope vapour pressure curve $[kPa \cdot °C^{-1}]$ and γ the psychrometric constant $[kPa \cdot °C^{-1}]$

Crop Evapotranspiration ET_c

Following the FAO recommendations [11], crop evapotranspiration is calculated via eq. (2.9) and is based on the crop coefficient K_c which depends on the crop type and the growth period.

$$ET_c = K_c \cdot ET_0 \tag{2.9}$$

Moreover the single crop coefficient (K_c), which incorporates averaged crop and soil characteristics, can be separated between two dual crop coefficients, K_{cb} for transpiration and K_e for evaporation. The calculation procedure follows chapter 6 and 7 from the FAO, 1998 [11]. A maximum crop coefficient $K_{c_{max}}$ can also be calculated using eq. (2.10) which reflects the case of a very frequently irrigated crop with maximal soil evaporation. Reference values for the transpiration coefficient K_{cb} are suggested by the FAO, 1998 [11] for different crops and growth stages but they need to be adjusted to the local climate

conditions as described in eq. (2.11). Finally the evaporation coefficient K_e can be calculated via eq. (2.12).

$$K_{c_{max}} = 1.2 + [0.04(u_2 - 2) - 0.004(RH_{min} - 45)] \cdot (h/3)^3 \quad (2.10)$$

$$K_{cb} = K_{cb} + [0.04(u_2 - 2) - 0.004(RH_{min} - 45)] \cdot (h/3)^3 \quad (2.11)$$

$$K_e = K_{c_{max}} - K_{cb} \quad (2.12)$$

Where u_2 is the wind speed at 2m height $[m \cdot s^{-1}]$; RH_{min} the relative humidity [%] and h the mean plant height during the specific growth stage $[m]$.

ET_c under soil water stress conditions

Previously we assumed optimal soil water availability for the crop and frequent wetting leading to maximal soil evaporation and transpiration. This is not applicable for all crops, especially where water is scarce. Indeed, the soil surface will dry which will reduce the actual evaporation rate and water stress may occur leading to reduced transpiration.
To account for those environmental conditions a water stress coefficient K_s is introduced (figure 2.7). The calculation of K_s is detailed in chapter 2.5.4.

2.5 Modeling soil water dynamics

We present here the main equations used in HYDRUS to simulate water flow in an unsaturated soil.

2.5.1 Governing water flow equations

The governing equation for a one-dimensional uniform flow of water in an unsaturated medium is based on the Richards' equation (eq. 2.13) [27].

$$\frac{\partial \theta}{\partial t} = \frac{\partial}{\partial t}\left[K(h,x)\left(\frac{\partial h}{\partial x} + cos(\alpha)\right)\right] - S(h,x) \quad (2.13)$$

$$K(h,x) = K_s(x) \cdot K_r(h,x) \quad (2.14)$$

Where h is the water pressure head $[L]$; θ is the volumetric water content $[L^3L^{-3}]$; t is time $[T]$; x is the vertical coordinate $[L]$; $S(h,x)$ is a sink term accounting for water uptake $[L^3L^{-3}T^{-1}]$; α is a the angle between flow direction and the vertical axis; $K(h,x)$ is the unsaturated hydraulic conductivity $[LT^{-1}]$; $K_s(x)$ is the saturated hydraulic conductivity $[LT^{-1}]$ and $K_r(h,x)$ is the relative hydraulic conductivity $[-]$.

2.5.2 Soil hydraulic properties

The model selected to characterize the soil hydraulic properties is based on the *van Genuchten - Mualem* equations (eq. 2.15 and 2.16) [28]. These equations have been broadly used and validated in the literature [29], [30]. They describe mainly the relationship between soil matrix potential, volumetric water content, effective saturation and soil hydraulic conductivity.

$$\theta(h) = \theta_r + \frac{\theta_s - \theta_r}{[1 + (\alpha h)^n]^{(1-1/n)}} \quad (2.15)$$

$$S_e = \frac{\theta(h) - \theta_r}{\theta_s - \theta_r} \quad (2.16)$$

$$K(S_e) = K_0 S_e^l [1 - (1 - S_e^{n/(n-1)})^{(1-1/n)}]^2 \quad (2.17)$$

With: h: Soil matrix potential $[cm]$ (taken positive for increasing succion); $\theta(h)$: Corresponding volumetric water content $[cm^3cm^{-3}]$; θ_r Residual water content $[cm^3cm^{-3}]$; θ_s: Saturated water content $[cm^3cm^{-3}]$; S_e: Effective saturation $[-]$; K_0: Hydraulic conductivity at saturation $[-]$; α: Calibration parameter $[cm^{-1}]$; n: Calibration parameter $[-]$; l: Calibration parameter $[-]$ (generally assumed to be 0.5)

2.5.3 Root water uptake

Two main models to characterize the root water uptake are implemented in HYDRUS 2D. The model based on Feddes et al., 1978 [31] contains a database on many vegetable crops and has been widely reviewed in the literature. It defines a linear water stress below a certain threshold (h_3) until the permanent wilting point (h_{pwp}) is reached (eq. 2.19) [32]. Additionally a water stress is implemented near soil water saturation due to deficient aeration conditions (anaerobiosis point).
The second model proposed by van Genuchten called *S-Shaped Model* [33], proposes a non-linear reduction function (eq. 2.20).

$$S(h,x) = \alpha(h,x) \cdot b(x) \cdot T_p \tag{2.18}$$

$$\alpha(h) = \frac{h_{pwp} - h}{h_{pwp} - h_3} \qquad if\ h_{pwp} < h < h_3 \qquad (Feddes) \tag{2.19}$$

$$\alpha(h) = \frac{1}{1 + (\frac{h}{h_{50}})^p} \qquad (Van\ Genuchten) \tag{2.20}$$

Where $S(h,x)$ is the sink term; $b(x)$ is the normalized water uptake distribution with depth [cm^{-1}]; T_p is the potential transpiration rate [$cm\ s^{-1}$]; $\alpha(h)$ Water stress reduction function [-]; h Soil matrix potential [cm]; h_{pwp}; Soil matrix potential at permanent wilting point [cm]; h_3 Soil matrix potential below which water stress occurs [cm]; h_{50} Soil matrix potential at which root water uptake is reduced by 50% [cm]; p Calibration parameter [-].

The spatial distribution of the root water uptake ($b(x)$) is a key parameter to characterize the soil water dynamics. The root water uptake function is however difficult to determine precisely. Most models are based on a root density function that can be measured experimentally on the field and the potential rate of transpiration [34],[35]. Indeed Coelho et al., 1999 [36] showed that root water uptake and root length density followed similar distribution during the plant growth and evolved similarly, though the root water uptake adapted very rapidly to the spatial availability of water, while the root length distribution adaptation was slower.
Patterns of root development vary greatly from the plant type, the irrigation pattern and the soil texture. Portas, 1973 [37] showed that the root system of melon, could either penetrate deep in the soil, with very tight lateral development in non-irrigated crops or either spread very brightly (5 times wider) with a shallow depth (2 times shallower) if frequently irrigated. The root elongation and direction in the soil depend indeed mainly on the soil resistance (mechanical impedance) and the water availability (water stress) [38]. In addition to the vertical and horizontal elongation of the roots, the root density function with depth can also vary. Some general patterns have been proposed by Coehlo et al., 1995 [39] for drip irrigation, the most commonly used 1-dimensional distribution consisting in a maximal density at the top, with a linear or Gaussian decrease with depth until the maximal root depth [10].

2.5.4 Transpiration reduction

In HYDRUS, the transpiration reduction is calculated as detailed in chapter 2.5.3, by calculating the sink term $S(h,x)$. Since root density is not homogeneous, some parts of the soil dry faster than others, due to higher root water uptake. Roots will suffer water stress earlier in those zones which will decrease their rate of water uptake. This may however not lead to transpiration reduction as many plant roots have the capacity to compensate this local water stress by taking up more water in others parts of the root zone where water depletion is lower [32]. A root adaptability factor accounting for root water uptake compensation has therefore been introduced in HYDRUS 2D [40]. This method allows to determine root water stress very locally within the root zone and enables the root water uptake to adapt very rapidly, but transpiration reduction occurs only when water is depleted below a certain level in the whole root zone (when full compensation is not possible anywhere).

Another method to assess transpiration reduction is based on the FAO, 1998 [11]. The general method from the FAO is based on the TAW and the p factor accounting for the fraction of the TAW that can be depleted before water stress occurs. The reduction of the transpiration was defined using a transpiration

reduction factor (K_s), dependent on the water deficit.

$$K_s = \frac{TAW - D_r}{(1-p)\ TAW} \tag{2.21}$$

$$ET_{c_{adj}} = K_c \cdot K_s \cdot ET_0 \tag{2.22}$$

This method is directly linked to the water availability in the whole root zone and does not assess the water stress in different parts like in HYDRUS. One inconvenient of this method is that the water depletion is dependent on the soil type, so that a depletion of the TAW of 40% for instance, corresponds to different values of soil matrix potential, from about -10 kPa for a loamy sand soil to -100 kPa for a clay texture (see figure 2.8). The FAO suggests therefore to adapt the p factor for very coarse or fine texture by about $\pm$ 10% [11].

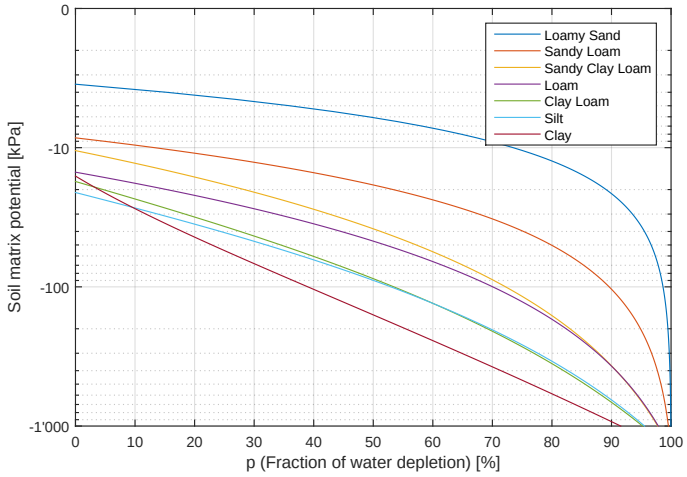

Figure 2.8: Relationship between the soil matrix potential and the fraction of water depletion p. Soil parameters were taken from Carsel et al., 1988 [29].

While the HYDRUS method seems more reliable as it assesses the water availability more precisely, some parameters are difficult to estimate such as the degree of water uptake compensation and the threshold values used for the water stress reduction function ($\alpha(h)$). Only a database from the Feddes model is available [16]. On the other side, the FAO method relies on a large set of literature and experiences making it also a realistic and robust model.

2.5.5 Calculation of yields

Calculating crop yield is a complex task as it relies on many different processes. Yield is linked to plant biomass, transpiration, water, salinity and temperature stress, CO^2 levels, soil fertility, etc. The HYDRUS software does not include a such module. The FAO model AquaCrop proposes a methodology to estimate yields [10]. It includes the major parameters influencing plant growth and yield formation. The model is relatively complex and falls beyond the scope of this study. The main processes are shown in appendix A.1.
The impact of water stress in this model influences different parameters. First, water stress at early growth stage will limit the green canopy development which will lead to reduced canopy (and transpiration) at the end of the development stage. Then during the mid-season, water stress leading to stomatal closure or early senescence will decrease transpiration rate. Reduced transpiration influences then the plant biomass. Biomass is finally linked to yield by using an adjusted harvesting index, which is also influenced by water stress through failure of pollination.

2.6 Towards the definition of a threshold to trigger irrigation

As discussed above, the soil water dynamics is spatially highly heterogeneous, due to the spatial root water uptake, the soil hydraulic conductivity and the water fluxes. The water dynamics is further influenced by the soil texture modifying the plant and soil response and the plant type with its own adaptability to stress and root development pattern. In this context, detecting water stress using a simple system in the field is a complex task. The proposed system used in this research is based on the monitoring of the soil matrix potential, which is directly linked to the ability of the plant to uptake water.

Different studies have proposed thresholds for a few crops using a similar system. Values differ however greatly and no general methodology has been proposed so that comparison between studies is difficult. Based on the Feddes model, Taylor, 1972 [16] has proposed a large database on values of soil matrix potential leading to water stress which is implemented in HYDRUS. Those values are considered too low in newer studies [41], most probably because it does not take into account the whole root zone dynamics and that other studies focused directly on maximal yield and not water stress. For tomato for instance, values as low as -60 to -150 kPa were proposed by Feddes, but Thompson et al., 2007 [41] reported a threshold between -38 and -58 kPa depending on the variety and growing season, with sensors placed at 10 cm depth in a sandy loam soil. Bower et al., 1975 [42] suggested even a lower threshold of -20 kPa in a clay loam soil at 15 cm depth and Wang et al., 2005 [43] found that irrigating only when the soil reached -30 kPa in a gravelly loam soil resulted to the highest yield. For other crops, Thompson et al., 2007 [41] measured a threshold of -35 kPa for melon and -58 kPa for pepper at 10 cm. In contrast, Smittle et al., 1994 [44] reported a maximal yield for pepper grown in loamy sand soils when the soil matrix potential was maintained higher than -25 kPa at 10 cm.
Based on these information it appears difficult to draw a general model. It can only be said that most sensors were placed at about 10 to 15 cm depth and that the best threshold is most likely in the range between about -20 to -80 kPa. Difference between plant species exist but seem to remain in a relatively similar range of soil matrix potential value. Most studies were also done on crops during the mid-season growth stage, that is when the plants are fully developed, during yield formation. Little data are available at earlier growth stage though triggered irrigation should be possible during the whole crop growth.

Based on the theory discussed above, we propose here a methodology to get a better understanding of the water and plant dynamics in order to define the most appropriate system to trigger irrigation.
The first consideration is that we want to design a system that can manage water during the whole growing season. It is therefore essential to distinguish the early growth stage and the mid-season stage. The processes of yield formation and the response to water stress are indeed very different during both phases.
One difficulty resides in determining which intensity of stress is harmful for the crop and results in lower yields. At early growth stage, it is suggested in the FAO AquaCrop model [10] that low level of soil water depletion already leads to reduced canopy expansion which leads to lower yields during the next stages. The most reliable information concerning this growth stage are given by the FAO, using p, the average fraction of TAW that can be depleted. It was however reported that exceeding this threshold had a less severe impact on final yield during early growth stage, than during yield and fruit formation. A mild stress during the crop development phase can even promote flowering [15]. During the mid-season, water stress is more directly linked to stomatal closure and transpiration reduction, since full canopy cover has already been reached. During this stage we can rely more easily on the literature cited above and also on the p values suggested by the FAO.

3 Materials and Methods

Two different approaches are presented in this study. The first part presents the experimental set-up that was installed in Burkina Faso, while a second part details the theoretical model that was implemented using HYDRUS 2D.
The experiments took place from October 2014 to March 2015 in a rural area very close to Ouagadougou ($12°20'24"N$, $1°27'8"O$). The crops were lent by *iDE*, an NGO working on the development of drip kit irrigation systems. iDE is one of the local partners collaborating on the project. Some of the locations where the system is tested are equipped with drip kits provided by iDE.
Two different crops were grown. A cabbage crop was grown on a 50 m^2 drip kit from October 29, 2014 to February 5, 2015. A second experiment took place from December 5, 2014 to March 25, 2015 on a drip-kit of 200 m^2 cultivated with eggplants. Both crops were prepared following the same practice. Before transplanting the crops were ploughed manually to a depth of about 10 cm. 1 kg / m^2 of an NPK soil amendment and 0.25 kg / 50 m^2 of urea were then applied.

3.1 Experimental set-up

3.1.1 Cabbage experiment

The cabbage species transplanted was *KK Cross*, a commonly used variety in Burkina Faso, that has a good tolerance to heat stress.
The drip irrigation system consisted of 12 sub-lines and each was connected to the main line with a valve. The main line was supplied by a 200 L water reservoir. The drip systems from iDE are equipped with micro-tubes and the water reservoir is usually placed at a height of about one meter, which allows sufficient pressure in the system with a micro-tube discharge rate of about 2 to 3 liters/hour. The sub-lines had a spacing of 40 cm and a micro-tube was placed every 40 cm. One cabbage seedling was transplanted in front of each micro-tube. The total surface covered by the system was about 50 m^2, the main line was 5 meters long and the sub-lines 10 meters long. A total of 180 cabbages were transplanted.
The system was divided into two equal parts and two different irrigation schedules were tested independently. The soil matrix potential was monitored continuously using Watermark 200SS sensors connected to the wireless sensor network as described in chapter 1.3. Figure 3.1 illustrates the system. Three sensors measured the soil matrix potential at 10 cm depth. Two sensors were placed in front of the dripper, 5 cm away perpendicular to the line. The third sensor was placed 20 cm away form the line. A fourth sensor was added to monitor the potential at 5 cm depth and 5 cm laterally. The same set-up was replicated for both experiments.

Two different experiments were performed (table 3.1). The treatment 1 (optimal, low depth) provided an irrigation amount of 100% of the calculated ET_c, with a typical irrigation depth and frequency. The typical irrigation depth applied in Burkina Faso is usually much lower than the RAW (readily available water), mainly due to small water reservoirs, so that the frequency of irrigation events is rather high.
For treatment 2, a certain water stress was applied to the crop by only irrigating about two third of the plant water needs (66% ET_c) with an irrigation depth equivalent to the RAW. The irrigation depth was increased with plant growth due to the roots development which increases the soil volume were water can be taken up.

During the whole study, we will refer to the irrigation amounts brought to the crop in terms of liters and not in terms of liter/m^2 or millimeters. Indeed, with drip irrigation systems, only a fraction of the crop is irrigated and this surface is difficult to determine a priori, so that dividing the irrigation amount by any surface may be confusing and not correct. This was also more convenient to describe that irrigation amount in HYDRUS in terms of liters per dripper (or per plant). As a consequence, we preferred to express the irrigation depth as a water volume that is applied on a drip kit system consisting of 90 drippers. As a result, the irrigation depth for treatment 1 consisted in applying an irrigation depth of 100 liters for 90 drippers, that is 1.1 liters per dripper. The irrigated area was estimated to be about 12 m^2 so that 100 liters corresponded to an irrigation depth of about 8.3 $[L/m^2]$ or $[mm]$. For 200 liters, it corresponded to an irrigation depth of about 16.5 mm.

	Treatment 1 (100% ET_c)		**Treatment 2 (66% ET_c)**	
Days after transplanting	Frequency [1/day]	Depth [L]	Frequency [1/day]	Depth [L]
0 - 20	1/1.5	70	1/2.5	70
21 - 40	1/1.5	100	1/2.5	100
51 - 90	1	100	1/3	200

Table 3.1: Irrigation schedule for the experiments on cabbage

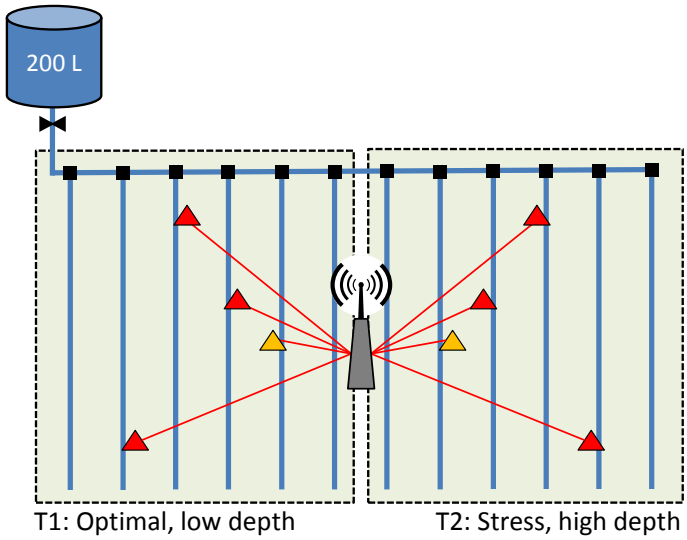

Figure 3.1: Set-up of the cabbage experiment. The crop was divided into two subplots with different irrigation schedules (T1 and T2) which are described in table 3.1. Red triangles represent Watermark sensors at 10 cm depth, yellow triangles are sensors at 5 cm.

3.1.2 Eggplant experiment

The species of eggplant selected was *Kalenda*. It is a common species used in Burkina Faso, with a good tolerance to heat stress and a reported resistance to different diseases (*Ralstonia solanacearum*, *Colletotricum lagenarium*, Tobacco mosaic virus)[45].
This drip system covered an area of 200 m^2 and consisted of a reservoir of 1 m^3 connected to a central main line, 10 meters long. 10 sub-lines were connected on each side of the main line and measured 12 meters with a spacing of 1 meter. The distance between micro-tubes was 50 cm and an eggplant seedling was placed in front of each micro-tube. The water discharge was 2 liters/hour per micro-tube.
The plot was divided into four different irrigation treatments of each 50 m^2 with each 90 eggplants. For each subplot the soil matrix potential was measured on 2 plants, at 5, 10 and 15 cm depth. In one case, the sensors were placed near the plant at an horizontal distance of 5 cm for all sensors, while on the second plant the distance was 12 cm. The set-up is illustrated in figure 3.2. Due to limitations in the number of available sensors, only the near sensors were placed on experiment 1 and the sensors at 10 cm depth were left away for experiment 3.
Additionally, two soil moisture sensors, one 5TE and one 5TM from Decagon, were also placed in front of a Watermark sensor to compare both measurements and to draw the relationship between soil moisture and soil matrix potential. The 5TE sensor could also measure the soil electrical conductivity, an indication of salinity stress. The sensors were displaced many times during the experiment to compare the data.

The crop was divided into four different experiments (table 3.2). The treatment 1 followed the traditional irrigation schedule used by iDE technicians, which consisted in a frequent irrigation with a low irrigation depth (100 liters) during the whole growing season. From our calculations this irrigation schedule corresponded to about 200% of ET_c at early growth stage and about 150% during the mid-season. The reason for this overestimation may be due to the fact that iDE agronomists considered that the whole drip kit surface is irrigated, whereas we estimated that only about 25% of it is actually wetted, due to wide spacing between sub-lines.
The second experiment used the same low irrigation depth but at a reduced frequency, leading to a certain

water stress (about 66% ET_c).
The third experiment provided 100% of the estimated ET_c but with a higher irrigation depth corresponding to the calculated RAW (400 liters).
The fourth and last experiment also used an irrigation depth that was equal to the RAW, but at a lower frequency than the third experiment, inducing water stress (about 66% ET_c).

The irrigation depth of 100 liters corresponded to about 8.3 mm, 200 liters to about 16.6 mm and 400 liters to about 33.2 mm.

	Treatment 1 (optimal - low irr. depth)		**Treatment 2 (stress - low irr. depth)**	
Days after transplanting	Frequency [1/day]	Depth [L]	Frequency [1/day]	Depth [L]
0 - 20	2	100	1/1	50
26 - 60	2	100	1/1.5	100
61 - 100	2	100	1/1.25	100
101 - 120	2	100	1/2	100

	Treatment 3 (optimal - high irr. depth)		**Treatment 4 (stress - high irr. depth)**	
Days after transplanting	Frequency [1/day]	Depth [L]	Frequency [1/day]	Depth [L]
0 - 20	1/1	100	1/2	100
21 - 60	1/2	200	1/3	200
61 - 100	1/3	400	1/4	400
101 - 120	1/4	400	1/5	400

Table 3.2: Irrigation schedule for the experiments on eggplants

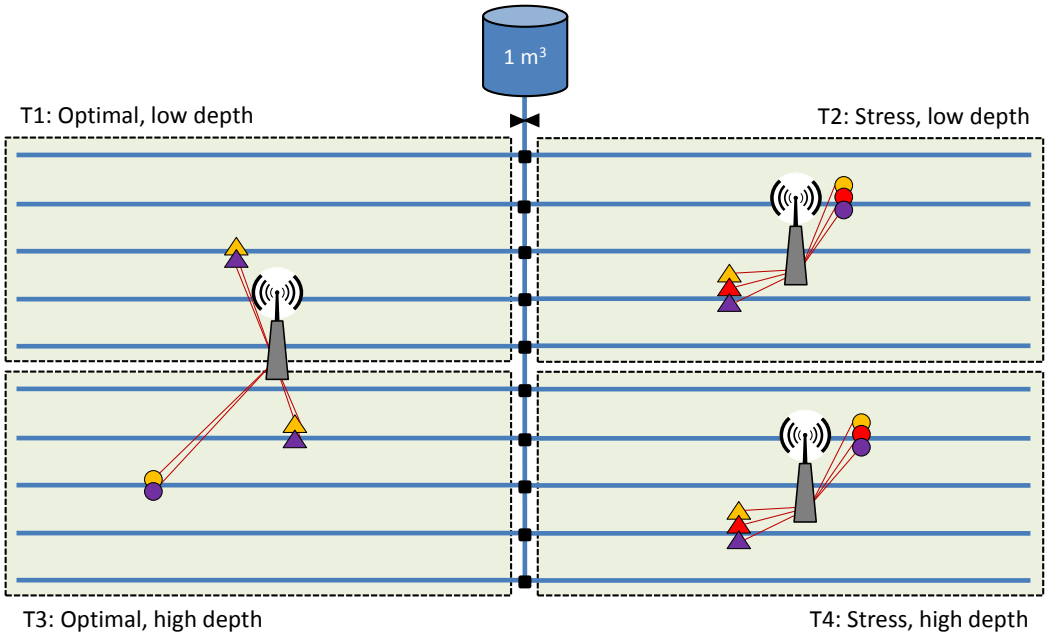

Figure 3.2: Set-up of the eggplant experiment divided in four irrigation treatments described in table 3.2. Triangles represent Watermark sensors placed near the plant (5 cm), circles are far sensors (12 cm away). Orange corresponds to 5 cm depth, red 10 cm depth and pink 15 cm depth.

3.1.3 Measurement of plant growth

Plant growth was monitored weekly during the whole growth.

Cabbage

The following measurements were performed:

- The diameter of the stem, 2 cm above ground;
- The mean diameter of the canopy cover of each cabbage;
- The diameter of the cabbage head (starting at the mid-season).

For each experiment, measurements were collected on a sample of 15 cabbage selected randomly among a total amount of 90.

Eggplant

The following measurements were performed:

- The diameter of the stem, about 2 cm above ground was measured;
- The mean diameter of the canopy cover of each eggplant;
- The plant height;
- The total number of leaves;
- The number of flowers.

For each experiment, measurements were collected on a sample of 10 eggplants selected randomly among a total amount of 90.

3.1.4 Root growth

Since the crops were small and soil preparation was done homogeneously, it is assumed that the mechanical impedance is relatively similar for each experiment, so that the main factor inducing a different root distribution is the water availability. It should however be noted that the soil was very hard, with a high density and a relatively rocky layer was found about 25 cm below ground. As a consequence, the root analysis may only be applicable for this specific location and does not represent the general case.
Measuring the 3-dimensional root length density is not easy in the field. One practice consists in collecting samples of soil cores in the root zone at different locations, to separate and wash the roots from the soil and to determine the total length of roots for each samples. By repeating this sampling at many locations and by extrapolating between each samples, a general profile of the root distribution can be obtained. However, due to the restricted instruments available and the compact soil texture a more simple procedure was selected to extract and analyze the root distribution. The ground around the plant was excavated and a large volume of soil containing the majority of roots was extracted. It was particularly difficult to dig deeper than about 25 cm in the soil due to the rocks, but it appeared that few roots reached deeper. The earth and rocks were then gradually washed away. Many smaller roots were lost during the process but the main structure remained. Sampling were done at each growth stage for the eggplant and only during the mid- and late growing period for the cabbage. Since the crops were relatively small, only one plant was extracted for each experiment which was assumed to be representative of the average state of the experiment.

The root distribution was assessed by image processing. A picture of the root distribution was taken, processed into a black and white image and the density with depth was measured by summing up, for each layer, the number of black pixels representing roots. The total biomass was also assessed by counting the surface of the image that was occupied by roots by counting all root pixels of the image.

3.1.5 Sap flow measurements

The sap flow within the plant stem is directly linked to plant transpiration. Heat pulse sap flow sensors have been successfully used to measure diurnal sap flow patterns and its correlation with stomatal closure and transpiration has been reported [14]. In order to monitor the rate of transpiration and to track potential transpiration reduction and water stress, sap flow meters were installed on some plants during the experiments. Concerning the cabbage experiment, four sap flow meters were placed on each experiments, on plants where Watermark sensors were also installed. Concerning the eggplant experiment, two sap flow meters were installed on the two eggplants for each experiments, again combined with Watermark sensors. The sap flow sensors were placed about 4 cm above ground, below the first branch or leaf.

We used eight sap flow sensors from the *East 30 Sensors* enterprise. The sensors consisted of a three stainless-steel needles spaced 6 mm apart, with the central needles containing a heater and the two outer ones equipped with thermistors sensors at three locations evenly spaced. Due to the small diameter only the middle thermistor was used. The sap flow meters were connected to a CR1000 datalogger from *Campbell Scientific* which was supplied by an external 12V battery connected to three small 10W 12V solar panels. Automatic measurements were collected every 30 minutes.
The sensors could only be installed at the beginning of the mid-season, since a minimum stem diameter was required in order to install the instrument in the stem. One challenge using sap flow meters was that those instruments were primarily used on trees and that because of the very thin stem diameter (about 10 mm), it was difficult to place the sensor precisely in the very thin xylem compartment. There was also more risk of noise in the signal due to the influence of external environmental factors.

Sap flow meters measure the diurnal velocity of sap flow in the xylem of the plant, which is directly linked to transpiration. For this reason, sap flow measurements are influenced by the meteorological parameters which influence the evapotranspiration rate, mainly relative humidity, wind speed, temperature and solar radiation as described in eq. (2.8). The sap flow velocity in $[m/s]$ was calculated by using the standard procedure suggested by East 30 sensors [46] and was automatically implemented in the datalogger code. The sap flow velocity can be linked to plant transpiration rate in $[liters/day]$ using the sectional area of the xylem, multiplied by the sap flow velocity [46]. The xylem radius was measured directly on a stem section at sap flow height, from plants that were extracted for root analysis. The area of the xylem was calculated by subtracting the pith area from the xylem and pith area. Finally the transpiration rate in $[liter/day/plant]$ was divided by the plant leaf area in order to compare it with calculated transpiration rate $[liters/m^2/day]$ or $[mm/day]$ from the meteorological station.
The signal from some sensors was not properly calibrated so that the minimum flow rate was much higher than others. All signals were smoothed by calculating the mean values on a mobile window of $\pm$ 30 minutes and were standardized by subtracting the minimum signal value on a time window of $\pm$ 2 days from the daily signal, so that all signals had a minimum near zero during the night.

In order to measure water stress via transpiration reduction, we extracted the daytime daily mean sap flow rate. Indeed, it was considered that transpiration reduction mainly occurred during the day and that comparing daytime mean was more significant. Daytime mean values for the calculated transpiration and the corresponding soil matrix potential were also calculated. Water stress could be assessed by comparing the day to day daytime mean reduction if correlated with soil matrix potential and not transpiration or by comparing the difference in signals between a plant subjected to low soil matrix potential and a reference plant.

3.1.6 Evapotranspiration estimation

Precise evapotranspiration estimation were needed to determine the irrigation schedules and to link it to the root water uptake, transpiration and soil matrix potential. It was also essential to have a good time resolution to calibrate the numerical model built with HYDRUS with the field measurements.

Meteorological data

The meteorological data necessary for the evapotranspiration calculation were acquired by a Sensorscope meteorological station. The station was not located directly on the site of experimentation, but in the center of Ouagadougou, about 8.4 km away from the experimental site. Those data were however the closest available to the site.
The meteorological station is equipped with diverse measurement devices from Sensorscope [47]. It includes wind speed and direction (Davis Anemometer), precipitation amount (Davis Rain Collector), air, surface and soil temperature (Sensorscope IRT, 5TE), relative humidity, wet and dry temperature (Decagon VP3) and radiation (Davis Solar Radiation). Data have a time resolution of 1 minute and are available from May 2013 until now, some gaps exist in the data due to maintenance or failure. Data were continuous during the period of this study.

It was however observed that wind speed measurements were much below the averaged values from other sources such as monthly values from the FAO Climwat 2.0 database [48] or hourly averages from the national meteorological institute. A second anemometer was installed in March 2015 directly in the middle of the eggplant crop at 2 meters height. Comparison of simultaneous measurements of wind speed on both sites has shown that wind speed were strongly correlated (R=0.785), but the wind speed magnitude was constantly lower in the center of Ouagadougou. The measurements of wind speed from the sensor in Ouagadougou were therefore adjusted by increasing the measured values by a certain correction

factor, in order to fit better with our experimental site. A correction factor was calculated by minimizing the root mean square error between both datasets and a value of 1.96 was found most adequate. The whole dataset of previous wind measurements in Ouagadougou was therefore increased by a factor of 1.96 for all calculations. Examples of recorded data and wind correction are shown in appendix A.2.

Evapotranspiration

Crop evapotranspiration was based on the procedure detailed in chapter 2.4.3. The calculated ET_0 was compared with other data and was proven to be consistent (figure 3.3). In particular, it was compared with monthly average over 15 years for Ouagadougou available from the FAO Climwat 2.0 database.

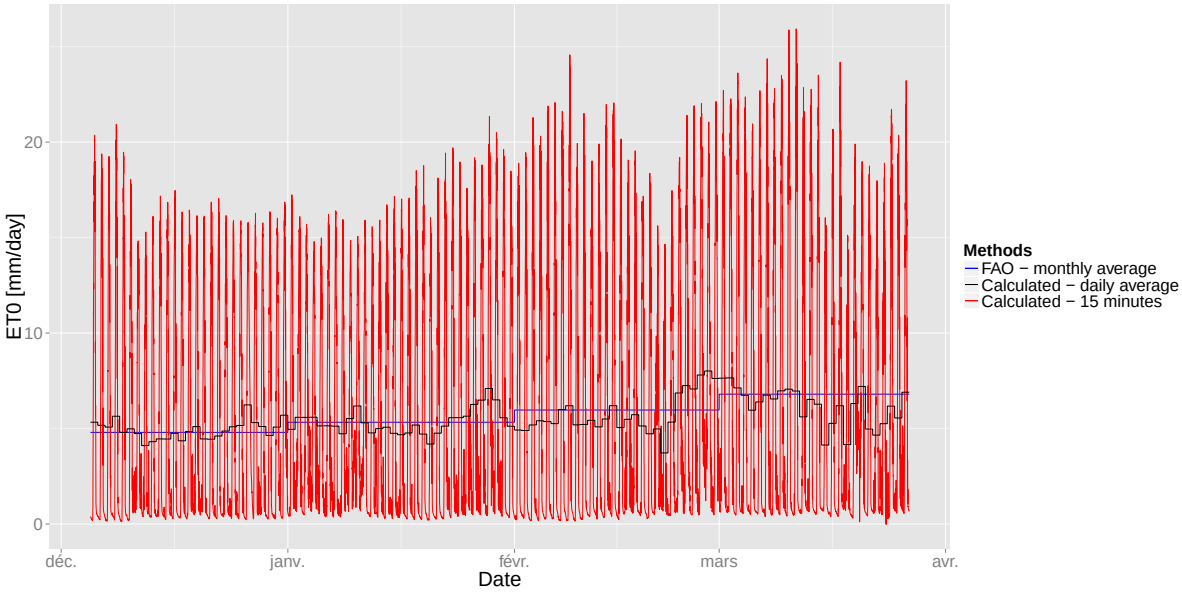

Figure 3.3: Calculated ET_0 for whole growth of the eggplant experiment.

The crop parameters used for the calculation of evapotranspiration for the eggplant and the cabbage experiments are summarized in table 3.4. Those data mainly come from the large database available from the FAO, 1998 [11] and were adapted with the consultation of local experts. In particular the duration of the stages and the maximal root depth (z_r) were adjusted.

	Duration [days]	K_c [-]	K_{cb} [-]	p [-]	z_r [m]
Stage 1: Initial	20	0.6	0.15	0.35	0.05-0.1
Stage 2: Development	40	»	»	»	»
Stage 3: Mid-season	40	1.05	1	0.45	»
Stage 4: Late season	20	0.9	0.8	0.55	0.2-0.4

Table 3.3: Growth parameters used for the eggplant experiment (adapted from FAO, 1998 [11]).

	Duration [days]	K_c [-]	K_{cb} [-]	p [-]	z_r [m]
Stage 1: Initial	20	0.7	0.15	0.4	0.05-0.1
Stage 2: Development	30	»	»	»	»
Stage 3: Mid-season	30	1.05	0.95	0.4	»
Stage 4: Late season	10	0.95	0.85	0.4	0.2-0.4

Table 3.4: Growth parameters used for the cabbage experiment (adapted from FAO, 1998 [11]).

Limitations

As stated before, the meteorological station was not located directly on the experimental site. Even though wind speed was corrected, other local variations are possible. Especially variations in relative humidity could cause some errors in the estimation of ET_0 and fluctuations in wind speed are still possible. Secondly, it has been shown that hot dry winds have a strong impact on K_c in Burkina Faso, especially during the dry fresh season [7]. This effect has been partially corrected by adapting the K_{cb} and K_c values for wind and humidity (see eq. 2.22). The crops at the experimental site are however small (50 m^2 and 200 m^2) which may lead to an "island effect", where the plants are more exposed to hot advective winds, leading to a higher rate of evapotranspiration. This also may lead to edge effects and may cause inhomogeneity within the plot, as the plants near the edges are exposed to drier winds.

3.1.7 Watermark 200SS specifications

The watermark sensor is a standard instrument that measures soil matrix potential based on the soil electrical resistance. It consists of electrodes embedded in a granular material that is in equilibrium with the pore soil water. It is a robust instrument that is relatively cheap, requires practically no maintenance if used correctly and calibration is easy by submerging the sensor before usage. It has a range of measurement from 0 to -200 kPa. Because of its high range of measurement the sensor is less accurate and sensitive than other more specific tensiometers, specially for high values of soil matrix potential from 0 to -20 kPa [49].

3.2 HYDRUS 2D simulation

HYDRUS 2D is a dedicated software that simulates water, heat and solute movements in 2 dimensional unsaturated soils. Among others, it allows to simulate soil evaporation, transpiration and root water uptake, as well as water stress. HYDRUS focuses only on water transports and does not include a crop growth module. Calculations relative to potential evapotranspiration, transpiration and evaporation, root and plant growth were done separately and then inserted in HYDRUS as input data.
HYDRUS 2D was used to accurately simulate the soil water dynamics and the water-soil-plant-atmosphere relationship. To build a realistic model different parameters had to be carefully calibrated. The main input parameters of the model are the followings:

1. Calibration of the soil texture using the equation of van Genuchten (eq. 2.15);
2. Defining the water stress reduction function and its parameters (eq. 2.20);
3. Rate of transpiration, evaporation and precipitation;
4. Determining the spatial root water uptake and its magnitude;
5. Irrigation duration and frequency must also be given, optionally a threshold can be used to trigger irrigation given a value of soil matrix potential and at certain depth (specific grid Node);
6. The geometry and the duration of the simulation must be defined.

3.2.1 Calibration of soil texture

Data collection

A sampling of the soil was performed in November 2012 (table 3.5). The soil texture corresponded to a sandy loam or a sandy clay loam texture. The soil was very compact and root penetration was limited.

Soil depth	% Sand	% Silt	% Clay	Comments
0 - 20 cm	54.9	25.49	19.61	relatively compact, very poor organic matter
20 -40 cm	47.06	31.37	21.57	very hard and compact, very rocky

Table 3.5: Sampling of the soil texture made in November 2012 at the research site.

In addition to this sampling, the soil matrix potential and soil moisture at a depth of 10 cm were recorded simultaneously during November 2014 to February 2015 for the cabbage experiment and between February and March for the eggplant crop.

Parametrization

In order to fit a soil model to the data, a soil water retention curve (SWRC) was drawn with the field data. The SWRC provides the relationship between the soil matrix potential and soil moisture given a soil texture and can be characterized by eq. (2.15) discussed in chapter 2.5.2. The unknown calibration parameters were θ_r, n and α. θ_s was measured by saturating the soil and was found to be around 0.32. The best combination of those 3 parameters was calculated by the minimizing the Root Mean Square Error (RMSE) between the measured and modeled water contents which corresponded to different values of soil matrix potential (eq. 3.1). Appendix A.3 shows the analysis of the parameters. Figure 3.4 shows the SWRC and the corresponding fitting.

$$RMSE = \sqrt{\frac{\sum_{i=1}^{N}(\hat{\theta}(h_i) - \theta(h_i))^2}{N}} \tag{3.1}$$

Where: $\hat{\theta}(h_i)$ is the predicted water content estimated by the model for a soil matrix potential value h_i; $\theta(h_i)$ is the measured water content corresponding to a soil matrix potential value h_i and N is the number of observations.

Two additional parameters were needed to calculate the readily available water (RAW): the water content at field capacity (θ_{fc}) and the water content at permanent wilting point (θ_{pwp}). They were determined using the calculated regression curve.

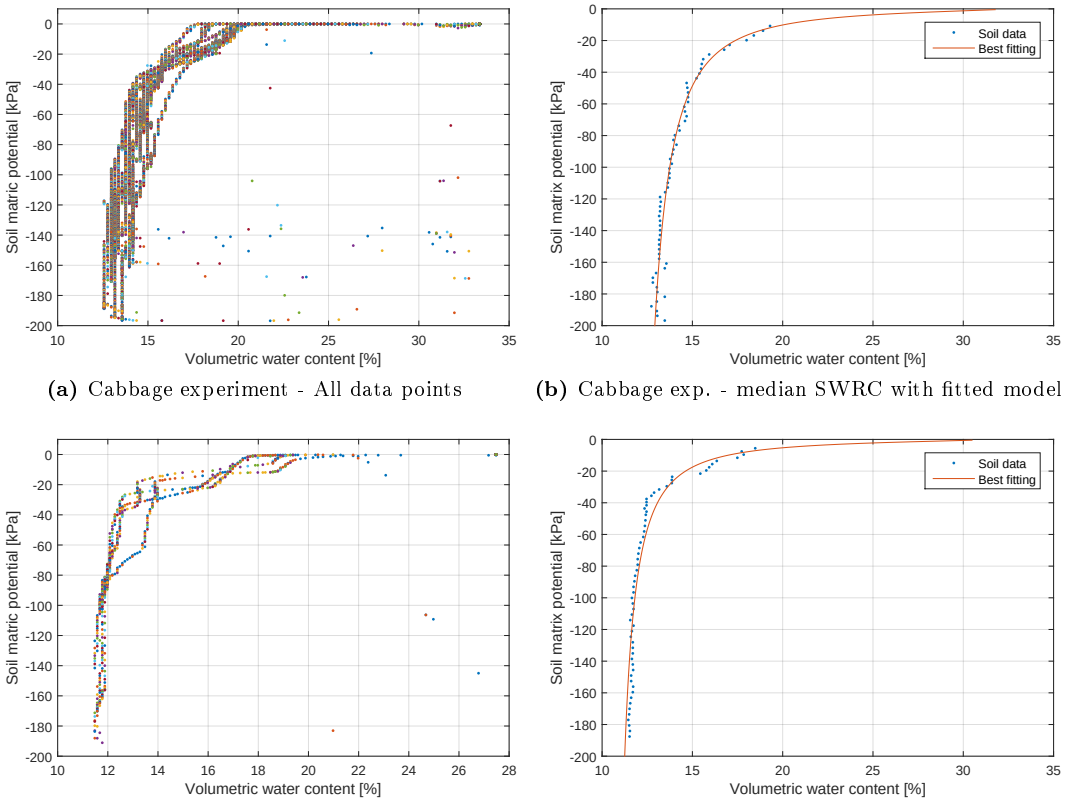

(a) Cabbage experiment - All data points **(b)** Cabbage exp. - median SWRC with fitted model

(c) Eggplant experiment - All data points **(d)** Eggplant exp. - median SWRC with fitted model

Figure 3.4: Comparison and fitting of the soil water retention curve for both crops.

To confirm this calibration, these values were compared with data from the literature. It appears that this calibration is similar to the one used to characterize a Sandy Clay Loam texture in RETC, which also corresponds to the soil sampling (table 3.5). Additionally, a similar parameterization was done by Mermoud et al., 2005 [50] in an experimental field about 17 km from our site and found relatively similar results.
The saturated hydraulic conductivity (K_s) was calibrated with our HYDRUS 2D simulation. A value of 15 cm/day was selected for the cabbage crop and 10 cm/day for the eggplant crop which is lower than the value used in RETC for such soil texture (30 cm/day) [29], since our soil is compact, but higher than the value used by Mermoud et al., 2005 [50] corresponding to 10.3 cm/day (0-30cm) and 6.48 cm/day (30-60cm).

The parameters used for the model are summarized in table 3.6.

	θ_r $[cm^3cm^{-3}]$	θ_{pwp} $[cm^3cm^{-3}]$	θ_{fc} $[cm^3cm^{-3}]$	θ_s $[cm^3cm^{-3}]$	α $[cm^{-1}]$	n [-]	K_s [cm/day]
Cabbage exp.	0.111	0.1169	0.1927	0.32	0.0463	1.5477	15
Eggplant exp.	0.102	0.1054	0.1612	0.315	0.0558	1.6328	10

Table 3.6: Calibrated soil model parameters for the cabbage (first row) and the eggplant (second row) experiments.

3.2.2 Geometry and Boundary Conditions

Our simulation domain consisted of a simple 2D vertical rectangular domain. It had a length of 1200 mm and a depth of 400 mm. The discretization of the domain consisted in a grid spacing of 2 to 20 mm for the z-coordinate (finer finite elements at the top) and 25 mm in the x-coordinate.

The simulation domain is illustrated in figure 3.5. The top boundary conditions consisted in an Atmospheric Boundary condition where the evaporation rate is applied. Every 0.5 meters, the top boundary conditions was defined as Variable Flux 1 to model the location of a dripper. The dripper flux was applied on a boundary length of 75 mm (3 nodes), which reduced the flux discharge rate on the boundary. The bottom boundary conditions were set to Free Drainage. This type of boundary condition was specially developed for freely draining unsaturated soil. A time step of 15 minutes was used for all input parameters. The time step used in HYDRUS for the simulations is 8 seconds but can be adapted by the model to face instability problems or to accelerate the calculation.

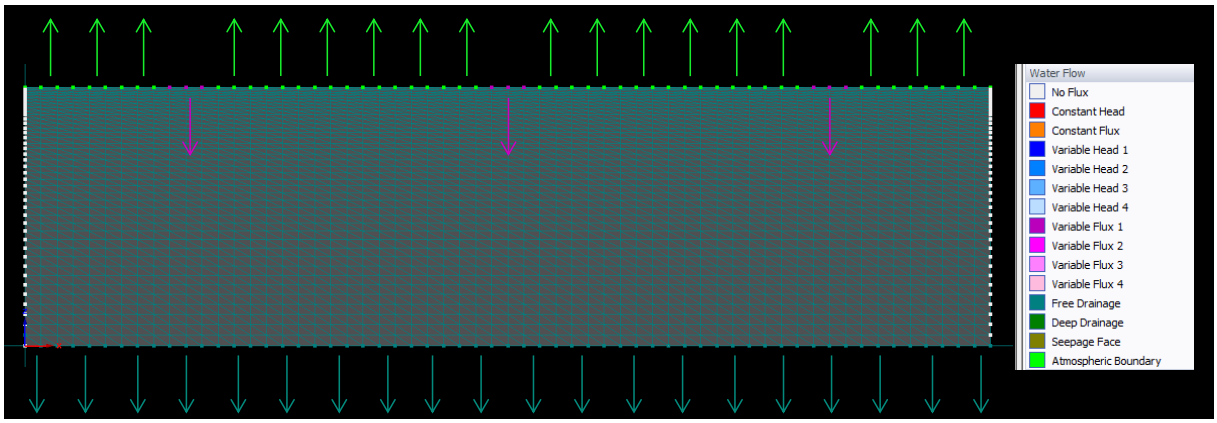

Figure 3.5: Illustration of the simulation domain in HYDRUS 2D. Arrows illustrate the different fluxes: Green - Atmospheric boundary conditions; Purple - Variable Flux 1 (for irrigation); Blue - Free drainage

Irrigation modeling

The characteristics of the irrigation (length and discharge rate) need to be implemented as an input of the time variable boundary conditions, under the "Variable Flux 1". Our drip system had the following characteristics for the cabbage experiment:

- Micro-tubes spacing: 0.4 [m] for the cabbage crop; 0.5 [m] for the eggplant crop
- Micro-tubes discharge rate: 2 [L/h]
- Number of micro-tube per treatment: 90 [-]
- Overall efficiency of water delivery: 0.9 [-]
- Width of wetted bulb: 0.3 to 0.4 [m]
- Length of Variable Flux 1 boundary for each dripper in HYDRUS: 75 [mm]

The micro-tube discharge rate represented a flux of 1600 mm/day which is much higher than the saturated hydraulic conductivity of our soil (150 mm/day), as a consequence a small water puddle formed on the soil surface in the field but this could not be modeled in HYDRUS 2D with Variable Flux. The

flux was therefore forced into the model which caused some stability problems in some cases. A solution was found by allowing postive pressure head at the soil surface which acts similarly to a water puddle on the surface. Moreover, the top 2 cm of soils were set with a higher hydraulic conductivity (300mm/day). We think that this is a correct assumption, as the soil was less dense near the surface and comparisons with measurements showed that the wetted diameter was correctly simulated.
One difficulty is that HYDRUS 2D assumes a homogeneous third dimension, meaning that the irrigation amount of a dripper is virtually applied on a length of one meter. In the case of drip irrigation where the soil in partially wetted, the volume of water is not applied along a whole meter, but only in a limited circular perimeter. For instance, we estimated the wetted diameter to about 0.3 to 0.4 meters depending on the irrigation depth. The width of the wetted bulb had a direct impact on the irrigation depth and was adapted carefully. Most of our simulations were done along a drip line, since interaction between the wetted bulbs may only occur in that direction.

3.2.3 Water uptake model

Among the different formulas used to describe water stress, the *S-Shaped Model* based on eq. (2.20) was selected . This model was the only one that modeled the reduction of water uptake similarly to the field measurements. In particular the Feddes model uses a linear water stress function, which could not be observed in our experiments. For the cabbage experiment we used a value of -80 kPa for the parameter h_{50} as suggested in HYDRUS [27] and which gave satisfying results in other simulations ([40],[51]) and a value of 5 for the calibration parameter p (instead of 3, as indicated in HYDRUS). For the eggplant crop the value of h_{50} selected was -50 kPa and a p value of 3.

Root water uptake compensation also needed to be defined. In HYDRUS, root water uptake can be compensated by increasing the water uptake in other parts of the root zone, which avoids transpiration reduction. A dimensionless water stress index ω_c is used so that the transpiration can be compensated until it falls below a fraction of the maximal transpiration. It has a value between 1 (no compensation) and 0 (full compensation). There is only few studies available on root water compensation and no clear values have been cited. It appears that root compensation reduces the importance of the spatial root distribution on plant transpiration [32] and that high compensation ($\omega_c < 0.5$) improves the simulation of water uptake from deep layers [52]. A value of 0.7 was finally selected for our simulation, allowing a mild compensation and relatively quick transpiration reduction.

The spatial distribution of root water uptake was a critical factor for the simulation. If the spatial root distribution exceeded the wetted zone from the dripper, a strong water stress would be induced in those zones, reducing transpiration. This phenomena could be partially compensated by the compensation function and the water stress index ω_c. It is however likely that little roots developed in those zones that remained very dry, so that the root distribution should match the wetted bulb. In our simulations, we rely on the root distribution measurements done in the field and we adapted this distribution if the modeled wetted bulb didn't match our observations of the root distribution.

4 Results of field experiments

4.1 Cabbage

4.1.1 Evolution of soil matrix potential

The cabbage seedlings were transplanted on October 29, 2014. The irrigation schedule detailed in table 3.1 could not be followed from the start. Instead, the same schedule was followed for both experiments until November 23, consisting of a daily irrigation of 100 liters, which corresponded to 100% of ET_c. After this date, that is at the end of the initial growth stage, the schedule from table 3.1 was used. The actual irrigation schedule followed is summarized in table 4.1.

	Treatment 1 (100% ET_c)		**Treatment 2 (66% ET_c)**	
	Frequency [1/day]	Depth [L]	Frequency [1/day]	Depth [L]
October 29 - November 22	1	100	1	100
November 23 - December 9	1/1.5	100	1/2.5	100
December 9 - February 5	1	100	1/3	200

Table 4.1: Actual irrigation schedule applied to the experiments on cabbage.

The evolution of the soil matrix potential is shown in the next page (figure 4.1) together with the calculated evapotranspiration fluxes and the Kernel density estimation of the soil matrix potential. The Kernel density estimates the probability density function of the soil matrix potential over time, that is the probability that the soil matrix potential takes a certain value. It is related to a smoothed histogram with its area normalized to 1. In order to calculate the probability density functions on a stable data set, the densities were estimated for each growth stage, which corresponded to the different irrigation schedules cited in table 4.1. Those probabilities must be considered with caution since the datasets were probably not long enough to consider an ergodic process.

From November 23 to December 9, it seems that the irrigation depth was not sufficient which led to a decrease in the soil matrix potential, which was accentuated by the increasing transpiration rate. During the mid-season stage, about after December 20, the behavior of the soil matrix potential was relatively steady for both experiments. For treatment 1, the soil matrix potential remained high (above -50 kPa) in the upper 5 cm of soils while it stabilized around -100 kPa deeper. Concerning treatment 2, the higher irrigation depth recharged the soil deeper illustrating the relatively similar soil matrix potential behavior at both 5 and 10 cm depth. The mean soil matrix potential values are represented in table 4.2.

	Soil matrix potential at 5 cm		**Soil matrix potential at 10 cm**	
	Mean [kPa]	Standard deviation [kPa]	Mean [kPa]	Standard deviation [kPa]
Treatment 1	-39.5	37.8	-62.4	38.9
Treatment 2	-41.2	47.4	-54.9	51.8

Table 4.2: Mean soil matrix potential over time, starting on November 23 (stage 2 and 3).

It appears that the mean soil matrix potential at 5 cm depth is relatively similar for both experiments and at 10 cm depth the potential is higher for treatment 2 than 1. The standard deviations are however higher for experiment 2, suggesting that lower values are reached. For treatment 1, the density plot below (figure 4.1) shows clearly that at 5 cm depth soil matrix potential was kept mostly above -50 kPa, which may have compensated the lower potential at 10 cm depth, whereas in treatment 2, it happened that both potential were below -100 kPa at the same time.

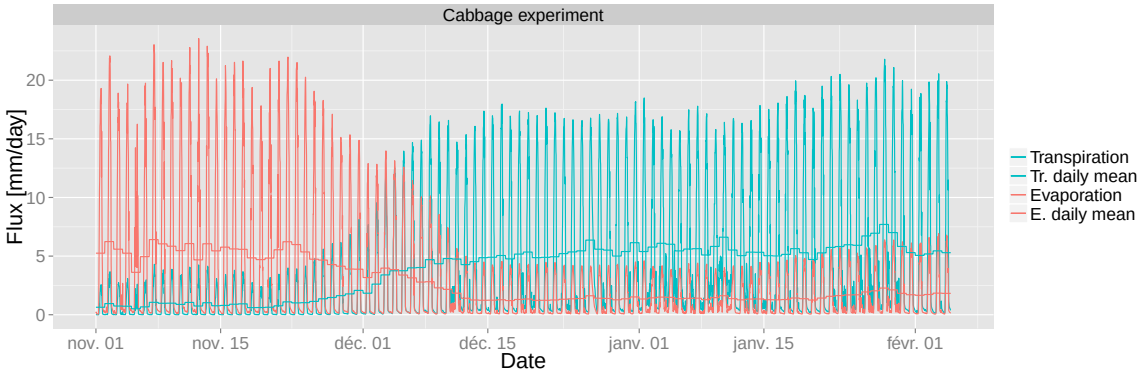

(a) Calculated evapotranspiration fluxes.

(b) Monitored soil matrix potential for both treatments.

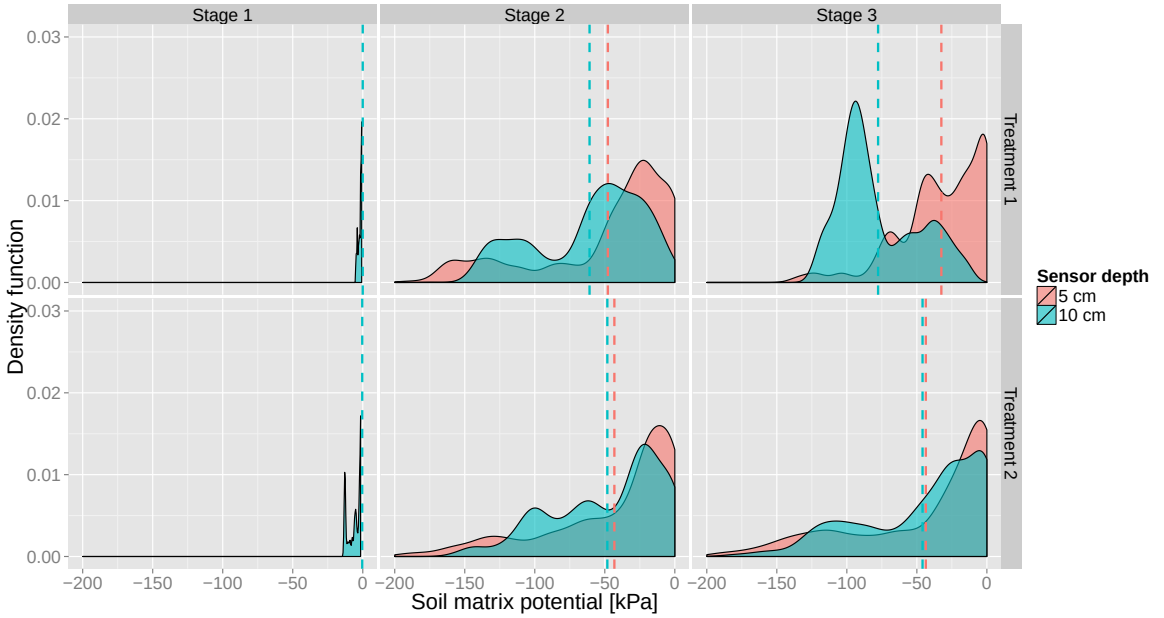

(c) Kernel probability densitiy function for each growth stage (see text for precision and table 3.1 for length of stages).

Figure 4.1: Comparison of evapotranspiration, soil matrix potential and corresponding Kernel density estimation for the whole cabbage experiment.

4.1.2 Plant growth

Due to some political instabilities in the country, the measurements of cabbage growth could only start about 50 days after transplanting at the start of the mid-season period, which is characterized by the beginning of the head formation.
Starting at the beginning of this stage, a pest gradually infested both cabbage experiments indiscriminately. The aerial pest colonized the leaves which were then eaten by larvae. A chemical pesticide ($lambda - cyhalothrin 2.5\% EC$) was vaporized on the plants which resulted in the death of the pest, but recolonization of the same pest occurred about a week later. The pest caused considerable damage on both crops, limiting or destroying the heads. Since the attack was not specific to one experiment, the comparison of final harvests seems still possible, though the yield will be below the maximal yield for this species.

Figure 4.2 shows the evolution of the growth parameters measured.

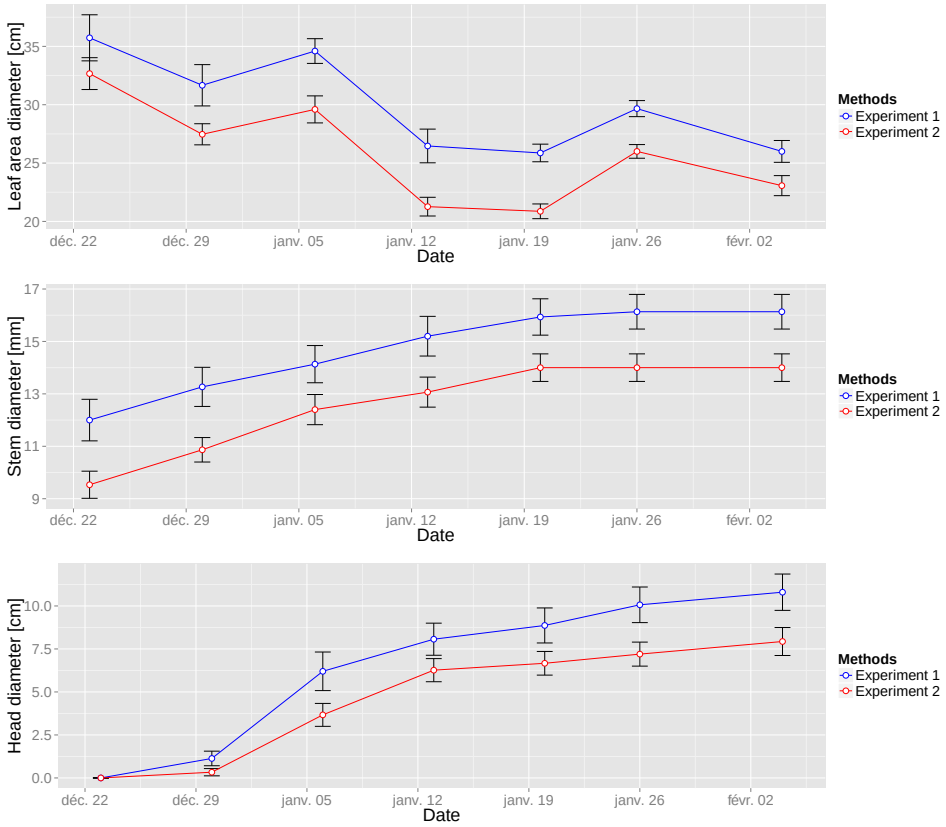

Figure 4.2: Evolution of cabbage growth, starting at the end of the development stage. The error bar represents one standard deviation.

The diameter of the leaf area appears to decrease with time. This is due to the fact that the local producer in charge of the site weekly removed the outer leaves of the cabbages to promote the formation of the heads. As a consequence, the leaf area does not appear as a good indicator of plant growth. It can only be noted that experiment 1 obtained a larger canopy diameter at the end of the crop development stage, indicating a certain water stress for experiment 2 during the previous stage. The same conclusion can be made for the stem diameter.

The formation of the heads was faster for experiment 1 and the head volume was higher. There are two possible explanations for this limited head growth. It may be due to the limited canopy expansion during the crop development stage or it is directly linked to the low soil matrix potential values during the head formation stage. It is not clear at that point which explanation is more likely.
At the end of the season, the cabbage heads were harvested. Table 4.3 shows the total harvests for both experiments and the corresponding total irrigation water used. The results are valid for a surface of 25 m^2 and corresponded to about 90 cabbage initially, though about a third did not produce marketable heads due to the pest. We introduce a Water Use Efficiency index (WUE) which is simply the ratio of harvest divided by the amount of water used. A higher ratio means a more efficient irrigation management.

	Harvest [kg]	Water consumption [m^3]	Water use efficiency [kg m^{-3}]
Treatment 1	67,8	10.92	6.21
Treatment 2	45,6	8.68	5.25

Table 4.3: Marketable harvests for the cabbage experiment.

Treatment 1 resulted in a higher yield, with bigger cabbage heads and the WUE was also higher for the first treatment. It can be concluded that experiment 2, was subject to water stress during its growth and resulted to lower yields. Moreover the water saved in treatment 2 did not compensate for the yield losses, indicating that irrigation management should aim at maximizing yields rather than trying to save water.

4.1.3 Sap flow analysis

8 sap flow meters were placed in the cabbage crop, four in each experiment, at the beginning of January, around 60 days after transplanting. The sap flow sensors within a treatment were given the name "a", "b", "c" or "d" to distinguish between them, but they were submitted to the same irrigation schedule. For each day, we calculated the daytime mean sap flow value and the corresponding daytime mean for ET_cb and the soil matrix potential. Daytime was considered from 8 a.m. to 18 p.m. The correlation between daytime means was then calculated. We use daily means to avoid the diurnal fluctuations in ET which would lead to a strong correlation with the sap flow so that we can focus on the daily trends. We compared only the daytime signals to avoid night fluctuations as well.

Due to the removal of external leaves about every 10 days, the interpretation of the sap flow measurements is difficult. Indeed, the removal of the leaves resulted in a sharp drop in the sap flow signal, which was then recovered in the next days. The different cabbages possessed a stem diameters at sap flow height of 18 to 27 mm. The pith had a radius of about 5 to 8 mm and the xylem a width of 2 to 5 mm.

Figure 4.3 shows the evolution of the signal for a specific period for treatment 2, which showed good correlation (0.90) between the mean daily daytime sap flow signal and the soil matrix potential. The signal of the sap flow was transformed in a transpiration rate as described in chapter 3.1.5. A decrease in the signal can be observed after an irrigation event, especially when the potential falls below -50 kPa. This daily behavior could however not be observed clearly for treatment 1, where the soil matrix potential remained higher and more constant.

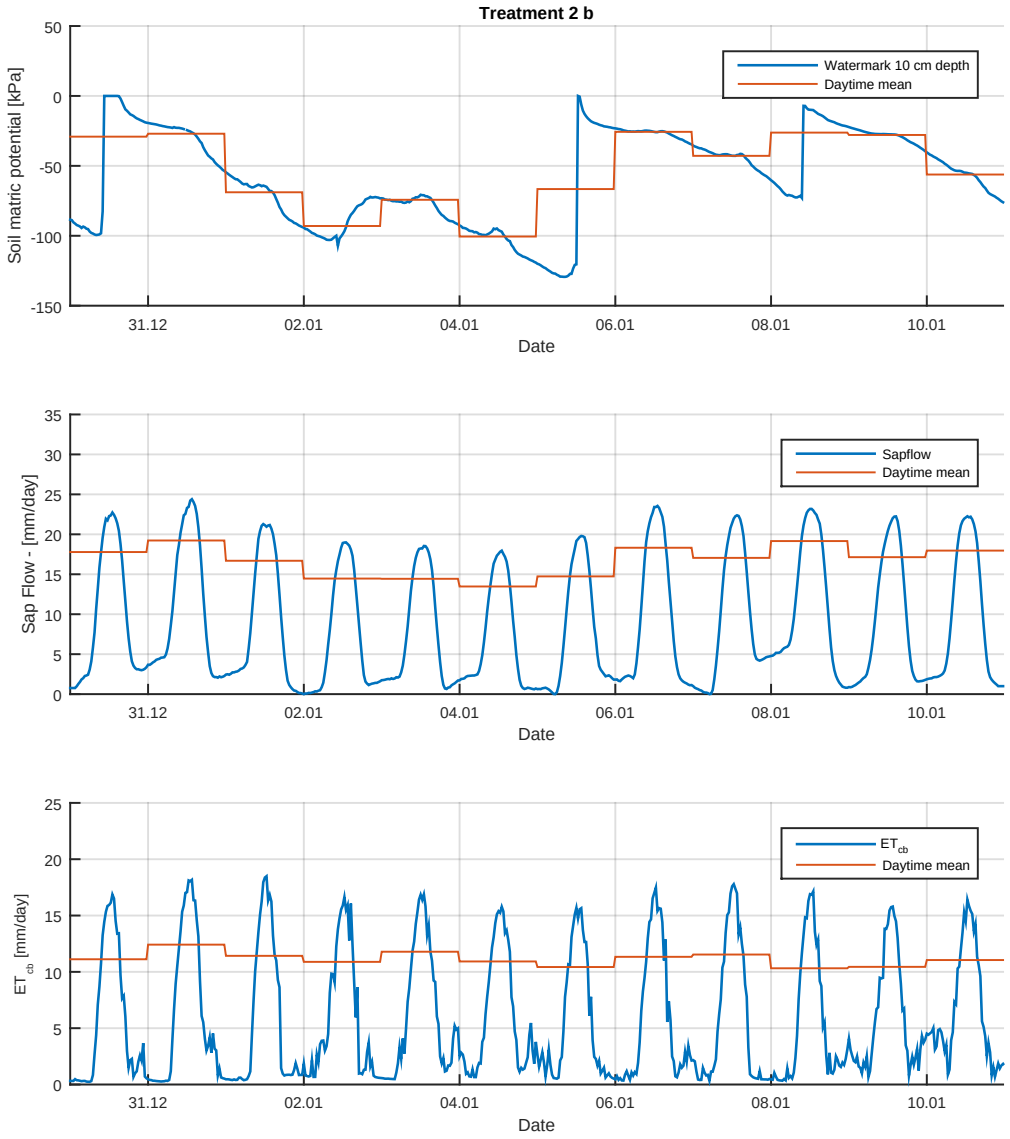

Figure 4.3: Comparison between the soil matrix potential and the transformed sap flow rate taken on cabbage "b" in treatment 2, at the beginning of the mid-season. The corresponding calculated transpiration rate (ET_{cb}) is also shown. The blue curves represent the 30 minutes time average for the sap flow signal and 15 minutes average for the both other signals. The red curves represent the mean daytime daily averages.

Some additional graphs are shown in figure 4.4 and also in appendix A.4, which show similar analysis, but for the late period, just before harvesting when leaves were no longer removed, except for treatment 1a, where leaves were removed on January 31. A relationship can also be observed on a longer time scale in all experiments and the corresponding correlations are shown in table 4.4. The correlations between the daily mean values of the sap flow velocity and the meteorological parameters were also tested but weren't very significant as they remained below 0.5.

Exp 1a	Exp 1c	Exp 2b	Exp 2c
0.74	0.73	0.83	0.41

Table 4.4: Correlation between the mean daily daytime sap flow and the corresponding mean daytime soil matrix potential.

The reduction of sap flow rate (and therefore transpiration) in figure 4.4 is particularly visible in treatments 1c and 2b where a strong reduction of the signal is observed below -100 kPa. The signal also reacted to the small increase in soil matrix potential that occurred around February 10. For treatments 1a and 2c shown in figure A.5 in appendix A.4, the signal reacted more slowly with a real decrease in sap flow signal when the potential was below -200 kPa.

These results seem to indicate that water stress occurs below about -50 kPa and is more severe below -100 kPa during the mid-season stage. This limit of water stress could explain the decrease in yield observed in experiment 2, where the soil matrix potential dropped below -100 kPa every third day, before an irrigation event is triggered. This value can however not be evaluated with more precision. From this analysis it is also difficult to conclude if the root distribution for treatment 2 adapted to the lower irrigation frequency by increasing deeper root biomass in order to improve its resistance to soil moisture depletion.

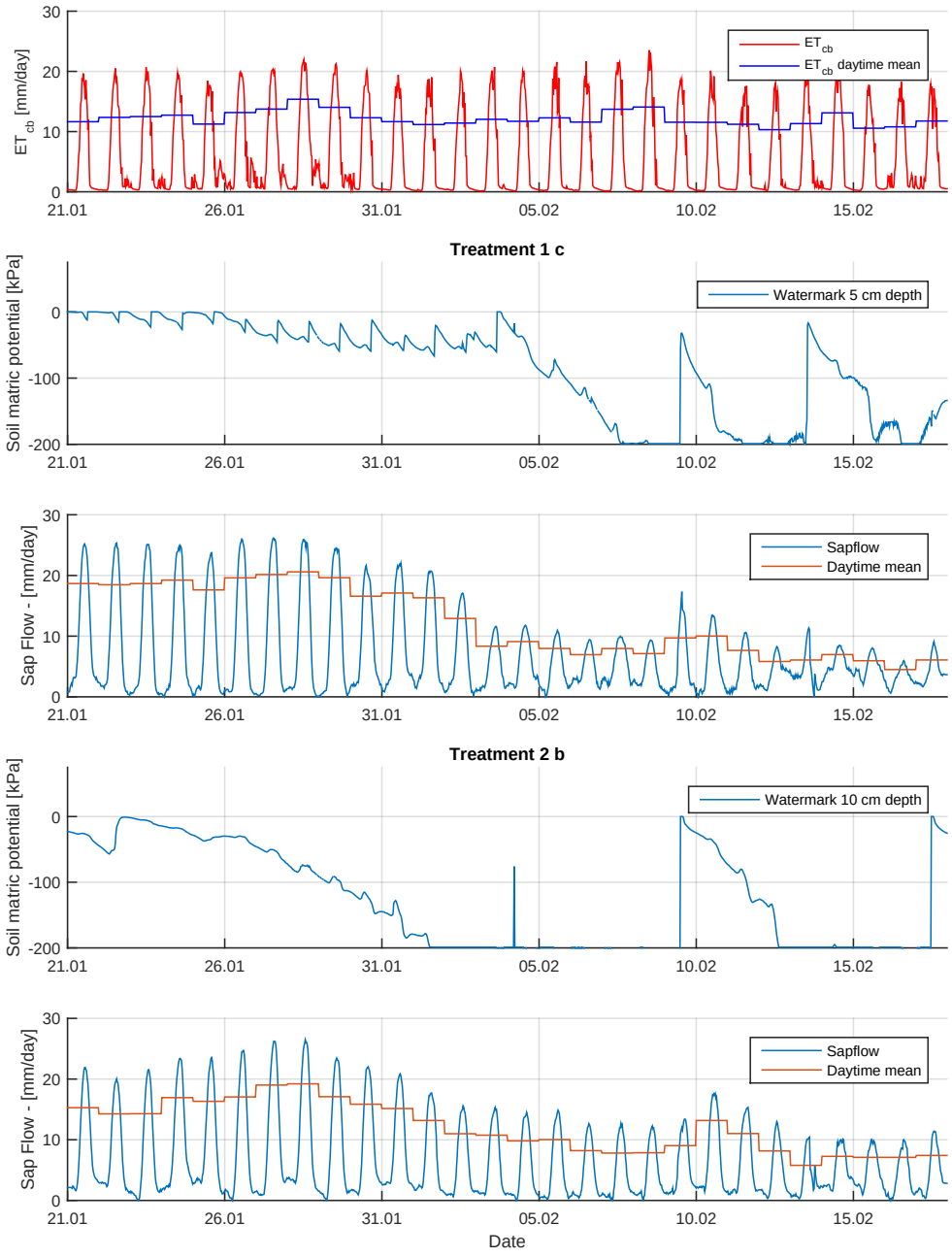

Figure 4.4: Comparison between the soil matrix potential, the transformed sap flow rate and the corresponding transpiration rate (ET_{cb}), for both treatments during the late season of the cabbage experiment. The blue sap flow curves represent the 30 minutes average, the blue Watermark curve the 15 minutes average and the red curves are the daytime means. For transpiration, the red curve represents the 15 minutes average and the blue curve the daytime average.

4.1.4 Root growth

At transplantation the seedling roots had a length of about 6 to 8 cm and about 1 to 2 cm horizontal radius. The first sampling of the root distribution could only occur during the mid-season due to political instabilities and government transition in the country which prevented field work so that the analysis had to be postponed. Around 60 days after transplanting, on December 27 the first root extraction could take place and the image analysis and density profiles are shown in figure 4.5. At that stage, the roots were already well developed. The roots reached a depth of about 20 to 25 cm. For treatment 1, a wide and dense network of secondary roots was observed in the first 5 to 10 cm, with only fewer roots penetrating deeper in the soil and a horizontal radial distance from the stem of about 20 to 30 cm. Concerning treatment 2, some main roots reached deeper in the soil to a depth of about 30 cm and more secondary roots could be observed below 10 cm. Nevertheless, most of the roots were contained in the upper 15 cm. The radial distance of the roots was similar to experiment 1. The main difference between both analysis is that roots were more concentrated near the surface for treatment 1 which can be explained by the lower irrigation depth applied more regularly that replenished the soil more superficially. Indeed, already at 10 cm, the measurement of the soil matrix potential remained steady around -100 kPa for a long part of the mid-season, indicating that the irrigation front did not reach much deeper (figure 4.1).

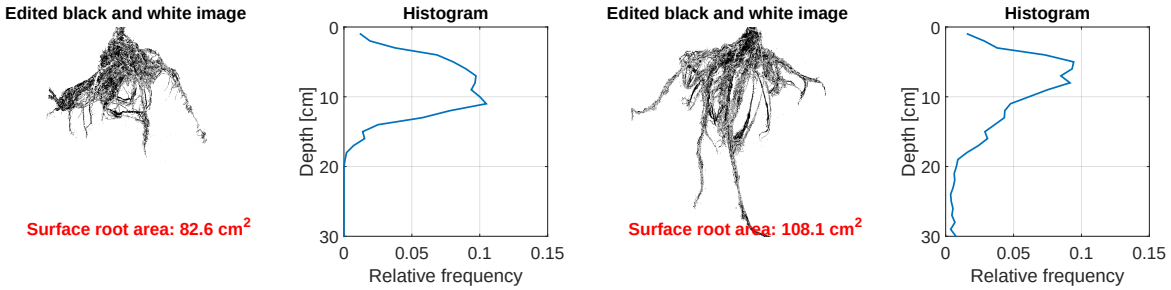

(a) Experiment 1 (optimal-low depth). **(b)** Experiment 2 (stress-high depth).

Figure 4.5: Evolution of the root distribution of cabbage - day 60 after transplanting.

A second extraction of the roots took place 90 days after transplanting, on January 26. There were relatively little differences in comparison with the previous analysis. As shown in figure 4.6, the roots developed a bit deeper for the experiment 1, with some roots reaching 25 cm. The root system was still mainly contained in the first 10 to 15 cm, though a bit less dense than before. Experiment 2 did not show much difference, except a few more deeper roots.

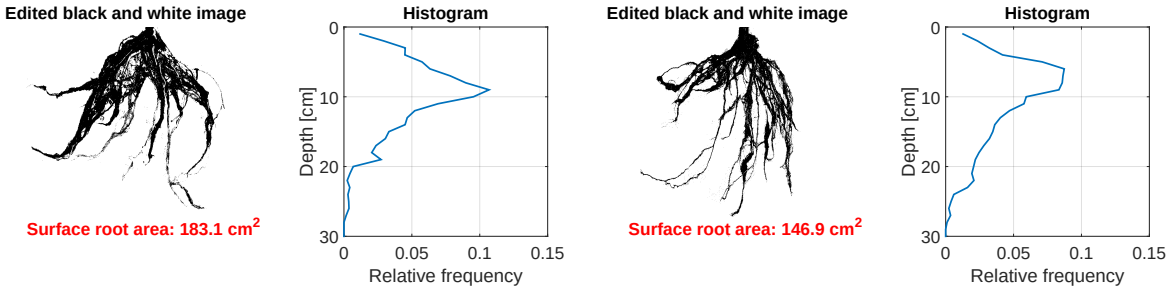

(a) Experiment 1 (optimal-low depth). **(b)** Experiment 2 (stress-high depth).

Figure 4.6: Evolution of the root distribution of cabbage - day 90 after transplanting.

4.2 Eggplant

4.2.1 Evolution of soil matrix potential

The experiment started on December 5, 2014, when the eggplants seedlings were transplanted. Due to political instabilities in the country, measurements and instruments could only be installed on December 14. The 7 first days the irrigation schedule was the same for all experiments consisting in irrigating twice a day with a depth of 100 L per experiment. The next 10 days (until December 22) the frequency was reduced to once a day. The proposed schedule detailed in table 3.2 was then followed. The actual schedule is summarized in table 4.5.

	Treatment 1 (optimal - low depth)		**Treatment 2 (stress - low depth)**	
	Frequency [1/day]	Depth [L]	Frequency [1/day]	Depth [L]
December 5 - December 12	2	100	2	100
December 13 - December 22	1	100	2	100
December 23 - February 3	2	100	1/1.5	100
February 4 - March 15	2	100	1/1.25	100
March 16 - March 25	2	100	1/2	100

	Treatment 3 (optimal - high depth)		**Treatment 4 (stress - high depth)**	
	Frequency [1/day]	Depth [L]	Frequency [1/day]	Depth [L]
December 5 - December 12	2	100	2	100
December 13 - December 22	1	200	2	100
December 23 - February 3	1/2	200	1/3	200
February 4 - March 15	1/3	400	1/4	400
March 16 - March 25	1/4	400	1/5	400

Table 4.5: Actual irrigation schedule applied for the experiments on eggplants.

The evolution of the soil matrix potential is shown in figure (4.7). The behavior is not very regular with time. This is due to different factors. First the evapotranspiration rate varies from day to day. Then the drip system does not assure a completely homogeneous water delivery, so that the irrigation depth may vary to some level between each irrigation events. It may have happened that the micro-tubes where not exactly in front of the eggplants stem, due to some manipulations on the sub-lines and the micro-tubes may also have been clogged, though regular checks have been done.

Experiment 1 presents a quite flat and constant behavior, the soil was kept very wet as irrigation occurred twice a day, so that the sensors remain close to 0 kPa. In particular the sensor at 15 cm depth was almost always saturated, indicating that the soil was recharged in depth and that leakages probably occurred. It should be reminded that the watermark sensors are not very reactive and precise in the 0 to -10 kPa range so that small daily fluctuations may not have been recorded.

Concerning treatment 2, the sensors that were placed near the stem horizontally (5 cm) kept relatively high soil matrix values. In contrast the far sensors placed at 12 cm from the stem laterally and at depths of 10 and 15 cm, were completely disconnected from the wetted bulb, as their potential decreased quickly below -200 kPa. Only two irrigation events recharged the soil to these depths, probably because the micro-tube was displaced closer to their position. The behavior of the sensors indicate that the wetted bulb had a narrow width and only reached a depth of 15 cm right below the stem. The root system is therefore expected to have been limited to a smaller soil volume. Due to the low irrigation amounts applied to this treatment and the restricted root system, a more rapid decrease in matrix potential was expected, specially for the sensors at 5 cm, which was not observed, probably due to the lower sensor sensitivity and precision above -20 kPa.

Treatment 3, received a higher irrigation depth but at lower frequency. As a result the potential decreased more than in the previous experiments, but the soil was more recharged as the far sensor at 15 cm depth usually reacted to the irrigation event, in contrast to treatment 2. When both sensors at 5 and 15 cm reacted to the irrigation event, the decrease was more abrupt for the shallow sensor illustrating a stronger water uptake at this depth. It appears also that the water uptake near the stem was stronger than far from the stem as the matrix potential reached lower values for the near sensor than the far sensor at 5 cm.

Finally, treatment 4 has a relatively similar behavior to treatment 3, with a soil matrix potential reaching lower values due to the lower irrigation frequency. It should be noted that for the experiment 4, near

sensors, the plant had a very slow initial development and had a canopy and height about half of the maximum at the beginning of the mid-season. Due to lower leaf area, transpiration was reduced which led to lower root water uptake. As a result, the soil matrix potential decreased slower compared to the other experiments.
In general the soil was recharged below 15 cm, though it can be noted that the far sensor at 15 cm did not always reached 0 after an irrigation event, indicating that the wetted front probably did not reach much deeper.

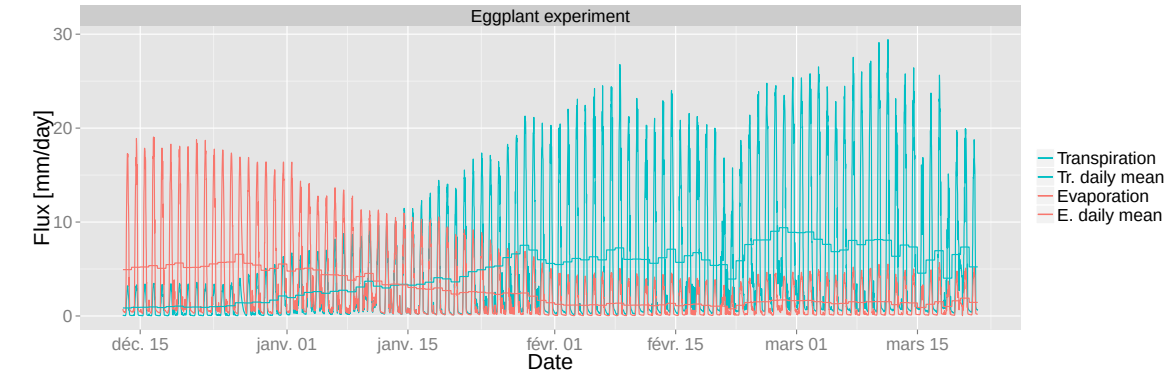

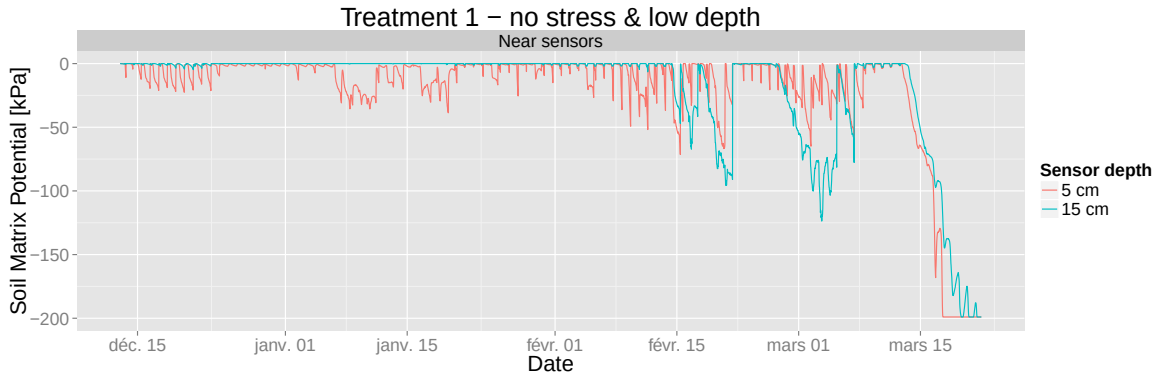

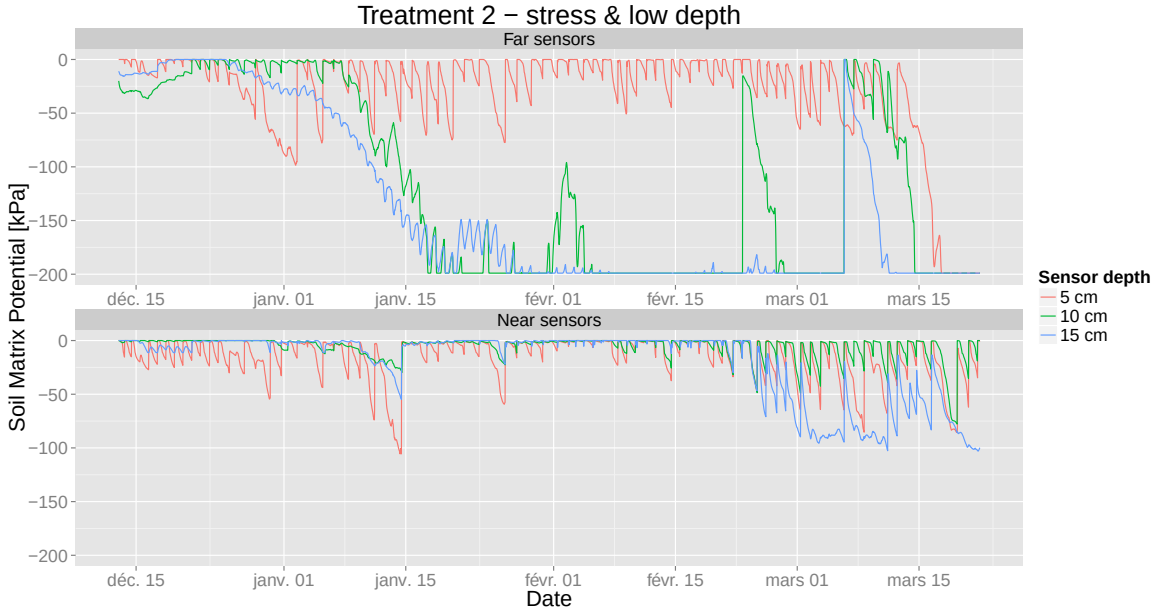

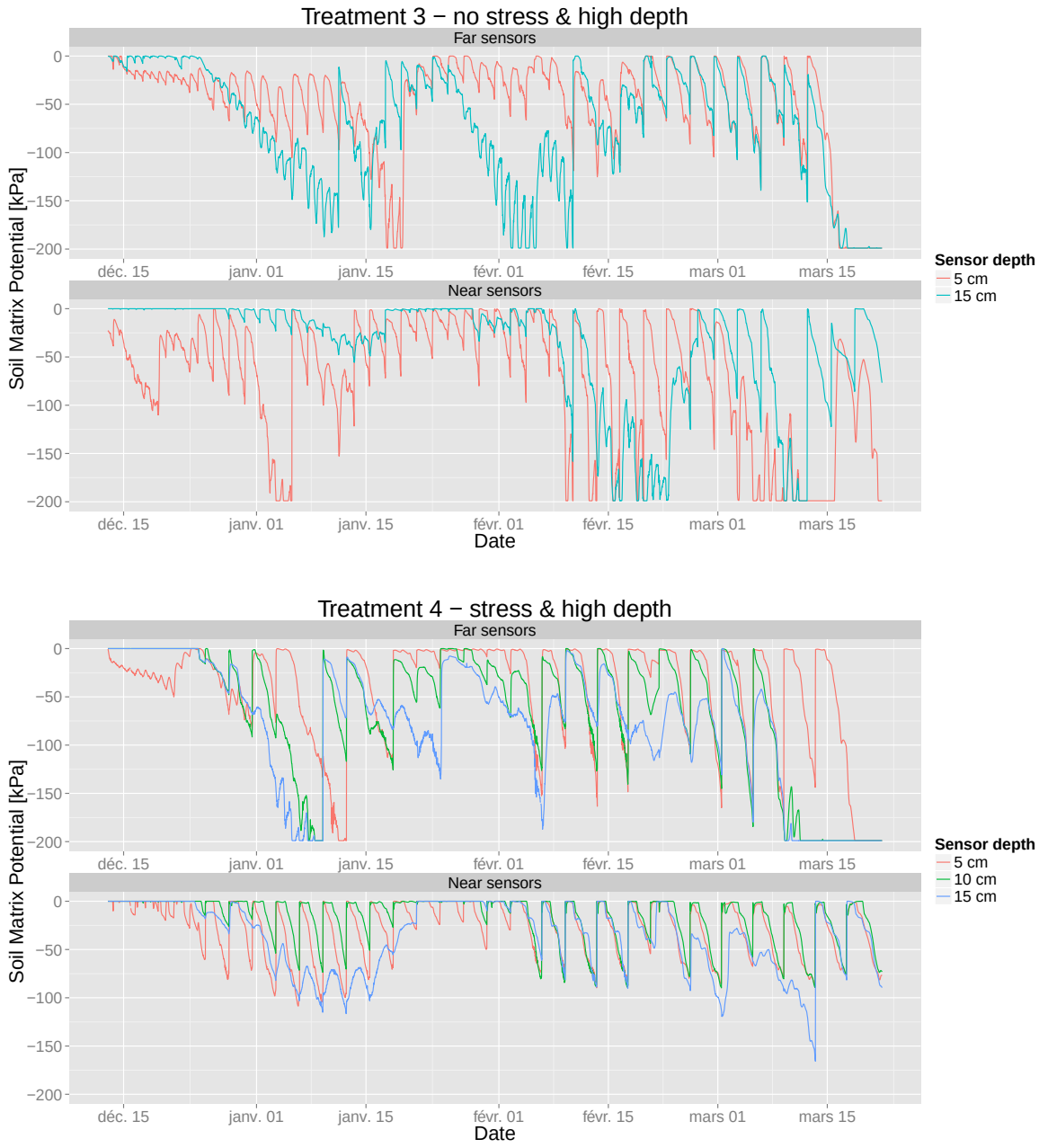

Figure 4.7: Comparison of the soil matrix potential evolution at different depths for the four treatments and for both locations (sensors near the micro-tube (5 cm) and sensors far from the micro-tube (12 cm), during the whole eggplant experiment.

Concerning water stress, the table 4.6, summarizes the mean soil potential for each growth stage and for each experiments for the far sensors, except for treatment 1 which possessed only near sensors. The drought period after March 15 was not taken into account.

	Mean soil matrix potential at 5 cm [kPa]			**Mean soil matrix potential at 15 cm [kPa]**		
	Stage 1	Stage 2	Stage 3	Stage 1	Stage 2	Stage 3
Treatment 1 (near)	-5.8	-6.1	-13.3	-0.5	-0.04	-20.7
Treatment 2 (far)	-4.1	-24.1	-19.3	-5.2	-113.8	-185.4
Treatment 3 (far)	-17.9	-46.4	-37.2	-2.1	-75.5	-64.0
Treatment 4 (far)	-20.4	-36.9	-36.8	-0.64	-70.7	-88.3

Table 4.6: Mean soil matrix potential for each development stage. Stage 1 from December 5 to December 24; Stage 2 from December 25 to February 3; Stage 3 from February 4 to March 15.

Figure 4.8 shows the Kernel density distribution of the soil matrix potential with time for each growth stage in the same way as discussed in chapter 4.1.1. The vertical dashed lines correspond to the mean values of table 4.6. This figure will be compared with the plant growth and sap flow results in the next chapters.

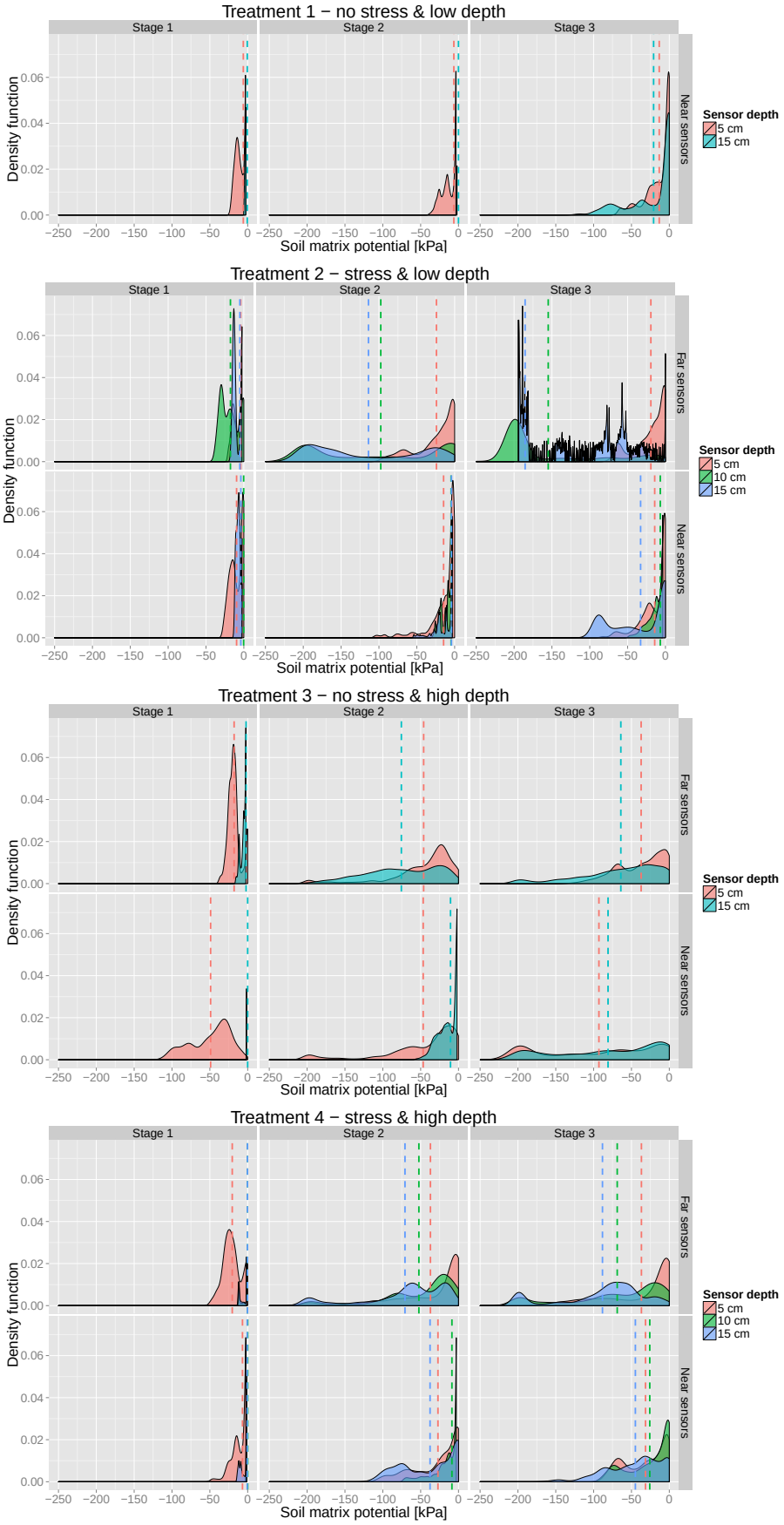

Figure 4.8: Kernel probability density estimation of the soil matrix potential over time for the four treatments and for each growth stage at different depths. The dashed lines correspond to the mean value.

4.2.2 Plant growth

Different measures were taken during the whole growth period for the four eggplant experiments. The results are shown in figure 4.9. The four first measures are indicators of the biomass development of the plants and were all correlated with each other. The last two graphs (number of flowers and cumulative harvests), are more directly linked to the productivity of the experiments.

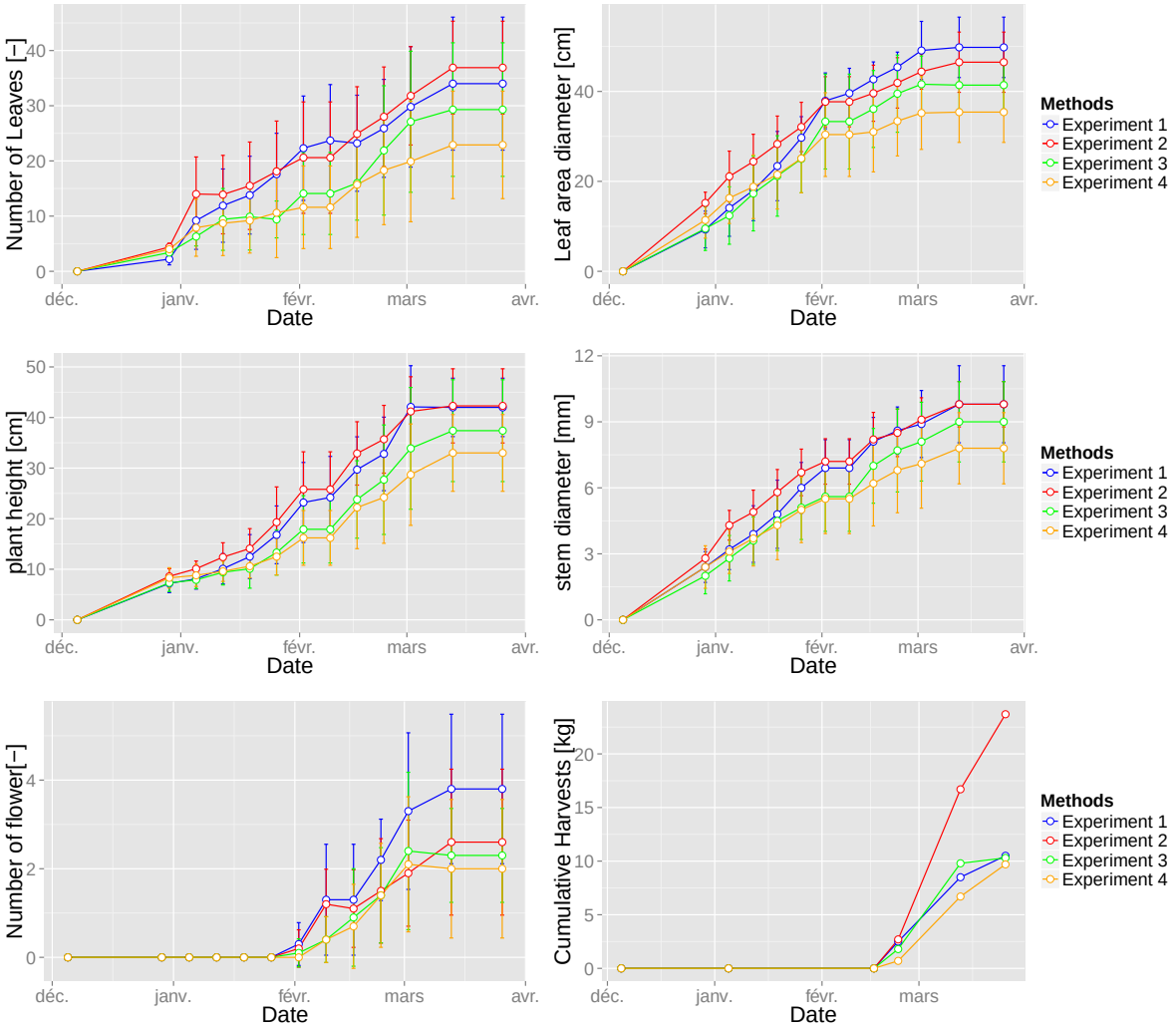

Figure 4.9: Evolution of eggplant growth parameters for the four treatments. The error bar correspond to one standard deviation.

Relatively rapidly after the beginning of the crop development stage, two groups can be dissociated, as experiments 1 and 2 showed higher growth parameters than experiment 3 and 4. The separation between those two groups occurred mainly during January which corresponded to the crop development growth stage. If the leaf area diameters did not differ greatly, the combined effect of the number of leaves and plant height reflects the lower leaf area index for both experiments 3 and 4. At the begging of February, this separation is most visible. Experiment 3, then catches up gradually but not completely with experiments 1 and 2, while experiment 4 remained lower. Treatment 1 and 2 had a good homogeneity in the plant development, with most plants having similar heights and leaf area index. More differences were observed in treatment 3 and 4, where some plants presented little growth and some were comparable with treatment 1 and 2. It can finally be noted that experiment 2, which had growth parameters below treatment 1 at the start of January caught up with experiment 1 at the beginning of February.

Concerning productivity and harvests, a few comments must be addressed first. Starting about at the beginning of the mid-season stage, at the beginning of the flowering, the crop was infected by a disease. The symptoms were yellowing and withering of the leaves starting from the stem to the top, followed by fruits decay and complete death of the plant occurred after about 10 to 15 days. The disease could not be identified precisely but it is strongly believe that the disease came from the roots. Extracted roots were rotten and a few small (1 mm) worms were observed, which may have wounded the roots and opened the

way to a parasite. A vascular disease may be the cause. The disease started only during fruit formation and hit firstly the treatment 1 followed by treatment 3 on a few different locations in the crop. From those locations the disease spread along the irrigation lines and infected the neighboring plants. The disease was specially virulent in experiment 1, where about 50% of the plants died at the end of February and only 20% were left in middle of March. Experiment 3 was also strongly affected with only 45% of the plants left alive at end of the experiment. Treatment 2 and 4 were also affected randomly but the disease did not spread and only about 10 plants died. It seems that the irrigation schedule was responsible for the spread of the disease, in particular it is likely that experiment 1 and 3, where irrigation was the highest, created wider wetted bulb in the soil, that connected to each other along the drip lines which allowed the spread of the disease. In experiment 2 and 4, the wetted zones were probably more disconnected which stopped the disease. Letting the soil dry during a few days did not reduce the disease strength as experiment 3 was strongly affected, even though the irrigation frequency was once every three days.

Regardless of the disease, the number of flowers per plant was the highest for experiment 1, and many plants grew 2 fruits at the same time. The production of treatment 2 was very homogeneous, but usually only one fruit grew at a time. Treatment 3 was less homogeneous, with some very productive plants and some that did not produce anything. Treatment 4 was similar to treatment 3, but less very productive plants were observed.
The most productive experiment was experiment 2, with a harvest 2 times larger than the other experiments. Since the disease infected strongly experiment 1 and 3, the productivity per living plants have been calculated and is shown in figure 4.10, since it corresponds more directly to the intensity of water stress.

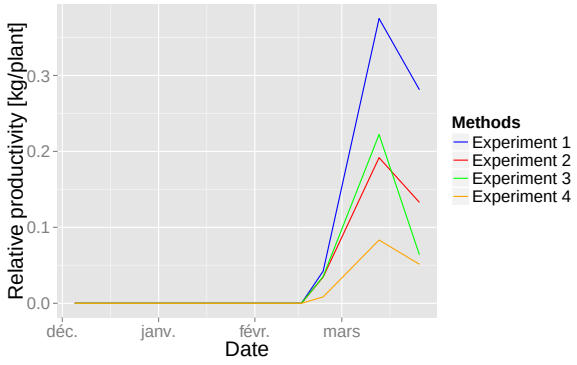

Figure 4.10: Relative productivity of the different treatments.

The production for all experiments was maximal at the beginning of March when most of the plants produced fruits. It appears that experiment 1 was the most productive experiment, followed by experiment 2 and 3 and experiment 4 was the less productive experiment. We can conclude that experiment 1 did not suffer any water stress and the productivity was near to maximal.
Treatment 2, which obtained a high biomass at the end of the growth stage, suffered from water stress during the flowering, which reduced its productivity. The soil matrix potential was kept above -50 kPa in the upper 5 cm, but was very low deeper (see table 4.6). The restricted root system may also have reduced the yield due to a limited water and nutrient reserve.
The plant growth was clearly limited during the crop development stage in experiment 3, which resulted in smaller plants. Water stress seems to have limited the yields indirectly due to this reduced development before flowering. Water stress during the flowering period in February seems to have been less significant, since some plants were still very productive in this experiment.
Finally, treatment 4 seems to have suffered from a water stress both during the plant growth and during mid-season, resulting in the lowest yields.

Table 4.7 summarizes the key results by comparing the yields with the quantity of water used.

	Harvest	**Relative productivity**	**Water consumption**	**Water use efficiency**	**Relative WUE**
	[kg]	[kg/plant]	[m^3]	[kg m^{-3}]	[g/liters/plant]
Treatment 1	10.5	0.375	22.5	0.47	1.50
Treatment 2	23.7	0.192	10.2	2.32	1.69
Treatment 3	10.3	0.222	14.2	0.72	1.41
Treatment 4	9.7	0.083	11.1	0.87	0.67

Table 4.7: Marketable harvests for the cabbage experiment.

A different analysis can be made, whether the disease is considered or not. With the effect of the disease, treatment 2 is by far the most productive experiment with a water use efficiency (WUE) almost 3 times higher than the other experiments. It is also interesting to note that it was the treatment that consumed the least water. Irrigating below 100% of ET_c seems to be therefore a solution to the spread of the disease. Another possibility to consider would be to use higher spacings between the micro-tubes, isolating each wetted bulb.

If the disease problem can be avoided, and if we focus on individual productive plants, it appears that treatment 2 has the highest relative WUE but less significantly. A higher WUE seems possible since treatment 2 did suffer from stress and productivity was higher in treatment 1. It appears that treatment 1 has a low WUE mainly because of over-irrigation and using an irrigation frequency between treatment 1 and 2 during the mid-season, would result to the highest yields with a lower water consumption. The schedule of experiment 3 could also be used for the mid-season.

4.2.3 Sap flow analysis

The sap flow velocity in 8 eggplants, two ("a" and "b" to distinguish them) for each experiment, was recorded during fruit formation, when the stem diameter was large enough to use the instruments. Based on measurements of the eggplant stem section, the stem diameters at sap flow height were about 9 to 12 mm, the pith had a radius of about 4 to 5 mm and the xylem a width of 1 to 2 mm.
During two weeks, the signal was measured continuously and then a drought period was initiated by blocking the micro-tubes (the one in front of the eggplant and the two adjacent ones) on one plant per experiment. The results are shown in the figures 4.11, together with the corresponding soil matrix potential evolution and transpiration rate during the mid-season stage.
As for the eggplant experiment, we calculated the daytime mean sap flow value for each day and the corresponding daytime mean for ET_cb and the soil matrix potential. Overall, all signals from the sap flow had a similar amplitude which corresponded relatively well with the estimated transpiration flux (ET_{cb}). Table 4.8 shows the correlation of the daily daytime sap flow fluxes with the meteorological parameters.

	Exp 1a	**Exp 2a**	**Exp 3a**	**Exp 4a**	**Exp 1b**	**Exp 2b**	**Exp 3b**	**Exp 4b**
ET_{cb}	0.66	0.42	0.33	0.80	0.54	-0.11	0.552	0.77
Temperature	0.39	0.32	0.23	0.62	0.38	-0.11	0.33	0.56
Radiation	-0.73	-0.77	0.11	-0.45	-0.82	0.03	-0.32	-0.64
Wind speed	0.29	0.43	-0.22	0.21	0.58	0.24	0.24	0.36
Rel. humidity	-0.65	-0.31	-0.41	-0.69	-0.35	0.28	-0.51	-0.64

Table 4.8: Correlation between the mean daily daytime sap flow and the mean daily daytime meteorological data.

It appears that correlations are in general relatively weak. The calculated transpiration is not strongly correlated with all sap flow signals, as we would have expected it. This could be due to water stress but it appears that the correlation between the daily mean soil matrix potential and the sap flow signals are also not strongly correlated (table 4.9). Moreover the experiments that were subject to the same treatment ("a" and "b") did not have a strong correlations either (table 4.10). Experiment 2b seems particularly not correlated with any other parameters.
The reason for this is not completely clear. It may be that the instrument precision was not very accurate

due to the small stem diameters (9-12mm), which was twice smaller than for the cabbage experiment, which gave better results. The noise was reduced for the calculation but relatively large daytime fluctuations could be observed in the sap flow signals. The time resolution of the measurements may also have been too long (30 minutes). The instruments may have been influenced by the meteorological parameters directly as well. Finally, there might be some uncertainties in the measurements of the meteorological parameters and the calculation procedure for evapotranspiration may not be completely accurate for a small time step. It seems therefore that comparing small daily sap flow variations is not accurate in this case.

Some conclusions can still be drawn. First, it seems that the value of soil matrix potential reached in all experiments did not lead to a significant reduction of the transpiration, since no correlation can be observed. Only treatment 4 may have induced a certain water stress since the correlation between the soil matrix potential and the sap flow signals is above 0.7 for both experiments, even though the reduction of transpiration was low.

After March, 7, a drought period was initiated in experiments 1 to 4 "a". A similar drought for the "b" experiments started on March, 14. In that case, the reduction of sap flow could clearly be identified but only below the maximal range of measurement of the sensors (-200 kPa). The drought had a specially severe impact on treatment 2 after 5 days of drought, leading to a reduction of about 50% of the signal. On treatment 3, no reduction could be observed for the "a" experiment, while a severe reduction was observed for the "b" experiment. This situation seem to illustrate some heterogeneity in the crop, where the plant in treatment 3a probably was able to develop a more extensive root system, allowing a longer resistance to water stress. For treatments 1 and 4 a decrease of the sap flow signal could also be observed but with a lesser effect. In all cases, the plant did not completely recover from the drought due to leaf senescence.

Exp 1a	**Exp 2a**	**Exp 3a**	**Exp 4a**	**Exp 1b**	**Exp 2b**	**Exp 3b**	**Exp 4b**
0.22	0.55	-0.58	0.71	0.57	-0.09	0.45	0.74

Table 4.9: Correlation between the mean daily daytime sap flow and corresponding mean daytime soil matrix potential.

Exp1 a+b	**Exp2 a+b**	**Exp3 a+b**	**Exp4 a+b**
0.72	0.26	0.41	0.14

Table 4.10: Correlation between the mean daily daytime sap flow velocity of the two sensors placed on the same experiment with the same irrigation schedule ("a" and "b" sensor).

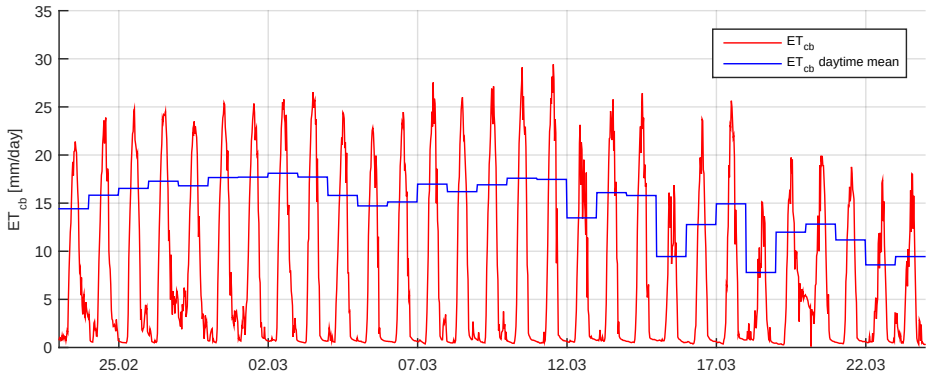

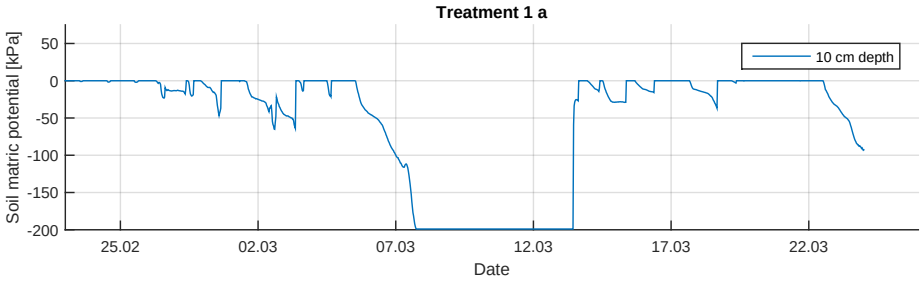
Treatment 1 a
Soil matric potential [kPa]
50
0
-50
-100
-150
-200
10 cm depth
25.02
02.03
07.03
12.03
17.03
22.03
Date

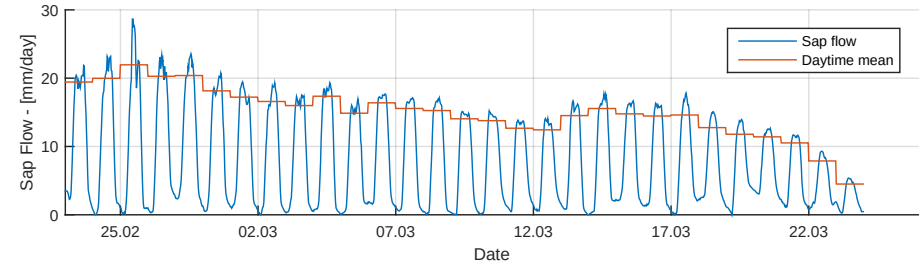
Sap Flow - [mm/day]
30
20
10
0
Sap flow
Daytime mean
25.02
02.03
07.03
12.03
17.03
22.03
Date

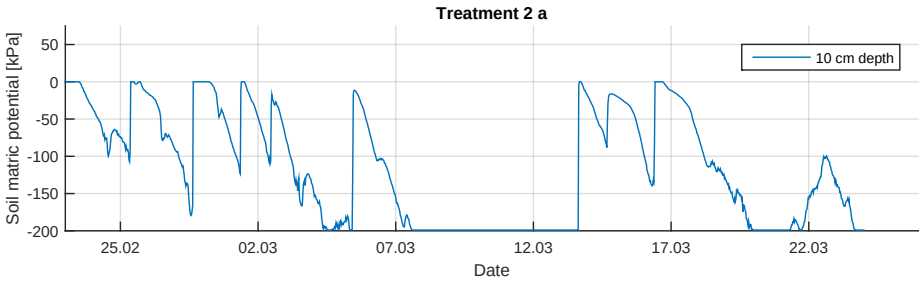
Treatment 2 a
Soil matric potential [kPa]
50
0
-50
-100
-150
-200
10 cm depth
25.02
02.03
07.03
12.03
17.03
22.03
Date

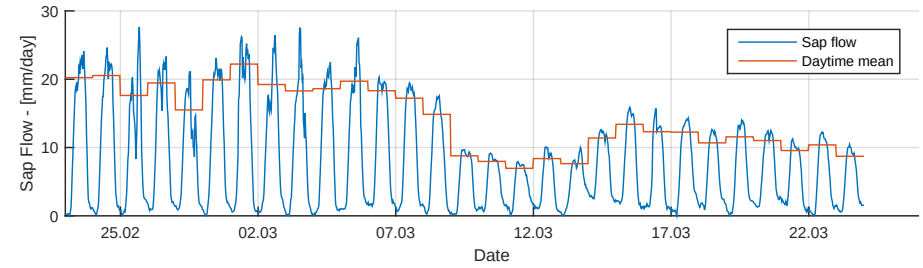
Sap Flow - [mm/day]
30
20
10
0
Sap flow
Daytime mean
25.02
02.03
07.03
12.03
17.03
22.03
Date

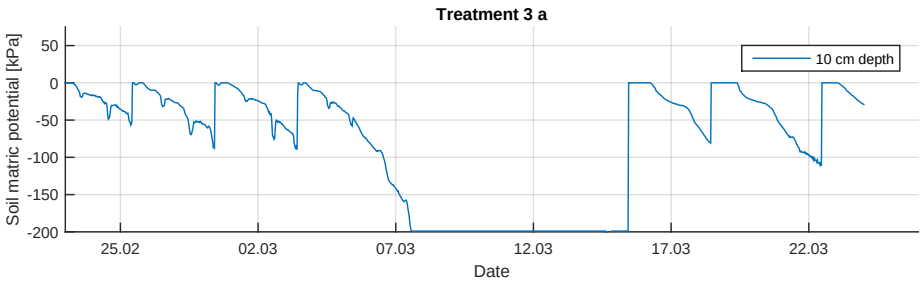
Treatment 3 a
Soil matric potential [kPa]
50
0
-50
-100
-150
-200
10 cm depth
25.02
02.03
07.03
12.03
17.03
22.03
Date

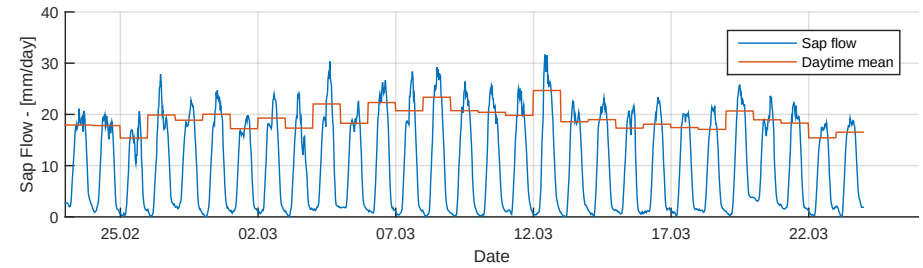
Sap Flow - [mm/day]
40
30
20
10
0
Sap flow
Daytime mean
25.02
02.03
07.03
12.03
17.03
22.03
Date

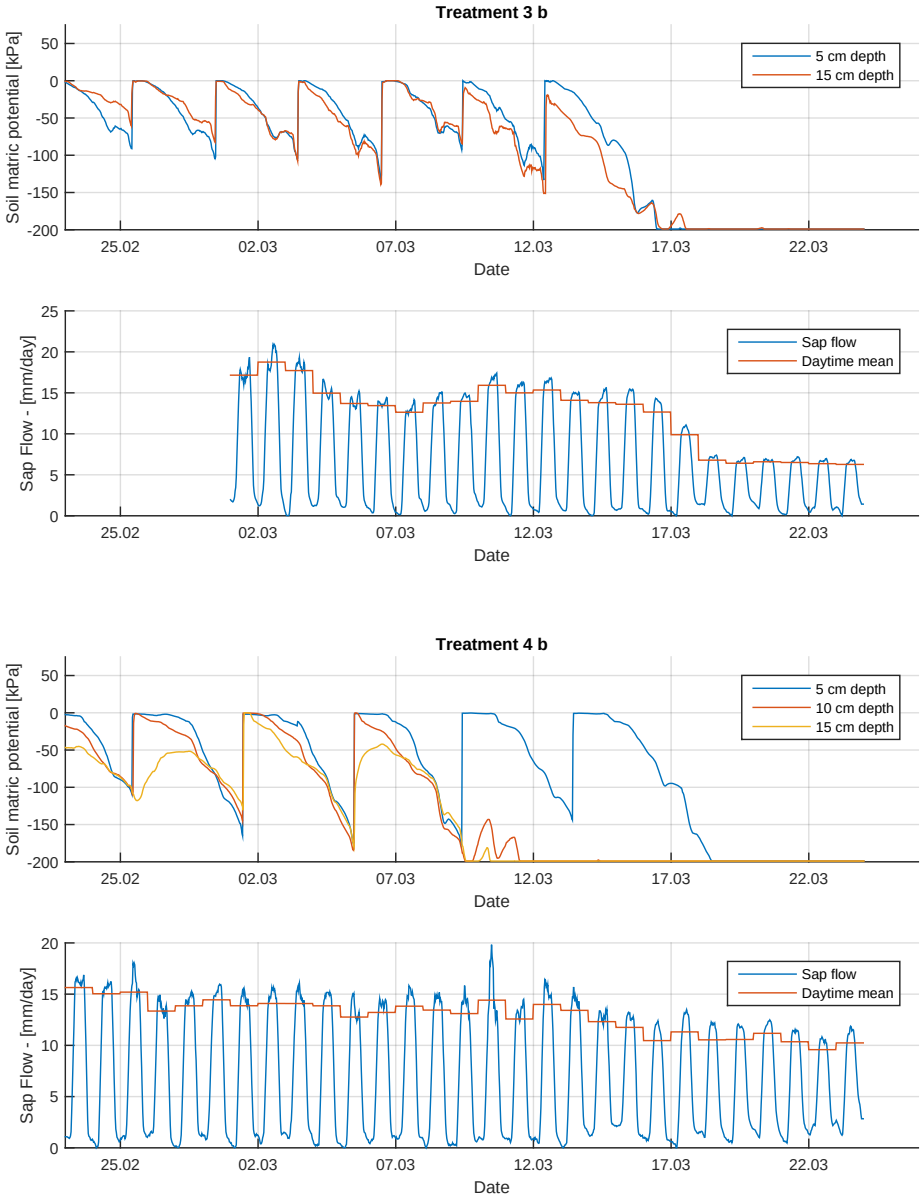

Figure 4.11: Comparison between the soil matrix potential, the transformed sap flow rate and the corresponding transpiration rate (ET_{cb}), for the four treatments during the mid-season of the eggplant experiment. The blue sap flow curves represent the 30 minutes average, the blue Watermark curve the 15 minutes average and the red curves are the daytime means. For transpiration, the red curve represents the 15 minutes average and the blue curve the daytime average. The signal of one sap flow per treatment is shown, except for treatment 3 due to different response to water stress.

The analysis of the sap flow signals seems to show that low values of soil matrix potential up to -200 kPa did not result in a significant reduction of transpiration. A mild water stress may have occurred below -150 kPa in treatment 4, though it could not be clearly observed. Moreover, it seems that treatment 2 was specially affected by the drought, which may be due to a smaller root system due to the irrigation schedule.

4.2.4 Root growth

The root analysis for the eggplant crop was done 30 days after transplanting, during the crop development stage, 55 days after transplanting, almost at the end of biomass formation and 75 days after transplanting during fruit formation.

30 days after transplanting

The first root extraction took place 30 days after transplanting, about at the end of the vegetative period. Some differences between the treatments could already be observed, though the general pattern was the same. Figure 4.12 shows the image analysis and the corresponding 1D distribution for the

four treatments. For all treatments, maximal root depth was about 15 to 20 cm. The root systems of treatment 3 and 4 (high depth) were not wide with a radius of only about 5 cm. Treatment 1 showed more secondary roots in the upper 10 cm and overall a higher biomass.

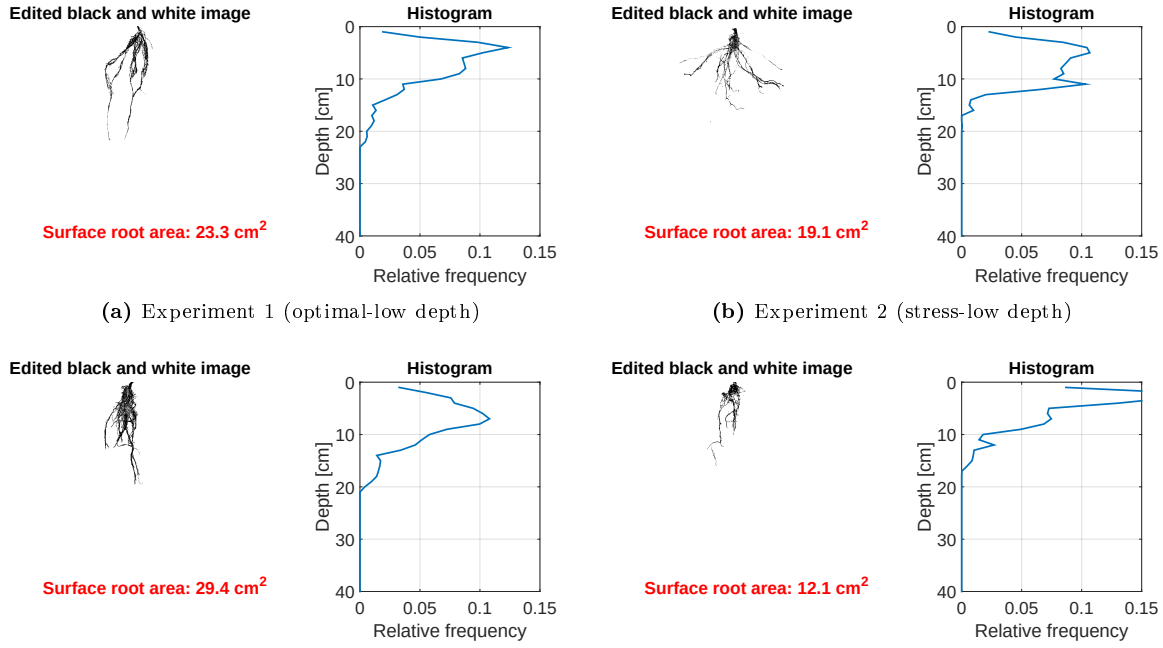

(a) Experiment 1 (optimal-low depth)

(b) Experiment 2 (stress-low depth)

(c) Experiment 3 (optimal-high depth)

(d) Experiment 4 (stress-high depth)

Figure 4.12: Evolution of the root distribution of eggplants - day 30 after transplanting.

55 days after transplanting

After 55 days, some differences can be noticed between the experiments. The image analysis is shown in figure 4.13.

For treatment 1, an extensive root system developed both on the surface and deeper. The longest roots reached about 25 to 30 cm depth, at a radial distance of about 30 cm from the stem. The upper 10 cm were occupied by a dense network of smaller roots, that reached about 20 cm from the stem. Since the soil is always wet for this experiment, the root system was not limited by water stress and the main limiting factor was probably soil resistance and the very dense and rocky soil layer at a depth of about 25 cm.

Concerning treatment 2, the root system was much less dense. It had many small roots in the upper 10 cm which extended horizontally to about 15 cm from the stem. Only a few main roots went deeper than 15 cm and lacked secondary roots. Maximal depth was about 15 to 20 cm and radial width about 15 cm. This behavior is understandable as only the upper part of the soil is replenished by the small irrigation depth.

Treatment 3 presented a relatively similar root system as experiment 1. The longest roots reached a depth of about 25 cm and with a radial distance of about 30 cm. A dense network of secondary roots also extended in the upper 10 cm. It seems that this treatment was not specially affected by the lower irrigation frequency, as the roots were essentially contained in the upper 10 to 15 cm.
The root system of treatment 4 was composed of many longer main roots with a less developed root system near the surface. The longest roots reach 30 cm depth with a radial distance of 20 cm. The main roots had many secondary roots below the top 5 cm. This distribution is explained by the lower water availability at the top, since irrigation occurred only once every 3 days.

It is interesting to note that all root networks analyzed had their main roots extending practically along one axis, along the drip line. Indeed, the water availability was higher between the drippers (50 cm spacing), than between the rows (1 meter).

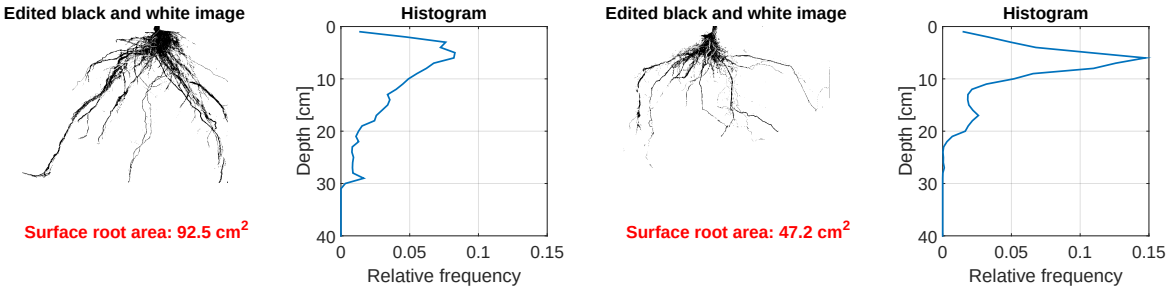

(a) Experiment 1 (optimal-low depth) **(b)** Experiment 2 (stress-low depth)

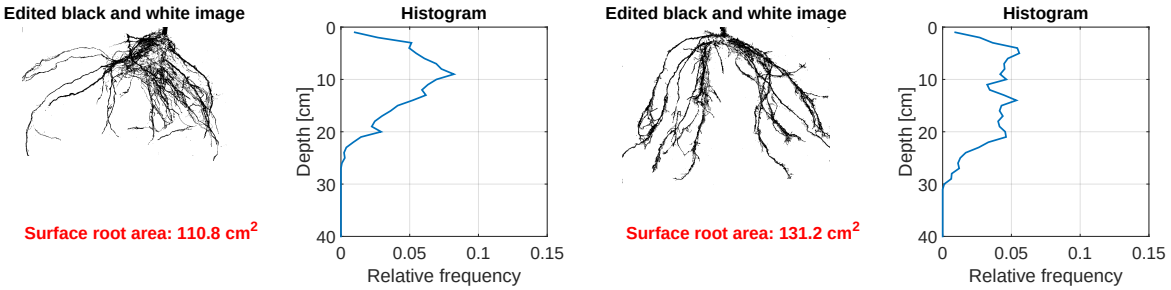

(c) Experiment 3 (optimal-high depth) **(d)** Experiment 4 (stress-high depth)

Figure 4.13: Evolution of the root distribution of eggplants - day 55 after transplanting.

75 days after transplanting

There were no notable changes in the root distribution after 75 days compared with the previous analysis, the patterns are relatively similar, with somewhat deeper roots as illustrated in figure 4.14. Only experiment 4 showed less longer roots than the previous analysis, though it had still the deepest root system.

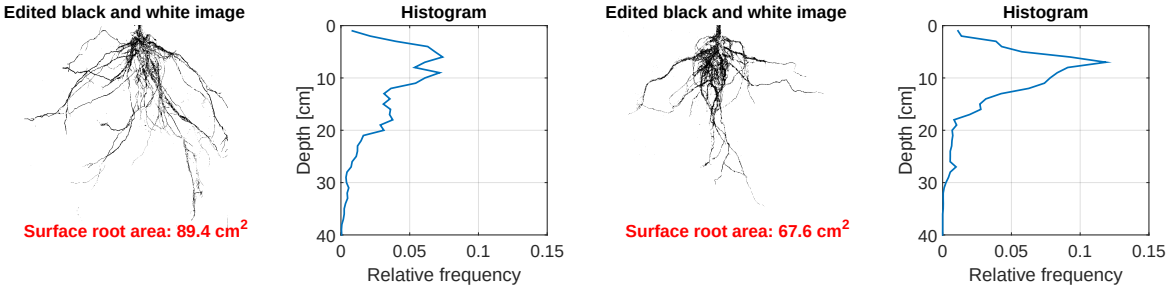

(a) Experiment 1 (optimal-low depth) **(b)** Experiment 2 (stress-low depth)

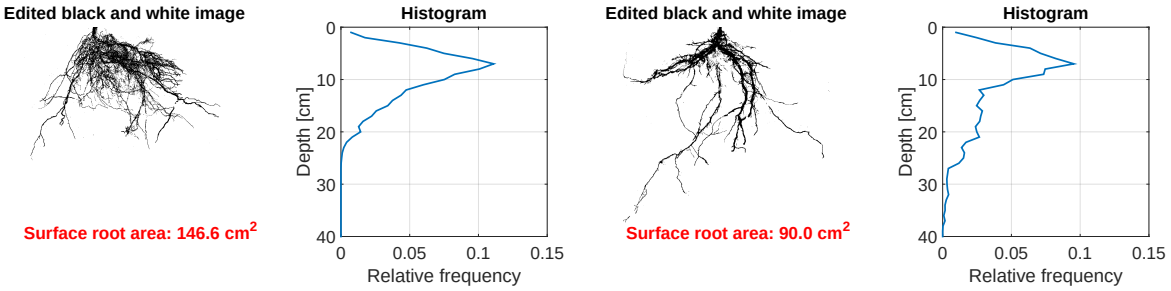

(c) Experiment 3 (optimal-high depth) **(d)** Experiment 4 (stress-high depth)

Figure 4.14: Evolution of the root distribution of eggplants - day 75 after transplanting.

The root analysis seems to confirm well the observations that were done earlier. In particular the root system of treatment 2 is comparatively smaller. Still even in treatment 2, where very low values of soil matrix potential where already observed at 10 and 15 cm, some roots did reach a depth of 20 to 30 cm. It seems therefore that the root system of the eggplants is able to develop even in zones with low soil matrix potential, probably because those zones were initially wet. Those roots become probably less active when the water depletion becomes too severe and is not replenished by the wetted bulb from irrigation.

4.2.5 Soil salinity and salinity stress

The soil electrical conductivity (EC) was monitored during the 75 first days of the eggplant experiment on treatment 4, and in the other treatments punctually to assess potential salinity stress. The electrical conductivity of the irrigation water was also measured. The irrigation water was pumped with a motor pump from an artificial lake about 250 meters away from the site. The electrical conductivity of the water was measured to be 0.35 dS/m which corresponds to a water with low salinity [53].

Concerning experiment 4, the soil pore EC was about 1.5 dS/m at the beginning of the growth and rose to about 4.5 dS/m in the middle of February. According to the database from by Maas, 1993 [21], eggplant is a sensitive crop with a salt tolerance of 1.1 dS/m. Passing this value, maximal yield starts to decrease at a reported rate of 6.9% per dS/m. This represents a yield reduction of 23.5% for experiment 4. It seems therefore that the lower productivity in treatment 4 may also be due to a certain salinity stress. In comparison the soil pore EC for treatment 2 reached about 3.5 to 4 dS/m during the mid-season and about 2.5 dS/m for treatment 1. Some studies suggest that drip irrigation usually avoid salinity stress by accumulating the salts only at edge of wetted zone [54], but since no leaching occurred in our experiments, the salt concentration did still increase as water was evaporated or taken up by roots.

In order to avoid salinity stress, it is recommended to over irrigate when the concentration becomes too high, in order to flush the salts with the leaching water [18]. Leaching occurred only in treatment 1 which explains the lower salt concentration. The difference in salt concentration between the other experiments is less clear and it is difficult to conclude if the irrigation frequency played a decisive role to limit salinity stress. One interesting observation was done during the drought period that occurred on March 7. As the soil matrix potential decreased below -200 kPa, the soil pore EC increased to a value up to 14 dS/m, which induced a strong salinity stress. From this perspective, using low irrigation frequencies may induce a stronger salinity stress.

4.2.6 Sensor precision

Simultaneous measurements of the soil matrix potential (Watermark) and the soil moisture (5TE and 5TM) were taken at adjacent locations (same depth and lateral distance) on the same plant. The aim was to compare both instruments to verify their accuracy. In order to easily compare the measurements, the soil moisture measurements from the 5TE were transformed to soil matrix potential values using the equation from van Genuchten (eq. 2.15). A comparison is shown in figure 4.15.

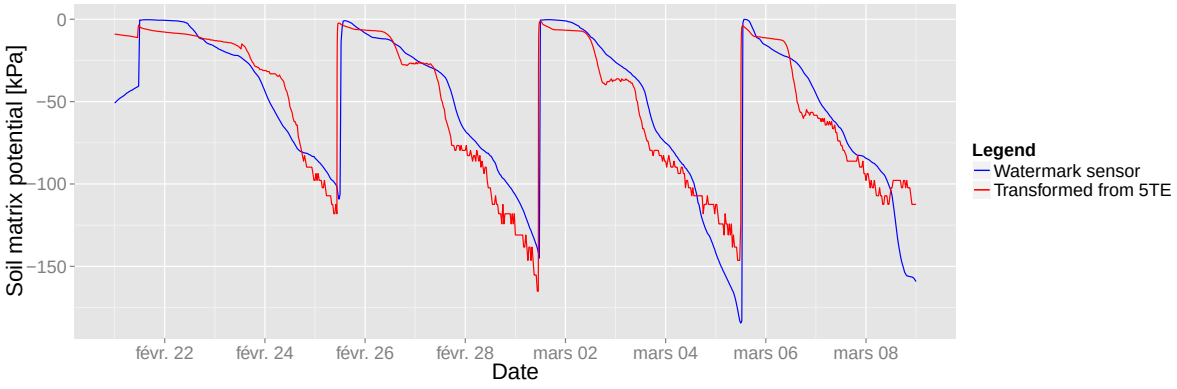

Figure 4.15: Comparison of the measurement between Watermark and 5TE sensors placed on treatment 4 of the eggplant experiment.

Two things appear from this analysis. First the 5TE sensor reacted more quickly to an irrigation event. Indeed there is usually a 30 minutes to 2 hours delay between the peak of the 5TE and Watermark sensor. The lag time was longer when the soil matrix potential was low but generally a 1 hour was most common. The time lag observed with the Watermark sensors may therefore not be due to the reaction time of the producer to trigger irrigation when an alert is sent, but rather to the reaction time of the sensor itself. Secondly, it appears that the Watermark sensor seems less reactive to changes in soil water fluctuations than the 5TE. This is particularly visible during night times, when the 5TE shows a very flat behavior, while the signal from the Watermark keeps decreasing. Both phenomenon have also been reported in other studies [55], and seem to come from a delay in the equilibrium that occurs between the soil matrix potential and the porous granular matrix in which the electrodes are embedded. Nevertheless, both devices gave similar values of soil matrix potential and their accuracy can be considered good and

adapted to triggered irrigation.

4.3 Discussion of preliminary results

The analysis of the root distribution seems to indicate that the irrigation effectively impacts on the development of the root system. If the treatment 1 is considered the reference, unstressed, root distribution, it appears clearly that the root system of treatment 2, was shallower which reflects well the irrigation schedule. In addition, the treatment 4 seems to show that the roots were less concentrated in the upper 10 cm and distributed more homogeneously with depth, this is specially visible at day 70. It is clear that this analysis only relies on a very small sample and that local variation in the ground may have played a role in the root development but the general trend seems to be realistic. A wider analysis was however not possible, mainly due to the reluctance of the local producer to destroy healthy plants.

The question that remains is to determine whether a deeper root system improves the plant development or sensitivity to stress. From our experiments, it seems that the experiments with longer roots (especially experiments 1 and 4), had a longer resistance to a punctual drought, as it was discussed in chapter 4.2.3. A deeper root system is probably also interesting in terms of nutrient uptake since it covers a larger soil volume. This point was however not investigated in the present study. In our experiments, treatment 2, with a shallow root system, produced the highest harvest, but productivity was not maximal. It is not completely clear if the restricted root system played a significant role in the limited productivity of treatment 2, or if it was only due to the magnitude of water stress. It seems however clear that a plant with a shallow root system will suffer quicker for water stress and therefore promoting a wider root system is probably beneficial in terms of water use efficiency.

It appears particularly clear that at early growth stage and until the end of crop development, a low frequency to promote root development also induced a certain water stress to the plant that limited canopy development, which was not beneficial for fruit formation. During yield formation it seems that water stress was less severe for the plant and that production was more dependent on the biomass formed during the previous stages, as long as the soil matrix potential was higher than about -100 kPa. Lowering the irrigation frequency during this stage may therefore be interesting to still promote root development. Another point that can be raised is more linked to the drip kit system. It appeared that drippers clogged more easily when the irrigation frequency was low. This may be to the fact that at high frequency (such as once a day), the micro-tubes do not completely dry so that the dirt is not solid is frequently washed away. When the frequency is lower the dirt accumulates more rapidly around the micro-tubes walls and are eventually clogged.

5 Results of HYDRUS 2D simulations

5.1 Model Calibration

5.1.1 Cabbage

To calibrate and validate our simulations, we compared the simulated and measured soil matrix potential and volumetric water content at different depths for the third growing stage (days 45 to 75 after transplanting) (figures 5.1 & 5.2).

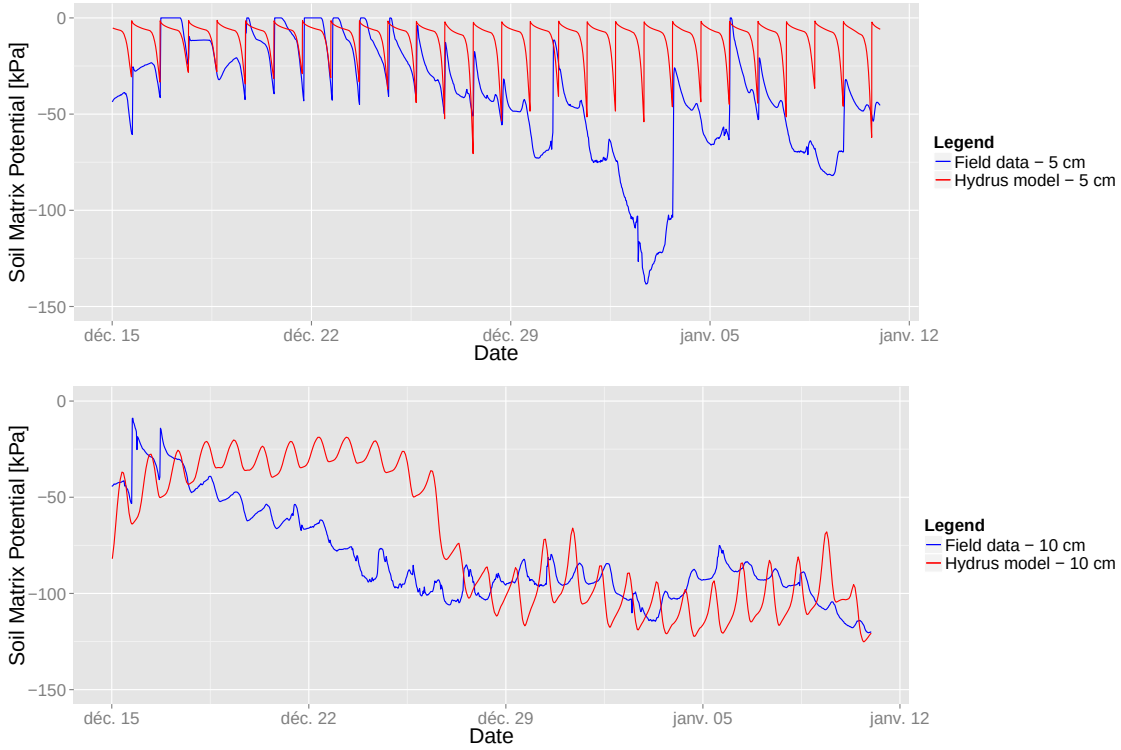

Figure 5.1: Comparison of the simulated and modeled water dynamics for the mid-season growth stage of the cabbage experiment at 5 and 10 cm depth and for treatment 1 (optimal, low irrigation depth).

The evolution of the soil matrix potential for treatment 1 (figure 5.1) was not completely regular. In particular there is a drop between the 1st to 5th January. This is most probably due to the drip system which uniformity is not very stable: the micro-tubes may partially get clogged; a small water puddle may form due to the relatively high discharge rate and due to crusting of the surface, resulting to some runoff, sometimes in the opposite direction of the sensor, which is about 10 cm away from the micro-tube. This drop is therefore only a local phenomenon and does not represent the overall state of the crop which was correctly irrigated.
Still, the model predicts relatively well the rate of water depletion, as the amplitude of the curves are similar.

Concerning treatment 2 (figure 5.2), the model appears relatively accurate as well. The behavior of the measured soil matrix potential was more steady in this case, due to the higher irrigation depth, which recharged the soil deeper and somewhat wider. The reduction of the water uptake (due to water stress) is also correctly modeled. This is particularly visible after December 29, as the water content drop is much smaller the last day before an irrigation event.

It should be noted that in HYDRUS 2D, the root distribution does not evolve with time, so that comparison over a long period may be difficult, as root adaptation can be relatively fast in reality [36].

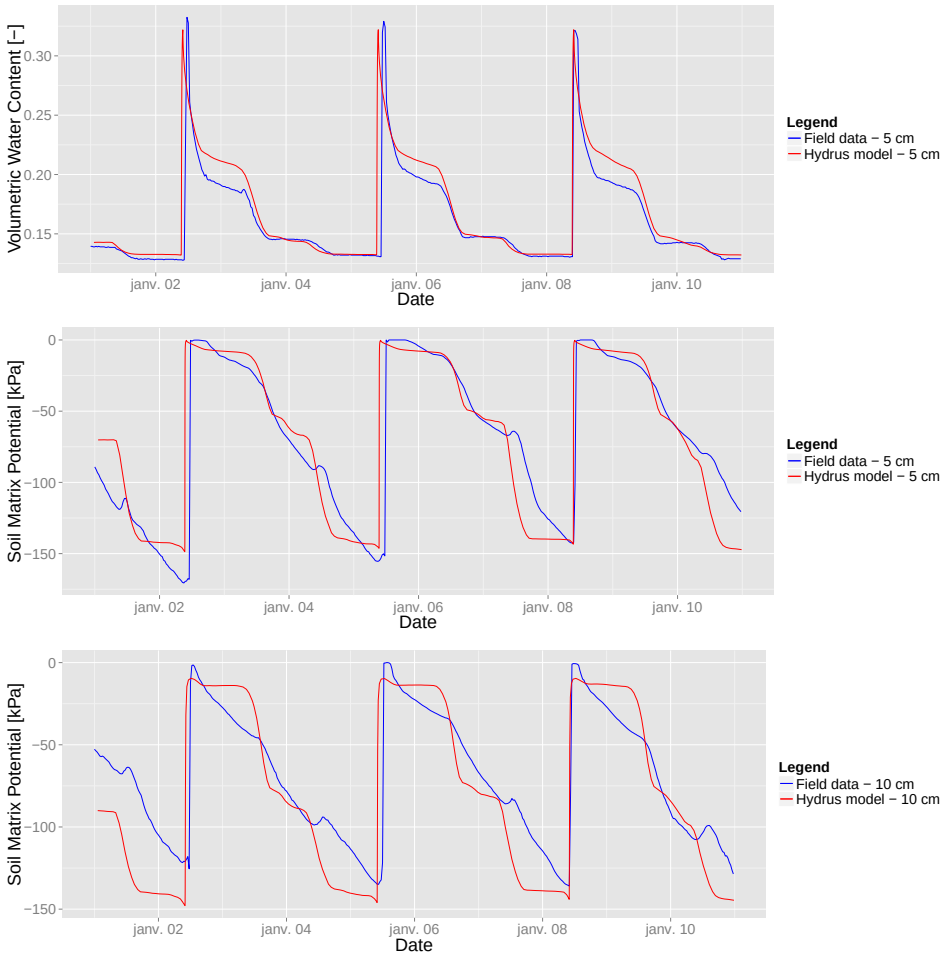

Figure 5.2: Comparison of the simulated and modeled water dynamics (soil moisture and soil matrix potential) at different depths for the mid-season stage of the cabbage experiment and for treatment 2 (stress, high irrigation depth).

Based on these two simulations, the actual evaporation and transpiration fluxes can be calculated. Table 5.1 summarizes the main results.

	Percentage of max. Transpiration [%]	**Percentage of max. Evaporation [%]**	**Total irrigation applied [L]**	**Leakages [L]**
Treatment 1	87.0	87.2	2700	0.5
Treatment 2	61.9	61.7	2000	2

Table 5.1: Results of the HYDRUS simulations during the mid-season of both treatments of the cabbage experiment.

These results suggest a strong transpiration reduction. This reduction is specially important for treatment 2, the last day before each irrigation event. This reduction was however not measured by the sap flow meters which showed no significant transpiration reduction. From the measurement it is clear that a reduction of the water uptake occurred in the central zone where measurements took place, but it seems that this reduction was compensated in other parts of the root zone, where the matrix potential was higher. Such root water uptake compensation has been reviewed in the literature, showing the strong ability of roots to adjust their water uptake, especially from deeper roots [56], [40].
Our model illustrates the amplitude of the potential water stress for both treatments, even if some compensation is likely to have occurred. We were however unable to simulate this water uptake compensation in our model. We believe this compensation is difficult to model because of the static character of the root distribution in HYDRUS, which does not allow roots to grow in zones of higher water content.
It may also be possible that the sap flow measurements were not completely accurate.

5.1.2 Eggplant

A similar calibration was done for the eggplant experiment. A period of 15 days was selected, starting about 80 days after transplanting during the fruit formation stage. The comparison is done with experiment 4, since it showed the lowest soil matrix potential values.

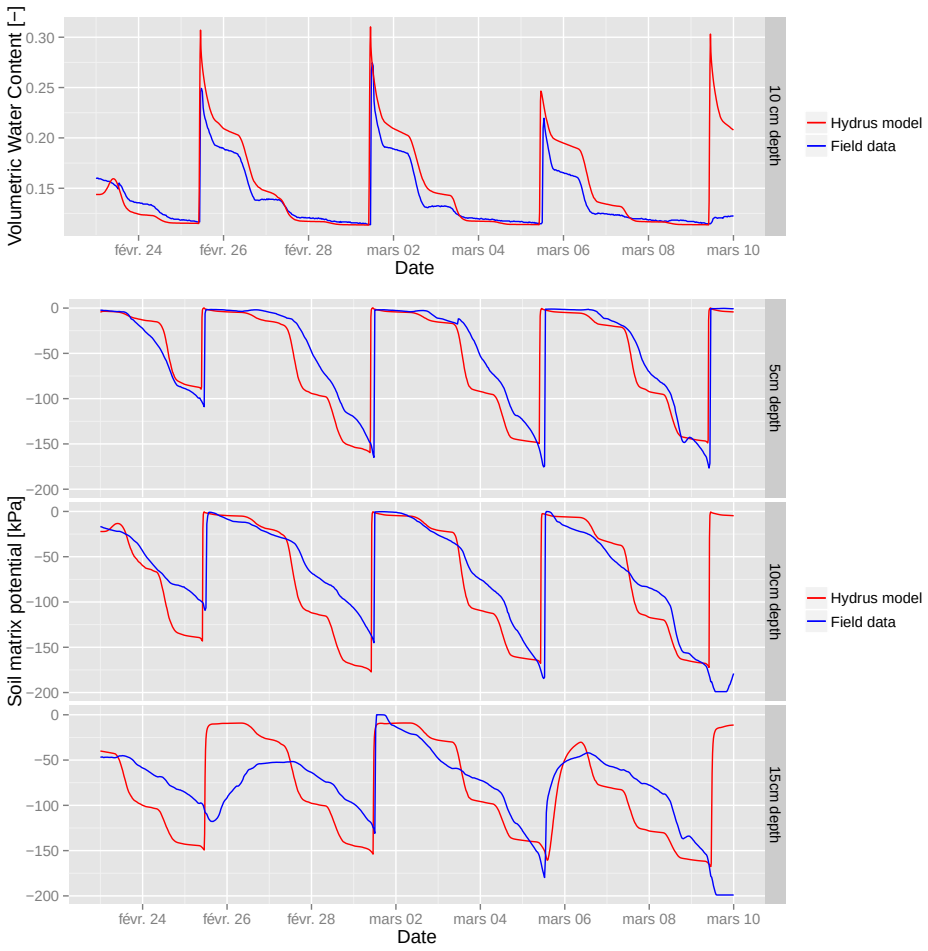

Figure 5.3: Comparison of simulated and modeled water dynamics (soil moisture and soil matrix potential) at 5, 10 and 15 cm depth, for the mid-season stage of the eggplant experiment and for treatment 4 (stress - high depth).

Simulations were done for all four experiments and good results were obtained using the same soil and plant parameters which supports that our calibration is correct. An overview of these simulations is shown in figure A.6 in appendix A.5.1. The table 5.2 shows the reduction of different fluxes as computed by our simulations.

	Ratio of max. Transpiration	**Ratio of max. Evaporation**	**Irrigation / ET_c**	**Leakages / Irrigation**	**Mean soil matrix potential**
	[%]	[%]	[%]	[%]	[kPa]
Treatment 1	99.9	89.9	90.1	5	-21.2
Treatment 2	76.4	55.5	69.7	0	-140.0
Treatment 3	84.1	67.6	78.6	0	-77.9
Treatment 4	65.3	48.3	61.9	0	-121.6

Table 5.2: Results of the HYDRUS simulations from February 23 to March 15 for the four treatments of the eggplant experiment.

Those results confirm well the previous discussed conclusion from the field experiments. During the mid-season experiment 2 and 4 were subject to water stress which limited the productivity, while Treat-

ment 1 suffered no stress and experiment 3, only a mild stress. Interestingly the mean root zone soil matrix potential calculated in HYDRUS, corresponds strongly with the mean soil matrix potential calculated at 15 cm for period 3 (see table 4.6).

Finally, figure 5.4 shows the mean soil matrix potential with depth over time for all four treatments. The profile was done at a distance of 7.5 cm laterally from the dripper. The drop in soil matrix potential indicates the lower limit of the wetted bulb, where the soil is only partially recharged by the irrigation events, but where roots are still present.

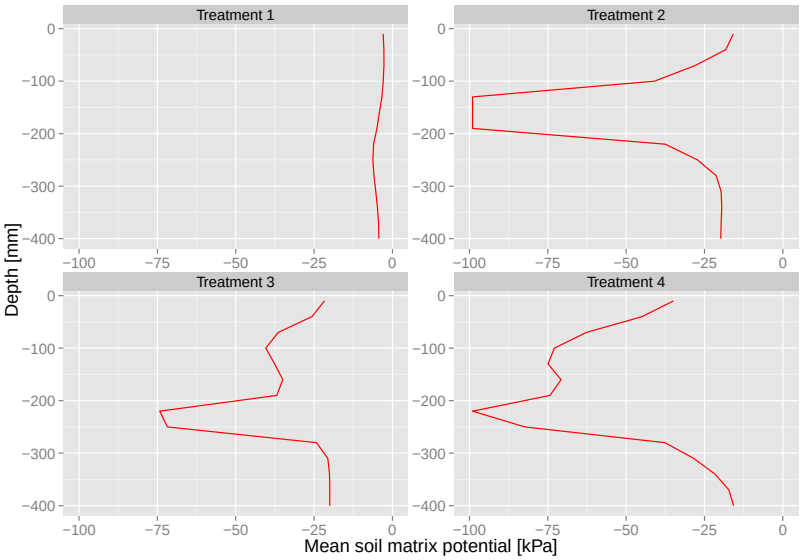

Figure 5.4: Vertical profile of the mean soil matrix potential over time with depth for all four treatments at a lateral distance of 7.5 cm from the dripper.

It appears that, for treatment 1, the soil is recharged completely and roots were not subject to any limitations due to water stress. For the three other treatments, the limit is located around 15 to 20 cm for treatment 2, 20 to 25 cm for treatment 3 and 4. The potential above those depth is higher for treatment 2, followed by treatment 3 and 4. These results also match relatively well the root analysis discussed previously. It seems however that some roots went deeper in the soil than the modeled wetted bulb, even though most of the root biomass was contained above the modeled depth.

We finally computed the mean soil matrix potential for the period of simulation along a horizontal profile at a depth of 10 cm from one dripper to the next one (50 cm). The results are shown in figure 5.5.

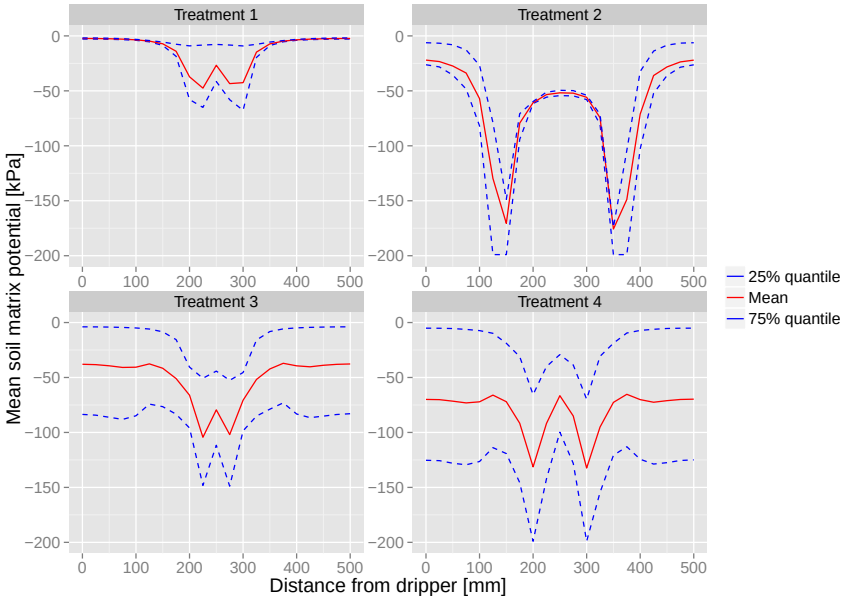

Figure 5.5: Horizontal profile of the mean soil matrix potential over time from a dripper for all four treatments at a depth of 10 cm.

The two drops represent the edge of the width of the wetted bulb. The higher soil matrix potential in the middle is due to low root water uptake. Concerning the spread of disease it appears that, particularly in treatment 2, the low matrix potential about 15 cm from the dripper is probably an important barrier against the movements of pathogens. In contrast the potential remains very high for treatment 1 which favored the dispersion of the disease. The analysis is less clear between treatment 3 and 4, though the mean values for treatment 4 are lower which was probably decisive to stop the spread of the disease.

5.2 Threshold and irrigation depth modeling

In this part we built different scenarios with different irrigation depths and different thresholds. We used for all scenarios the same plant and soil calibration as for the eggplant experiment and the simulation duration, the evaporation and transpiration fluxes were the same for all scenarios. The model is based on the drip irrigation system from iDE.
Scenarios were run with a threshold to trigger irrigation which was placed at a depth of 5 cm and 5 cm away from the dripper horizontally. Because the irrigation events are short (about 30 minutes to two hours) and hydraulic conductivity is relatively low, the wetted front from an irrigation application infiltrates slowly in the soil and only reaches a depth of about 5 cm at the end of the irrigation event. As a consequence, if the threshold was placed deeper, HYDRUS would trigger a second irrigation event directly because the soil matrix potential is still below the threshold at that time, which doubles the irrigation depth and influences our scenarios. This is a limitation of the model and as a consequence the threshold could only be placed at a shallow depth of 5 cm.

We analyzed two different periods. The first period corresponded to the initial growth stage, between day 10 to 30 after transplanting. The second period considered corresponded to the beginning of the mid-season, during yield formation, about 80 days after transplanting also during 20 days.

For the first period, the thresholds tested were: -5, -10, -15, -20, -25, -30, -40, -50 and -100 kPa. These scenarios were also tested with different irrigation depths corresponding to 25, 50 and 100 liters.
For the mid-season period, the thresholds were: -5, -10, -20, -30, -50, -70, -100, -150 and -200 kPa. These scenarios were also tested with different irrigation depths corresponding to 100, 200 and 400 liters. For the irrigation depths of 200 and 400 liters, the longer irrigation time allowed to place the threshold at 10 cm depth as well.

As already mentioned in chapter 3.1.1 we chose to express irrigation depth in terms of water volumes in *liters* instead of mm/m^2 as the estimation of the effective irrigated surface is not straightforward and depends on the sub-lines and drippers spacing, as well as the irrigation depth. For the HYDRUS simulations we based our calculations on the drip kit system of the eggplant crop. As a result, the irrigation depths supplied 90 drippers, which allowed us to express the irrigation depth in terms of liters per dripper in HYDRUS. Since the wetted area at the surface fluctuated given the irrigation volumes applied to the crop, the net irrigation depth in [liter/m^2] may very given the amount of water applied. Using water volumes provided a fixed quantity in HYDRUS and avoided confusion. A general procedure to calculate the irrigated area and to calculate irrigation depth is discussed further in the study in chapter 6.4.

For each simulation, the root zone was adapted to match the simulated wetted bulb in order to avoid water stress in zones that are not reached by the irrigation water. The evolution of the soil matrix potential at different depths was evaluated and the percentages of actual over maximal transpiration and evaporation were evaluated. Before recording the results of the simulations, we let the model run for three days, so that a certain equilibrium was reached in terms of water distribution in the soil.

5.2.1 Early growth scenarios

Figure 5.6 shows the evolution of the soil matrix potential for all simulations with an irrigation depth of 25 and 100 liters, the scenarios with a depth of 50 liters are shown in appendix A.5.

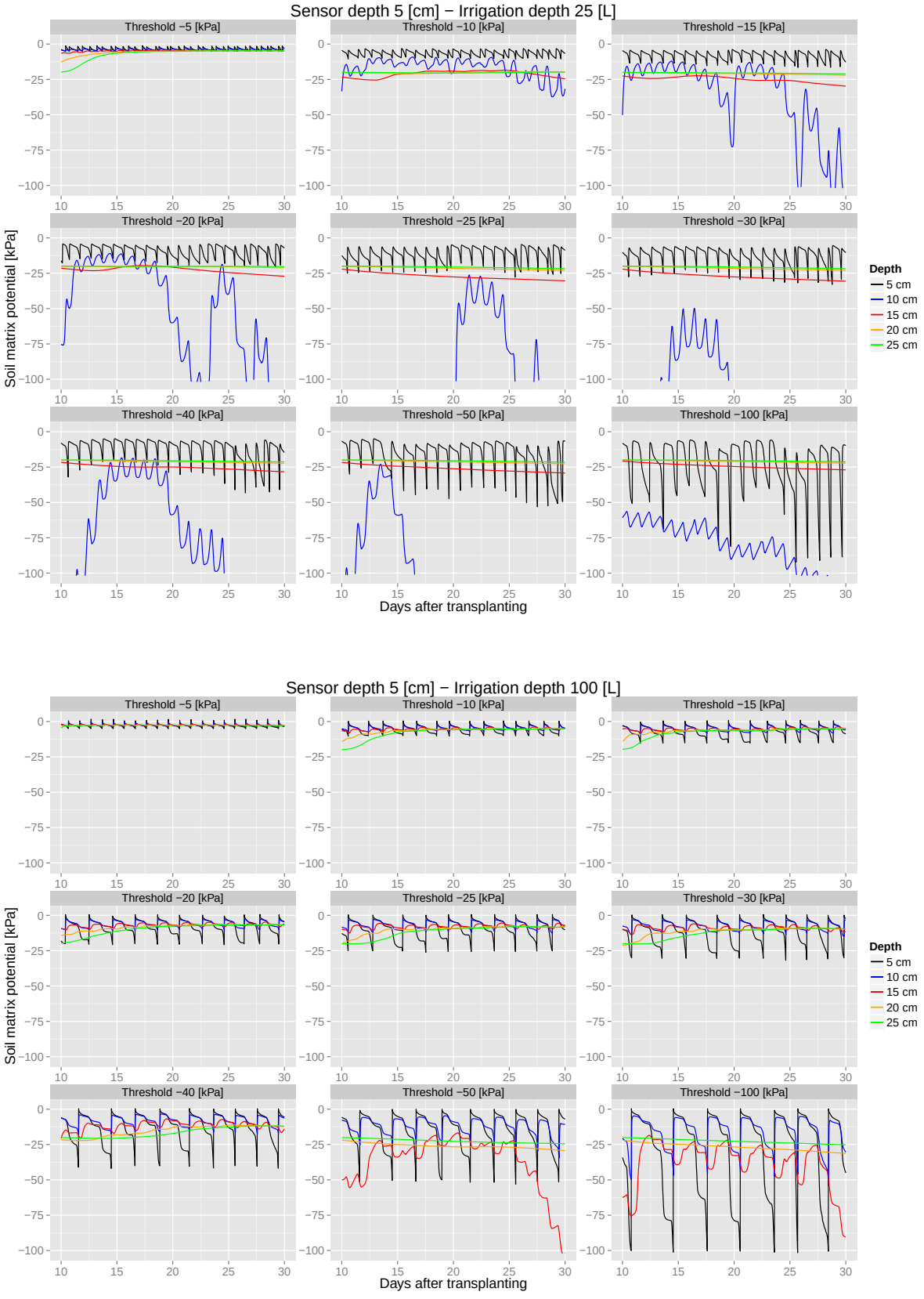

Figure 5.6: Evolution of the simulated soil matrix potential at various depths for all scenarios during the early growth stage and using an irrigation depth of 25 liters and 100 liters.

For all scenarios it appears clearly that the soil matrix potential below 15 cm does not fluctuate with time. Even at 15 cm the evolution of the potential hardly fluctuates, except for the last scenarios with an irrigation depth of 100 liters and a threshold lower than -50 kPa. Indeed, the roots at that stage only reach a depth of 10 to 15 centimeters, so that the water uptake is very limited below 10 cm. Moreover, depending on the threshold, the irrigation either saturates the whole soil (high threshold), so that the

potential stays very high, or when the soil is drier only the upper part of the soil is recharged by the low irrigation depth. The figure A.9 in appendix A.5 shows the mean soil matrix potential over time at different depths. The drop that occurs at a certain depth corresponds to the edge of the wetted bulb. It shows that with a depth of 25 liters, only the first 10 cm are reached by the irrigation front, for the 50 liters scenarios the depth is about 13 cm and for the 100 liters scenarios the depth is 170 cm.
The first conclusion that can be done is that placing the sensor below 10 cm is not recommendable as the sensor will only measure low variations and the placement will not be representative of the water availability in the root zone.

This represents a major limitation of our irrigation management system. If we want to control irrigation using only one sensor during the whole growth, a maximal depth of 10 cm is required for the sensor. This depth seems however justified as it corresponds also to the depth of maximal root density from our root analysis (see figure 4.12 from chapter 4.2.4).

The figure 5.7 shows the reduction of transpiration depending on the threshold used, as well as other relevant results.

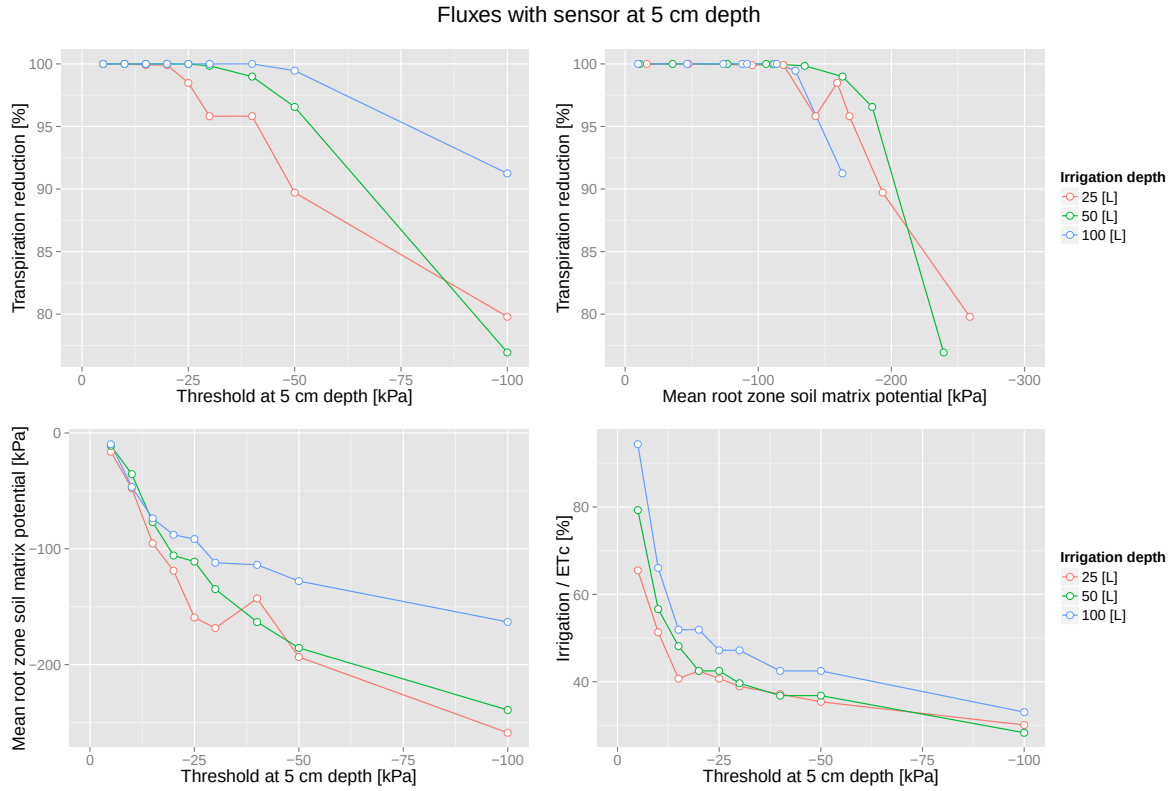

Figure 5.7: Summary of all scenario results for the early growth stage and given the irrigation depth. The upper-left plot represents the simulated cumulative actual transpiration volumes over the cumulative potential transpiration amounts given the irrigation threshold used at 5 cm depth. The bottom-right plot shows the relationship between the mean root zone soil matrix potential over time and the soil matrix potential threshold used. The upper-left plot shows the ratio of transpiration reduction given the mean root zone soil matrix potential. The bottom-right plot represents the reduction in irrigation water applied using the ratio of cumulative irrigation amounts over the cumulative amounts of potential transpiration and evaporation given the threshold used.

For the early growth stage, it has been discussed that water stress could already affect plant growth before transpiration actually starts to decrease. In our models, it was shown from the calibration that the transpiration reduction function overestimated the actual transpiration reduction (but not the local root water uptake reduction), so that we consider the transpiration reduction as a good indicator of water stress.
For this early stage, we propose to fix the optimal threshold just before transpiration starts to decrease. Looking at the first plot of figure 5.7, with a sensor at 5 cm, this threshold is -20 kPa with an irrigation depth of 25 liters, -30 kPa for 50 liters irrigation depth and -40 kPa for 100 liters. When looking at the last plot, we observe that the ratio of irrigation over evapotranspiration is strongly reduced for high thresholds and then presents a very flat slope. The proposed threshold are located near at the start of this plateau, confirming that the threshold seem optimal for the purpose of both water stress avoidance

and water savings. For more security, the threshold could be increased a bit, and placed exactly at the beginning of the plateau, about 5 kPa higher. If we want to place the sensor at 10 cm depth, the threshold should be adapted. The table 5.3 summarizes the selected thresholds.

Irr. depth	**Threshold at 5cm**	**Threshold at 10cm**	**Irrigation/ET$_c$**	**Irr. frequency**
[L]	[kPa]	[kPa]	[%]	[1/day]
25	-20	-20	40	1.5
50	-25	-20	39	1/1.3
100	-30	-15	42	1/2

Table 5.3: Summary of the selected optimal thresholds and irrigation schedules for the early growth stage based on all HYDRUS scenarios.

It is interesting to note, that at deeper depth, the threshold must be lower when the irrigation depth is higher, due to the higher recharge of the soil after an irrigation event.

The irrigation depths selected for our scenarios do not lead to significant differences in terms of water savings compared to water stress. One hypothesis of the study was that increasing the irrigation depth and lowering the irrigation frequency would save water as the soil surface is less frequently wetted, limiting the top soil evaporation. This conclusion was proposed by Mermoud et al., 2005 [50] who used HYDRUS 1D to simulate surface irrigation in semi-arid zones. The model has shown that there was no clear difference in evaporation reduction between the scenarios for triggered irrigation. Since the soil is only partially wetted (in contrast to surface irrigation), the reduction of evaporation by decreasing the irrigation frequency is compensated by an increase of the wetted diameter at the soil surface, due to the higher irrigation depth. The evaporation reduction was in the end very similar for each irrigation depth. Irrigating with a higher depth increases the depth of the wetted bulb, which may promote a deeper root system, however it reduces the irrigation frequency and field experiments have shown that a higher frequency slowed the plant growth.
From the simulations, using a very low irrigation depth seems to hardly reach 10 cm which is probably not optimal.

To conclude, we propose to use an irrigation depth corresponding to 50 liters, with a threshold of -20 kPa at 10 cm depth and located about 5 cm away from the stem.
Our simulations show that great water savings can be achieved at that early growth stage. A part of the water savings are directly linked to the drip kit system since a part of the soil is not irrigated, limiting the evaporation flux, which is the major source of water loss. Controlling irrigation shows that greater water savings can be made by avoiding leakages and controlling the soil moisture at the soil surface. It should be noted that in these simulations we use a value for the crop coefficient K_c corresponding to its maximal value (around 1.2) and not the mean value proposed by the FAO, which already takes into account evaporation reduction, but which can vary greatly depending on the irrigation frequency. As a result the calculated ET_c values to its maximal value and the ratio Irrigation / ET_c appears thus lower.

5.2.2 Mid-season scenarios

The same methodology was repeated to build scenarios during the mid-season, when water needs are the highest. The same evapotranspiration was used for all scenarios and the root zone was adapted for each scenario. The results are shown in figure 5.8 for the irrigation depth of 100 liters and 400 liters, the results for 200 liters can be found in appendix A.5.

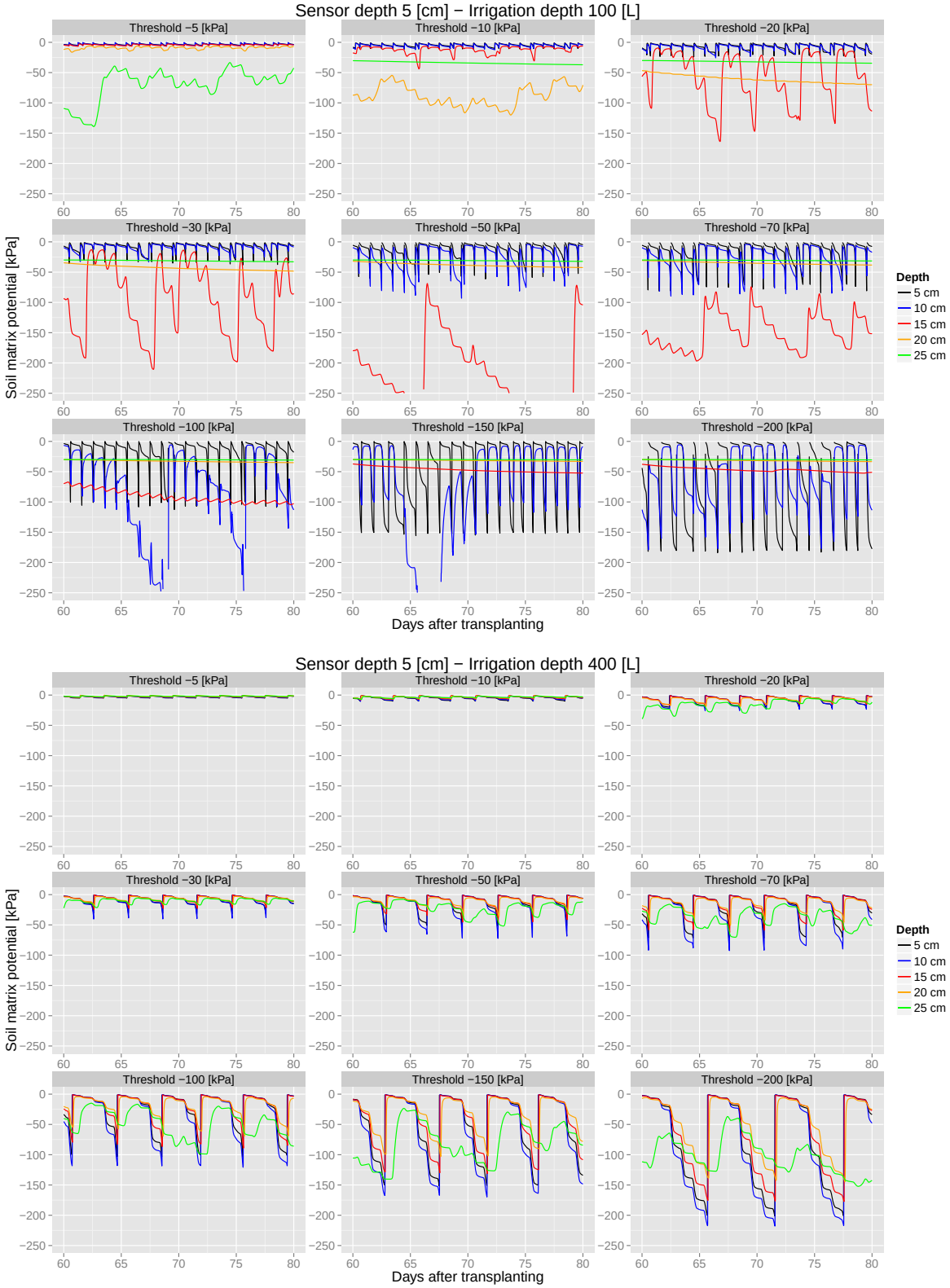

Figure 5.8: Evolution of the simulated soil matrix potential at various depths for all scenarios during the mid-season stage and using an irrigation depth of 100 liters and 400 liters.

The main difference between the two different irrigation depths is that the highest depth allowed to recharge the soil more deeply, below 25 cm, while the lowest depth only reached about 15 cm. The figure 5.9 shows the different fluxes at a depth of 5 cm. For the irrigation depths corresponding to 200 and 400 liters, the scenarios were also run with the threshold at 10 cm depth.

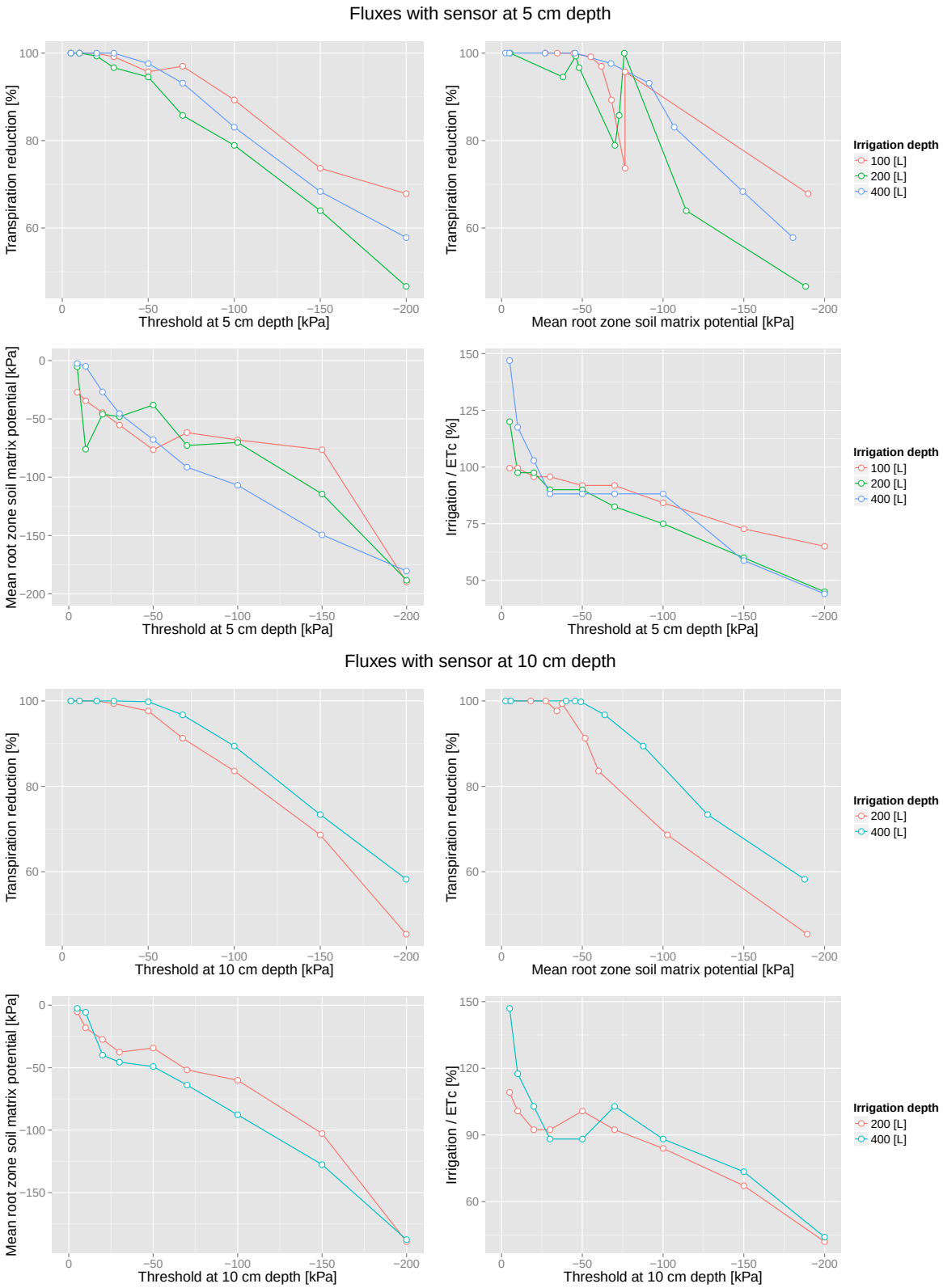

Figure 5.9: Summary of all scenario results for the mid-season growth stage and given the irrigation depth and for a threshold placed at a depth of 5 cm (upper graphs) and 10 cm (lower graphs). The upper-left plot represents the simulated cumulative actual transpiration volumes over the cumulative potential transpiration amounts given the irrigation threshold used at 5 cm depth. The bottom-right plot shows the relationship between the mean root zone soil matrix potential over time and the soil matrix potential threshold used. The upper-left plot shows the ratio of transpiration reduction given the mean root zone soil matrix potential. The bottom-right plot represents the reduction in irrigation water applied using the ratio of cumulative irrigation amounts over the cumulative amounts of potential transpiration and evaporation given the threshold used.

It appears that there was little differences between the scenarios with different irrigation depths in

terms of transpiration reduction and water savings. The reduction of transpiration and irrigation amounts are relatively similar for all irrigation depths, with a slightly higher transpiration with a 400 liters depth. The main difference resides more in the frequency of irrigation but the results in terms of water savings and water stress are similar.
An interesting observation, looking at the bottom right figure, is that for a low irrigation depth (100 liters) and a low threshold, the mean root zone soil matrix potential is lower than the threshold, indicating that the soil is more saturated near the center where the sensor is placed. This is mainly due to the high irrigation frequency. However, at lower thresholds, the tendency is inverted and the potential at the sensor location is lower than the mean root zone soil matrix potential, due to the higher water uptake in this zone and the lower irrigation frequency. The point were the tendency inverses is around -50 kPa. For high depths this phenomenon is less pronounced and the relationship more linear.
We propose for this growth stage to allow a small transpiration reduction and choose a threshold corresponding to 95%. Indeed, as discussed, plants are more tolerant to water stress during this stage and our model showed a much higher transpiration reduction than the field experiments. For all experiments this corresponds to a threshold of about -50 kPa. When looking at the ration irrigation over ET_c, it appears that this threshold is located on the same plateau as for the previous growth period, but which corresponds to 90% of ET_c this time. The plateau is higher due to the much lower importance of the evaporation flux at the stage, so that irrigation is much more linked to transpiration. It is also interesting to note that -50 kPa corresponds to a value representative of the mean soil matrix in the root zone.

The table 5.4 summarizes the values for the different fluxes at the corresponding thresholds.

Irr. depth	**Threshold at 5 cm**	**Threshold at 10 cm**	**Irrigation/ET$_c$**	**Irr. frequency**
[L]	[kPa]	[kPa]	[%]	[1/day]
100	-30	-50	90	1
200	-50	-50	92	1/2
400	-60	-70	89	1/3

Table 5.4: Summary of the selected optimal thresholds and irrigation schedules for the mid-season growth stage based on all HYDRUS scenarios.

Each irrigation depth seems appropriate and will depend more on the producer's needs or on the size of the water reservoir. Using higher depth allows to spend less time in the field since the irrigation frequency is reduced. A drawback that needs to be more studied is the possibility that the drip system get clogged more easily with lower frequency. Using a low irrigation depth may restrict the root system expansion which may limit the nutrient availability. This was however not investigated in this study.

5.3 Influence of the soil texture

In this section, we evaluated the influence of the soil texture on the transpiration and irrigation amounts with the proposed thresholds discussed previously. Different soil textures were tested, from relatively coarse soil textures (sandy soils) with high hydraulic conductivities at saturation, to fine soils (clay soils). The textures where classified by decreasing particle sizes, which also corresponds to decreasing values of the parameters n and α from the van Genuchten equation (eq. 2.15). Coarse textures are characterized by high hydraulic conductivity near saturation but rapidly decreasing with lower soil matrix potential. The decrease in potential is also very steep with decreasing soil moisture (see chapter 2.2.3). Fine textures in contrast have lower hydraulic conductivity, but become higher than coarse textures at lower matrix potential. The decrease in matrix potential with soil moisture is also less steep. We used 6 soil textures that are available in HYDRUS and were parametrized by Carsel et al., 1988 [29]. They represent mean values for a large set of soils defined in the same class. The textures selected were Sandy loam, Sandy clay loam, Loam, Clay loam, Silty loam and Silt.

For both early growth we built three scenarios for each soil textures with irrigation thresholds corresponding to -20, -30 and -50 kPa and for the mid-season stage the thresholds tested were -10, -50 and -100 kPa. The irrigation depth used for all scenarios was 50 liters for early growth and 200 liters for mid-season. The figure 5.10 shows the ratio of maximal over potential transpiration and evaporation as well as the ratio of irrigation amounts over crop evapotranspiration.

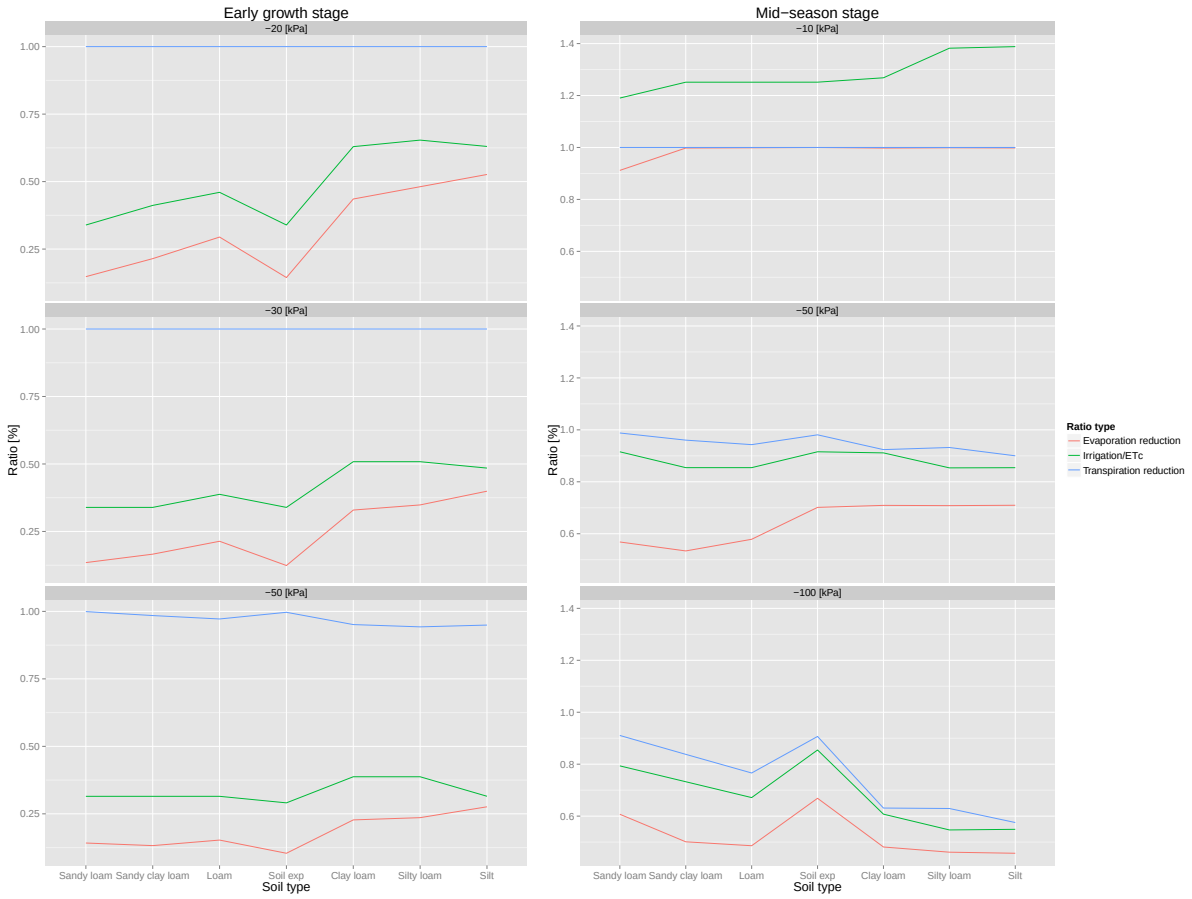

Figure 5.10: Ratio of maximal over potential transpiration and evaporation as well as the ratio of cumulative irrigation amounts over cumulative potential evapotranspiration given different soil textures and using three different thresholds at a depth of 5 cm. Simulations for the early growth stage (left) and the mid-season stage (right).

It appears that for the optimal scenarios (-30 and -50 kPa) transpiration reduction is relatively similar for all soil textures and the ratio is between 90 and 100%. Fine texture soils tend to have a higher irrigation frequency, this is due to their lower matrix potential at field capacity (around -40 kPa, against -10 kPa for coarse soils), leading to faster drainage of the soil. This implies higher irrigation amounts as well.
Fine texture soils have also a more homogeneous soil matrix potential in their root zone. This is due to their higher hydraulic conductivity at low matrix potential, balancing the differences within the root zone. In our previous scenarios with our calibrated texture, which is relatively sandy, the potential tended to be lower in the central part of the root zone, where the sensor is placed, with higher values of soil matrix potential deeper, which allowed more root water uptake compensation. In fine soils, the decrease is more homogeneous, leading to less compensation and higher water stress with low thresholds.
It is usually assumed that sandy soils are subject to important leakages, this seems to happen however only when it is saturated. When the threshold and the irrigation depth is controlled, leakages appear to become rapidly marginal even for coarse soils.

To conclude it appears that the thresholds proposed previously seem to be adequate for any soil texture, during both early growth and mid-season stages. Those results are very encouraging regarding the piloting of irrigation using a threshold since the system seem to be applicable on a widely range of soil texture, making it very flexible without much adaptation.

Concerning Burkina Faso, it was shown that most soils could be identified as sandy loam or sandy clay loam textures as discussed in chapter 2.1. Those soils responded well to our models in terms of transpiration and water savings so that it is believed that the proposed thresholds are well adapted.

5.4 Horizontal spread of the wetted bulb

Concerning the sensor location, not only does the sensor depth matter but also its horizontal distance to the dripper. It was already shown from the field experiments that the far sensors placed at a horizontal distance of about 12 cm did not systematically react to the irrigation events, as they were disconnected from the wetted bulb. This was particularly significant for experiments with low irrigation depth. This could also be due to a displacement of the dripper or runoff in the opposite direction from the sensor.
In figure 5.11, a horizontal profile of the mean soil matrix potential at a depth of 10 cm was computed. All scenarios were done for the mid-season period, with an irrigation depth of 200 liters and using three different thresholds. The same six textures were also tested.

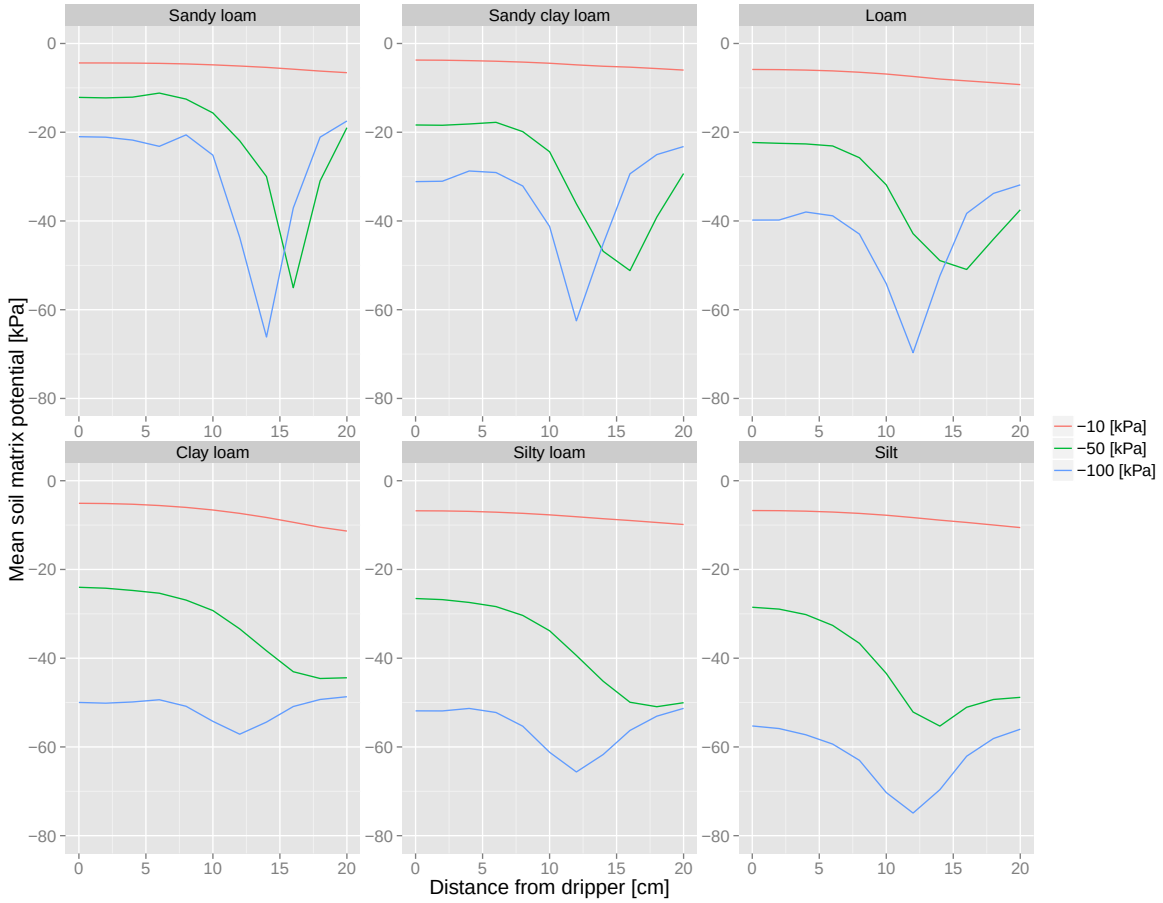

Figure 5.11: Horizontal profile at 10 cm depth of the mean soil matrix potential with time during the mid-season and using different thresholds and soil textures.

It appears that the soil matrix potential is constant until a horizontal distance of about 10 cm from the dripper. Beyond this distance, the soil matrix potential drops more or less steeply depending on the soil type. We suggest therefore to place the sensor at a horizontal distance of 5 cm. Placing it further may result in a lower response of the sensor, especially at early growth stage and may be less representative of the root zone soil matrix potential.

6 Discussion

6.1 Water stress and threshold

The field experiments and numerical modeling were conceived and performed as complementary approaches, and conclusions seem to converge towards a general irrigation management system that is discussed here.

First, it was shown that measuring water stress directly is not a straightforward operation and that sap flow measurements may not be the most efficient method to assess water stress and yield reduction on plants with small diameter. In addition, it seems that stress conditions may appear before transpiration reduction occurs, especially when biomass is building up. As discussed earlier, other effects of water stress can occur before transpiration reduction such as reduction of cell growth and wall synthesis [14] at early growth and pollination failure (disturbance in embryo formation) during mid-season [15]. An alternative approach was successfully used by Thompson et al., 2007 [41] who assessed water stress by measuring leaf water potential with a pressure chamber, and was able to measure pressure reduction at soil matrix potential values as high as -39 kPa for tomato. Measuring stem water potential with psychrometers was attempted in this study but was not successful due to device failure. The relationship between water stress and effective reduction of yield is also not clear, especially with regard to the different plant growth stages. Field experiments where soil water availability or soil matrix potential is directly compared to yield reduction seem to give the best evidence of water stress, but comparison between experiments is difficult due to external local parameters characteristic of the site. It is also not easy to distinguish between the different phenomenon which may also induce yield reduction such as salinity stress, nutrient availability, temperature stress, etc.

From our experiments, the cabbage crop appears more sensitive to water stress than the eggplant crop since a small reduction of transpiration could be observed below -50 kPa for the cabbage, whereas no significant reduction was observed for the eggplant before -200 kPa, though the sap flow measurements were probably not completely accurate. A database for the Feddes water stress model is available in HYDRUS based on Taylor, 1972 [16], and p values (faction of water depletion) are proposed by the FAO, 1998 [11]. No values were available for eggplant so we used the data for tomato, which belongs to the same family and has similar characteristics. They are summarized in table 6.1.

	Feddes (h_3 and h_{pwp})		**FAO** (fraction of water depletion - p)		
	higher threshold	lower threshold	early stage	crop development	mid-season
	[kPa]	[kPa]	[-]	[-]	[-]
Cabbage	-60	-800	0.4	0.4	0.4
Eggplant	-80	-800	0.3	0.4	0.5

Table 6.1: Summary of thresholds for the start of transpiration reduction proposed for the Feddes model (based on Taylor, 1972 [16]) and for the FAO model (based on FAO, 1998 [11])

Both database seem to confirm our observations since, during the mid-season, eggplants tolerate a lower soil matrix potential threshold and has a lower p value. The p value usually increases with plant growth, which reflects the higher plant tolerance to stress due to a more extensive root system. For the early growth stage, the p values proposed correspond to the start of transpiration reduction. In FAO's AquaCrop model [10], a lower value is proposed for reduction of canopy development. A p value of 0.15 is proposed for the tomato which is much lower than the value of 0.3 indicated previously and reflects the need of a higher threshold at the beginning.

The values proposed for the Feddes model were tested with our calibrations, but did not simulate correctly the local root water uptake reduction. We used for our models a higher threshold for root water uptake reduction (50% uptake reduction at -50 kPa) but also allowed water uptake compensation. We believe that root water uptake can decrease at higher soil matrix potential but does not lead to transpiration reduction as long as water uptake can be compensated in other parts of the root zone. Therefore the values used for the Feddes model reflect more a "point" or mean root zone soil matrix potential below

which transpiration decreases, but not the local ability of the roots to uptake water. In the Feddes model, the relationship between root water uptake and transpiration reduction is therefore not clear.

Our models showed that the root zone soil matrix potential cannot be considered homogeneous and that it is therefore very difficult to find a reference threshold among the different studies that have been conducted in the literature, since there are no consensus on the depth and location of the sensors. From this perspective the model from the FAO, which assesses the state of the water depletion in the whole root zone, seems more reliable, but unfortunately the depletion is difficult to monitor in the field and it cannot be linked to a soil matrix potential threshold, as the relationship is not linear and depends on the soil type.

Given the difficulty to define precisely water stress, our combined experiments and models have shown relatively clear results, though they might not be completely plant specific. It appears that defining a very specific threshold for each plant may not affect greatly the irrigation amounts. Indeed we have shown that a strong reduction of the irrigation volumes occurs at high soil matrix potential thresholds, around -20 kPa for the early growth stage and around -30 kPa for the mid-season. This rapid reduction comes from the reduced water losses due to evaporation and leakages. For the mid season, water needs were not significantly different for thresholds between -30 and -75 kPa and lowering the threshold resulted then mainly in transpiration reduction. We recommend here a system that limits unnecessary water losses and optimizes transpiration. It is also interesting to note, that according to the database from Taylor, 1972 [16], most plants have a stress tolerance in a range between -30 kPa and -80 kPa, which corresponds to that plateau. Deficit irrigation which would consist in limiting transpiration and partially plant yield to save water is not considered here. This practice seems however not profitable, as yield losses decrease faster than transpiration reduction for most vegetable crops [15].
The influence of the soil texture on the discussed thresholds was also assessed. It was found that, though the wetted zone differed given the soil type, the thresholds did not change significantly. In our models, this was partially due to the fact that we considered that the root distribution fitted well with the wetted zone so that the root system was directly influenced by the depth of the sensor and the irrigation schedule. Our root zone therefore adapted automatically its main root zone density near the sensor location. This assumption was confirmed by our analysis of the root density in the experimental crops but should be tested at other locations with different soil textures. In particular, the impact of the very hard soil layer at 25 cm depth was unclear.

From these observations we estimate that the thresholds proposed in this study allow a good compromise between saving water, assuring plant yield and proposing a simple and flexible system adapted to most vegetable crops and soils.

6.2 Proposed irrigation system

The goal of this research was to understand the plant and water dynamics in order to propose an optimized support system for piloting irrigation in semi-arid regions. A decisive factor in order to propose a new technology in poor rural areas is the price of the system, its robustness and its simplicity of use. These constraints orientated the research towards the definition of a cheap system, that is using the least number of sensors, which makes a large part of the price. In this perspective placing only one sensor at a single depth was the primary system envisaged, though other options were also investigated.

The main difficulty with using a sensor at a single depth is that it is not possible to assess the soil water availability in the root zone but only at a point. There are no indications on the soil matrix potential elsewhere. The consequence is that the system does not give any information about the irrigation depth that is applied at each irrigation event. If a too high irrigation depth is applied at once or if the soil is very sandy with a high hydraulic conductivity, water may infiltrate below the root zone, leading to unnecessary leakages, but the only information from the sensor will be that the soil was replenished at the sensor depth. Moreover, especially at early stage, there is a risk of over saturation of the soil which may limit the sensor reactivity.
On the opposite, if the irrigation depth is low, the system will insure that the soil is irrigated at least up to the sensor depth, but the behavior below is again unknown. This may limit the wetted zone of the soil and hence limit root development. A shallow root system did not cause real problems concerning water stress but nutrient availability was not investigated. As a result using only one sensor can only manage the irrigation frequency of the system and water stress can be avoided by recharging the soil at regular interval but this is the only feature of the system.

Nevertheless, our analysis showed encouraging results and proved that it was possible to place the sensor at a relatively representative location within the root zone especially during the mid-season and that the threshold is relatively stable given the irrigation depth. At early growth stage we propose to use a higher threshold since the sensor location is less representative of the root zone soil matrix potential and water stress tolerance is lower. It is also believed that this sensor depth can be used for plants with different maximal root zone depths. Indeed, the root distribution and the root water uptake depended strongly on the irrigation schedule so that roots will grow mainly in the wetted zone of the soil. As a result, the sensor depth, combined with the irrigation depth will directly influence the root distribution so that the sensor depth will promote a strong root development near its location, which makes it sensitive to plant water stress. The proposed thresholds seemed to perform well for different soil textures, though some finer adjustments may be possible, but would restrict the flexibility of our system. Therefore using one sensor at a depth of 10 cm seems to be the best alternative. Still too low irrigation depth may lead to some water stress as it was shown that the threshold should be a bit higher. Given the fact the we selected thresholds with a model allowing rapid water stress, a certain safety margin can probably be considered so that the system may still be efficient. The system can however not manage too high irrigation depths (much above 400 liters) very well and the main risk is water losses due to leakages and therefore over irrigation. Putting the system into the context of Burkina Faso shows that this may not be a problem during the mid-season, since water reservoirs are usually small, so that irrigation depth is hardly too high. For example, using iDE drip kit, the 500 m^2 kit can only irrigate 1000 liters at once when using a full water reservoir for a surface of 500 m^2. This represents a low depth of 100 liters per 50 m^2 as used in our simulations. The 200 m^2 can apply a maximum depth of 200 liters per 50 m^2. The main risk with those drip kit concerns the early growth stage where too high irrigation depths may lead to system failure by saturating the soil at 10 cm depth.

As discussed, the threshold needs to be adapted with time. One constraint here was that we did not want to displace the sensor during the experiment, so that the depth must be adequate for the whole crop growth. 10 cm was found to be the most convenient depth. Nevertheless, the threshold must be adapted with plant growth, as the roots penetrate deeper in the soil and plant transpiration increases.
A distinction must be made between plants that are transplanted or seeds that are directly sown in the crop. For our models we assumed that plants were transplanted and that they possessed a rooting depth of about 10 cm after 10 days. In this case we can rely on the thresholds used in the early growth scenarios. However, just after transplanting, roots may hardly reach the sensor location, so that the main process reducing the soil matrix potential is due to soil drainage. For sandy soils, field capacity is very high (around -5 to -15 kPa), so that the matrix potential hardly decreases beyond this value. In parallel, the soil evaporation in sandy soils only affects the top 5 cm of soil so that high soil moisture is available for the deeper roots. During this phase, piloting irrigation with the sensor at 10 cm depth is difficult in sandy soils. The threshold should be set at -10 kPa to allow an irrigation event about every 2 days, but the reaction of the sensor may not be adequate as discussed in chapter 4.2.6.
If the soil has a finer texture, matrix potential at field capacity is lower (around -30 kPa), so that the soil will reach this potential faster than coarse soils. However, the influence of soil evaporation for such soils reaches a depth of about 10 cm, so that water depletion occurs deeper than for coarse soils. Table 6.2 summarizes reference values of field capacity for the texture class defined in HYDRUS and based on Carsel et al., 1988 [29].

	Sandy loam	Sandy clay loam	Loam	Soil exp	Clay loam	Silty loam	Silt
Matrix potential at field capacity [kPa]	-5	-10.5	-15	-12.5	-17.5	-40.5	-21.0

Table 6.2: Reference soil matrix potential value corresponding to field capacity for different textures.

We recommend therefore to test a threshold corresponding to field capacity but to switch to manual irrigation if an irrigation event is not triggered about every 2 to 3 days, which, according to our models, corresponded to the time needed for a soil to reach field capacity after an irrigation event. The irrigation frequency is difficult to determine precisely since limited data were acquired at that stage and it is not completely clear how the plant reacts to water stress just after transplanting. These recommendations should therefore be validated experimentally.
Concerning Burkina Faso, most soil textures correspond to sandy loam 2.1 and their field capacity is around -10 kPa. We recommend therefore to test a threshold at -10 kPa. We consider that using the threshold may be useful at that early stage because it was observed that most water savings could be

achieved when soil evaporation is high.

If the crop is sown, the same remarks are valid except that the period until roots reach a depth of 10 cm is longer.

As a result a minimum of four thresholds is required. The first threshold corresponds to the very early growth stage when roots are very limited, The second threshold covers the initial growth stage and can be extended to a third of the crop development stage. The third threshold lasts until the end of the development stage and finally the last threshold covers the mid-season. Optionally a lower threshold can be used for the late period, during fruit ripening, to save water just before harvest, and in particular irrigation can be stopped about 5 days before the end of the harvest. For the last period, lowering the threshold may be risky if the growth period are not clearly defined, as it could induce water stress when the fruits are still growing.
The length of the growing periods depends on each plant and also on the climate. General durations for most vegetable crops are proposed by the FAO, 1998 [11] but the information should be verified given the climate (semi-arid for Burkina Faso) and the plant species. A visual observation can also determine these stages by following the description of chapter 2.2.2. Taking eggplant as an example the plant growth stage length are (1) 20 days; (2) 40 days; (3) 40 days and (4) 20 days and the thresholds are detailed in table 6.3.

Days after transplanting [day]	0 - 10	10 - 35	35 - 60	60 - 100	100 - 120
Threshold at 10 cm depth [kPa]	-10	-15	-30	-50	-50

Table 6.3: Proposed evolution of the irrigation threshold with eggplant growth

The alternative to the proposed system discussed above is to use a second sensor at a deeper depth, although this would raise the cost of the system significantly but would reduce the risks of failures and would allow a finer control of the irrigation. The second sensor must be placed at a depth corresponding to the wanted depth of the wetted zone, which would correspond more or less to the depth above which most of the root biomass is contained. Concerning our experiments, the sensor depth would be around 20 to 25 cm. The above sensor can still be placed at 10 cm with the same threshold and its purpose is the same, that is controlling water stress and managing the irrigation frequency. The deeper sensor works differently, it does not trigger irrigation but gives an indication about the irrigation depth. The soil matrix potential for this sensor must remain between an upper threshold and a lower threshold. The upper threshold corresponds to the soil matrix potential at field capacity. A default value of -20 kPa can be used in Burkina Faso, since soils are coarse. The lower threshold can be set a bit lower than the irrigation threshold used for the first sensor, a value 30 kPa lower than the threshold seems realistic, though this value was not investigated in more details. If the soil matrix potential is higher than the upper threshold of -20 kPa, an indication is sent to decrease the irrigation depth by 20 % the next time, if the potential reaches 0 kPa, the irrigation must be decreased by 50%. On the opposite, if the lower threshold is reached, irrigation must be increased by 20%. The system is summarized in table 6.4 but must be seen as a draft and was not completely validated by numerical models or field experiments. Note that this scenario corresponds to the model using a threshold of -50 kPa with a depth of 200 liters illustrated in figure A.12 in appendix A.5. We discussed here only the functioning during the mid-season stage, but the system could be also adapted to early growth stage, by using higher thresholds, in a smaller range around field capacity for the deep sensor.
While this system is more costly, it allows more reliability. Costs and benefits should be assessed experimentally. It might also be more profitable specifically for scientific purposes and may also be an interesting alternative for an automation of the irrigation system, where valves would be opened automatically.

Sensor depth	Threshold	Action
[cm]	[kPa]	-
10	lower than -50	Trigger irrigation
20	0	Reduce irrigation depth by 50%
20	higher than field capacity (-10 to -30)	Reduce irrigation depth by 20%
20	lower than -80	Increase irrigation depth by 20%

Table 6.4: Summary of the functioning of the alternative proposed system using 2 sensors.

A point that was not discussed so far concerns the number of locations where the sensor must be placed. The main discussion is whether using only one location per irrigation kit is representative enough of the whole crop. There are many risks if using only one location. The main problems come from the irrigation homogeneity of the drip system. The crop development was not completely homogeneous and relatively big differences were present between plants. Indeed, the experiments have shown that water delivery can vary due to pressure problems, partial clogging of the dripper, or the formation of a small water puddle, resulting to runoffs. Inhomogeneity in the soil texture, the presence of rocks or the availability of nutrients may also play a role in the plant development. If the sensor happened to be placed on a plant that presented lower growth, the transpiration rate and root water uptake would be lower, which would lead to an underestimation of the crop water needs. If the dripper gets completely clogged, the sensor will not respond to irrigation and the producer may over irrigate the crop. It may also happened that the dripper irrigates more than the rest of the system, underestimating crop water needs.
The uniformity of water delivery along the sub-lines and at the beginning and end of the drip kit was however relatively uniform, as plants with optimal growth could also be found at the end of the sub-lines. The uniformity problems come mainly from random clogging of the drippers.
In these conditions, it seems delicate to rely on only one sensor in order to achieve a good appreciation of the crop state. This configuration is recommended only if a very regular and careful control of the system can be provided and may require to displace the sensor. It is therefore proposed to use three sensors and to rely on the median value to achieve a better control. The three sensors must be placed on different sub-lines in order to avoid pressure problems and at the exact same position from the dripper (5 cm) and at the same depth (10 cm) so that the median value relies on measurements that would be the same if homogeneity was perfect.

A last possibility would be to use only two sensors at two locations, and to send an alarm when the measurements between both sensors differ more than a certain value, 10 kPa for example. It would then require an intervention of the producer to fix the problem.

6.3 Installation procedure of the irrigation management system

The procedure to put the system into function properly is summarized here and a few advices concerning its deployment are given.
We suggest to use three sensors per drip kit system. The sensors must be placed on three different sub-lines of the drip kit. The location on the line does not really matter, since water distribution did not significantly decrease with distance from the water reservoir. We recommend to place the three sensors between the middle and the last fourth of the sub-lines.
All sensors must be placed at an horizontal distance of about 5 cm from the dripper and at 10 cm depth. Note that the sensor's porous medium has a length of about 4 cm so that the sensor tip must be placed 2 cm deeper in order to place the center of the medium at the wanted depth. The sensor is also usually attached to a PVC pipe and is directly inserted into the soil with a certain angle. As a result the effective drilling length is a bit longer and the horizontal distance at the soil surface a bit further. Eq. (6.2) and (6.2) give the calculation procedure for any sensor depth (s_{depth}) and table 6.5 summarizes the exact placement of for a sensor at 10 cm depth (s_{depth}) and 5 cm away ($d_{dripper}$) from the dripper, given the angle.

$$d_v = \frac{s_{depth}}{cos(\alpha)} + 3 \tag{6.1}$$

$$h_h = d_{dripper} + s_{depth} \cdot tan(\alpha) \tag{6.2}$$

Where d_v is the length (depth) of the drilling corresponding to the sensor tip in the soil [cm]; h_h is the horizontal distance from the dripper at the surface [cm]; s_{depth} is the wanted sensor depth (10 cm)

[cm]; $d_{dripper}$ is the wanted horizontal distance from the dripper (5 cm) [cm] and α is the angle of the PVC pipe in the soil (0° if the sensor is inserted vertically in the soil).

Angle (α)	**drilling depth (d_v)**	**Horizontal distance (d_h)**
[°]	[cm]	[cm]
0	13	5
30	14.5	10.75
45	17.1	15
60	23	22.3

Table 6.5: Exact placement of a sensor at 10 cm depth, 5 cm away from the dripper.

The sensors should be installed a few days before the transplantation or sowing of the crops and a light irrigation event can be triggered to humidify the sensor. Careful attention should be taken to not completely saturate the soil before the piloting of irrigation as this would prolong the drainage time and may prevent the sensor response. On the opposite it is suggested to follow the sensors indication from the start.

Finally, the thresholds required and their evolution with time are summarized in table 6.6.

Days after transplanting	**Threshold at 10 cm depth**
[day]	[kPa]
0 - 10	-10 (or field capacity (see table 6.2))
10 to a third of the development stage	-15
First third of the development stage to mid-season	-30
Mid-season to end	-50

Table 6.6: Summary of the procedure to determine the irrigation threshold given the plant growth stage.

6.4 Irrigation schedule

In this section, we give some recommendations concerning the irrigation schedule for producers independently of the sensor network.
From our observations and modelings, it appears that water savings can be achieved especially at the beginning of plant growth where soil evaporation and leakages can be limited. During these periods, producers tend to irrigate the field abundantly in order to promote seedling growth. It seems however that the water quantities used are mainly lost and that optimizing the schedule can insure good soil moisture without losses. During the mid-season, less savings can be made.

A difficulty when assessing plant water needs with drip kit system is to estimate the effective area that is irrigated by the system. In particular the drip kits may have different spacing between sub-lines and between drippers. Instead of using the area of the drip kit itself, we suggest to base the calculation on the number of drippers. As a basic estimation, one can assume that each dripper irrigates a diameter of about 0.4 meters, which corresponds to the wetted diameter modeled with a depth of 400 liters. This value is somewhat overestimated for lower irrigation depths so that it can take into account water losses and uncertainties. If the spacing is smaller than this value, the dripper spacing must be used. All equations to calculate the irrigation schedule as discusses in chapter 2.4.2 are summarized below.

$$Irrigation\ volume\ [L] = \frac{Irr_n \cdot A_{dripkit} \cdot f_w}{e_t} \quad (6.3)$$

$$Irr_n = \frac{ET_c \cdot f_{leaf}}{F_{irr} \cdot f_w} \quad (6.4)$$

$$ET_c = K_c \cdot ET_0 \quad (6.5)$$

$$f_w = A_w / A_{dripkit} \quad (6.6)$$

$$f_{leaf} = A_{leaf} / A_{dripkit} \quad (6.7)$$

$$A_w = n_d \cdot \pi \cdot d_w^2 / 4 \quad (6.8)$$

$$A_{leaf} = n_{plant} \cdot \pi \cdot d_{leaf}^2 / 4 \quad (6.9)$$

Where Irr_n is the net irrigation depth $[liters/m^2]$ or $[mm]$; $A_{dripkit}$ the area of the drip kit $[m^2]$; f_w the fraction of soil wetted by irrigation $[m^2 m^{-2}]$; e_t is the overall efficiency of water delivery to the plant (assumed to be 0.9) [-]; ET_c the crop evapotranspiration $[L/m^2/day]$ or $[mm/day]$; f_{leaf} the fraction of soil covered by vegetation (at full development stage) $[m^2 m^{-2}]$; F_{irr} the irrigation frequency $[day^{-1}]$; K_c the crop coefficient [-]; ET_0 the reference evapotranspiration; A_w is the effective wetted area $[m^2]$; A_{leaf} area covered by plant canopy (at full development stage) $[m^2]$; n_d the number of dripper; d_w the wetted diameter (assumed to be 0.4), n_{plant} the number of plants and d_{leaf} the maximal diameter of the plants (at full development stage).

For all our estimations on the eggplants each subplot had a drip kit area of 50 m^2 and consisted of 90 drippers. The effective irrigated area can be estimated to about 12 m^2 which is much below the area of the subplot. The irrigation depth used in the models corresponded therefore to a net irrigation depth (Irr_n) of 8 mm (100 liters), 17 mm (200 liters) and 33 mm (400 liters).

The fraction of soil wetted by irrigation f_w, can be estimated to 25% in our case. The fraction of soil covered by vegetation (f_{leaf}) can be estimated using the maximal canopy diameter during the mid-season. For eggplants, the maximal diameter was about 0.5 meters so that the area can be estimated to 20 m^2, which represents 40% of the surface. Note that normally the dripper spacing matches the maximal canopy diameter.

The table 6.7 suggests reference irrigation frequencies and irrigation depths for the different growth stages in Burkina Faso. The depths may be increased by 20% for the months of March and April.

	Early growth	**Crop development**	**Mid-season**	**Late season**
F_{irr} [1/day]	once a day	once a day	every two days	every three days
Irr_n [mm]	3.5	6	16.5	16.5

Table 6.7: Proposed irrigation schedule for Burkina Faso.

Month	**1**	**2**	**3**	**4**	**5**	**6**	**7**	**8**	**9**	**10**	**11**	**12**
ET_0 [mm/day]	5.33	5.97	6.8	7.13	6.61	5.42	4.06	3.9	4.17	5.06	5.06	4.8

Table 6.8: Reference evapotranspiration values for Ouagadougou (from FAO's Climwat 2.0 database [48]).

Finally, some plant specific values such as K_c and the length of each growth stage can be found in the FAO database [11].

7 | Conclusion

In this study a great attention was given to the physical processes linking the soil water, the plant and the atmosphere. Complex interactions were demonstrated and encouraging results seem to converge towards a general model adapted to most vegetable crops. In particular, one of the key aspect of the study was to assess the response of root distribution to the irrigation schedule and the root water uptake adaptation. From our analysis, it seems clear that the root development is directly influenced by the wetted bulb and that water uptake compensation can be a rapid process. Based on this observation we have shown that using a sensor at 10 cm depth was most appropriate for vegetable crops to pilot irrigation during the whole growth stage.
We also highlighted the lack of a general consensus in the literature to pilot irrigation, as the measurements were taken at different depths and were very plant specific. We propose here a less precise irrigation management system based on thresholds which are assumed to be tolerated by most plants. Such system is more adapted to the local producer needs, as it gives simple and flexible recommendations. However, we did not assess the plant specific tolerance to water stress, which may even vary among a same specie given their genetic properties.
Our approach only considered the dry season during which precipitations do not occur and where water scarcity is most severe. The system may however also be adequate during the rainy season, as drought pockets may occur between two irrigation events, may save water by allowing more rain water to be stored in the soil and may avoid diseases by avoiding soil moisture saturation and by keeping the soil in a medium wet state.

Due to the great complexity of the processes, the approach used in this study focused primarily on an analysis of the physical processes of the soil and plant dynamics. The biological interactions between the soil and the roots were not considered in this study, in particular the influence of symbiotic effects with mycorrhizae on nutrients and root water uptake may play a significant role. We propose here one system to improve agricultural practices in semi-arid areas but it may be used together with other practices. For instance, reducing soil evaporation may be achieved by covering it with soil mulching which may also promote biological activity. Other interesting practices could include intercropping, using a deep and shallow-rooted crops together to better exploit the soil moisture.

To conclude, this study has demonstrated the great potential of using an irrigation support system in semi-arid areas, which can be adapted to the producers needs, requires low maintenance, is easy to use and offers good flexibility. Still, the financial aspects which will be a decisive factor for the distribution of the system have not been investigated in this study, even though the first project results seem encouraging. I am confident that this technology may contribute to a more sustainable use of the scare water resources and may secure plant yields and producer revenues and I am looking forward to following the development of this exciting technology in the near future.

A | Appendices

A.1 Schematic calculation of yield from FAO

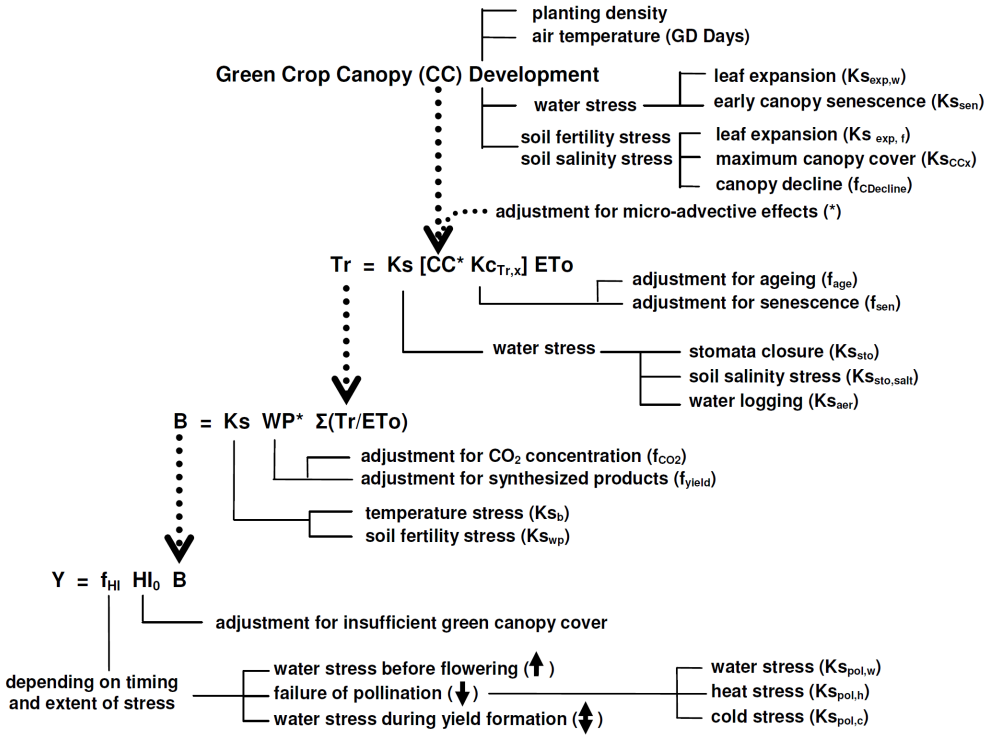

Figure A.1: Schematic calculation of yield based on the AquaCrop model from the FAO (from Raes et al., 2012 [10]).

A.2 Meteorological data

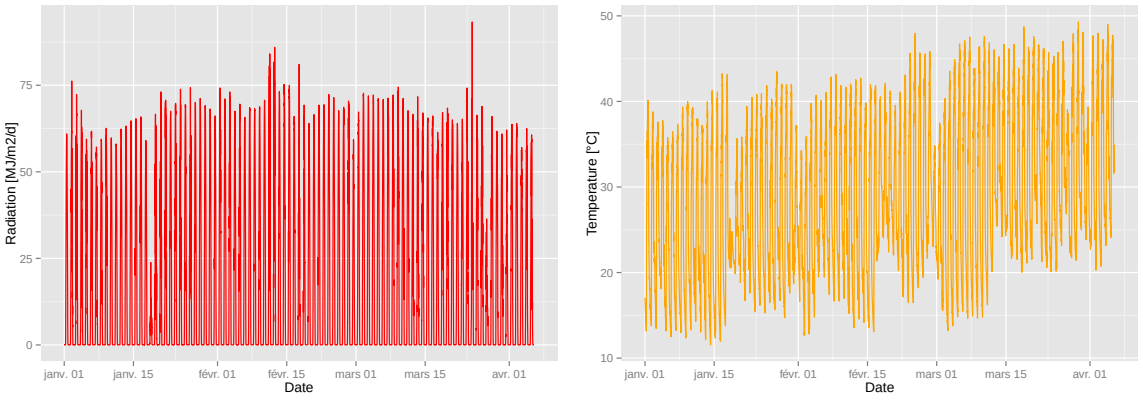

(a) Radiation $[MJ/m^2/day]$ **(b)** Temperature [°C]

(c) Relative Humidity [%] **(d)** Wind $[m/s]$

Figure A.2: Data used for ET_0 calculation and measured by the Sensorscope hydro-meteorological station based at Meteorological Institute in Ouagadougou for the whole duration of the eggplant experiment.

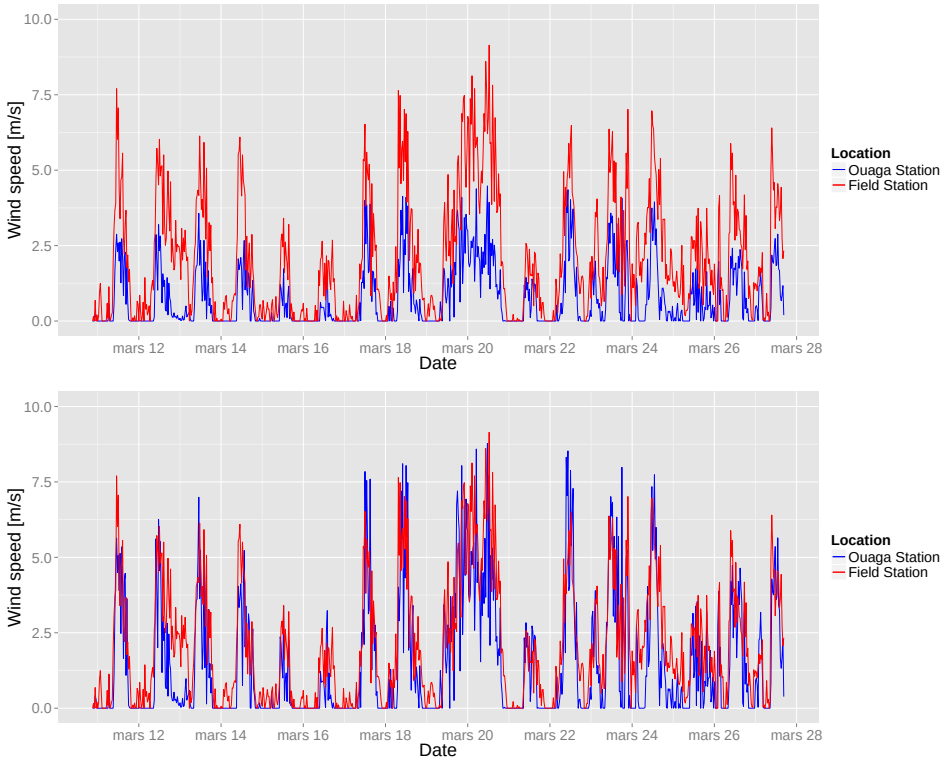

Figure A.3: Correction of wind speed. Up: Original dataset; Down: Adjusted measurement with a correction factor of 1.96 for the Ouagadougou station

A.3 Fitting of the soil water retention curve

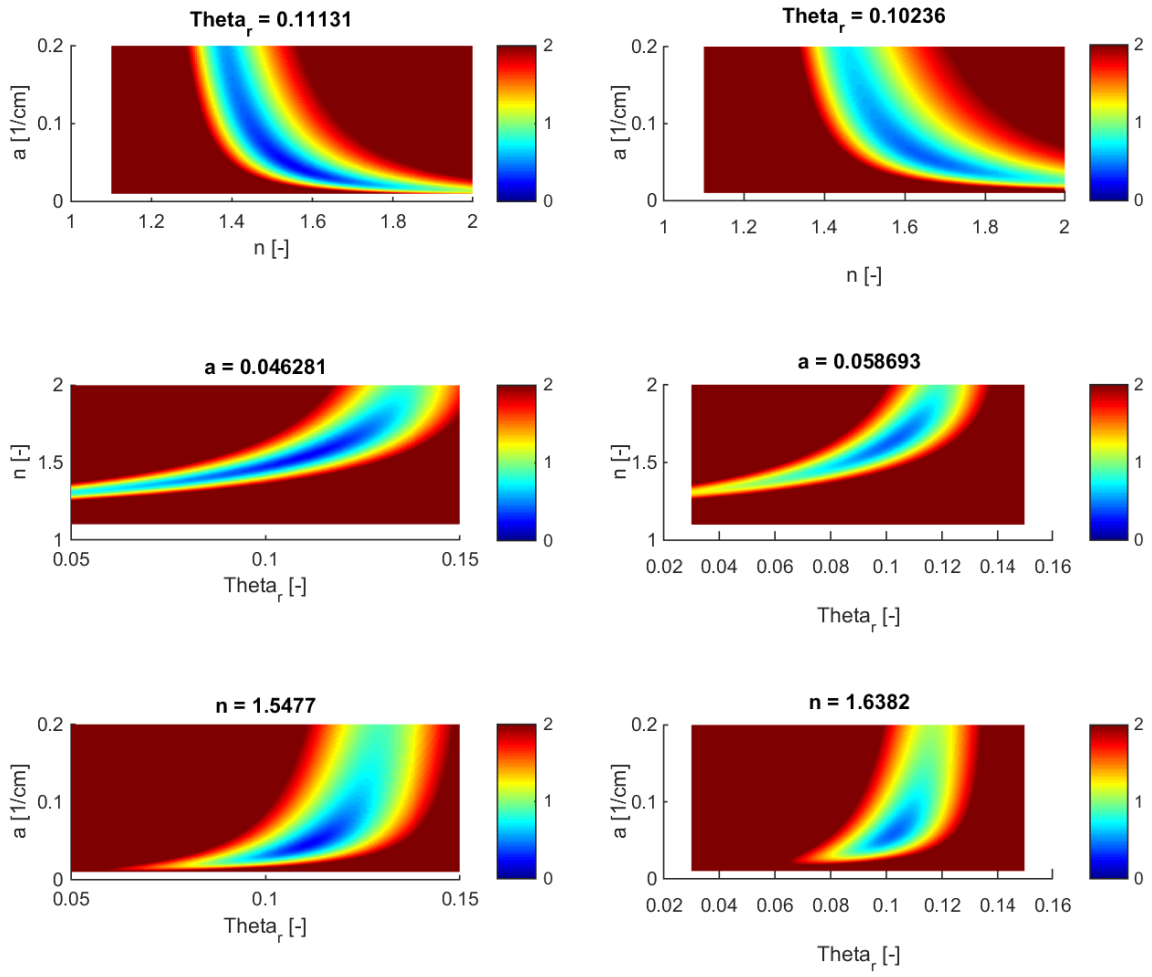

(a) Cabbage crop **(b)** Eggplant crop

Figure A.4: Root Mean Square Error (RMSE) between the modeled and observed points calculated by varying the 3 unknown parameters used for calibration of the soil texture from the van Genuchten equation (eq. 2.15): α, n and θ_r. 2 parameters are tested, while the third is kept at the best value. The blue zone shows the area where the RMSE is minimum, corresponding to the best combination of parameters

A.4 Sap flow results

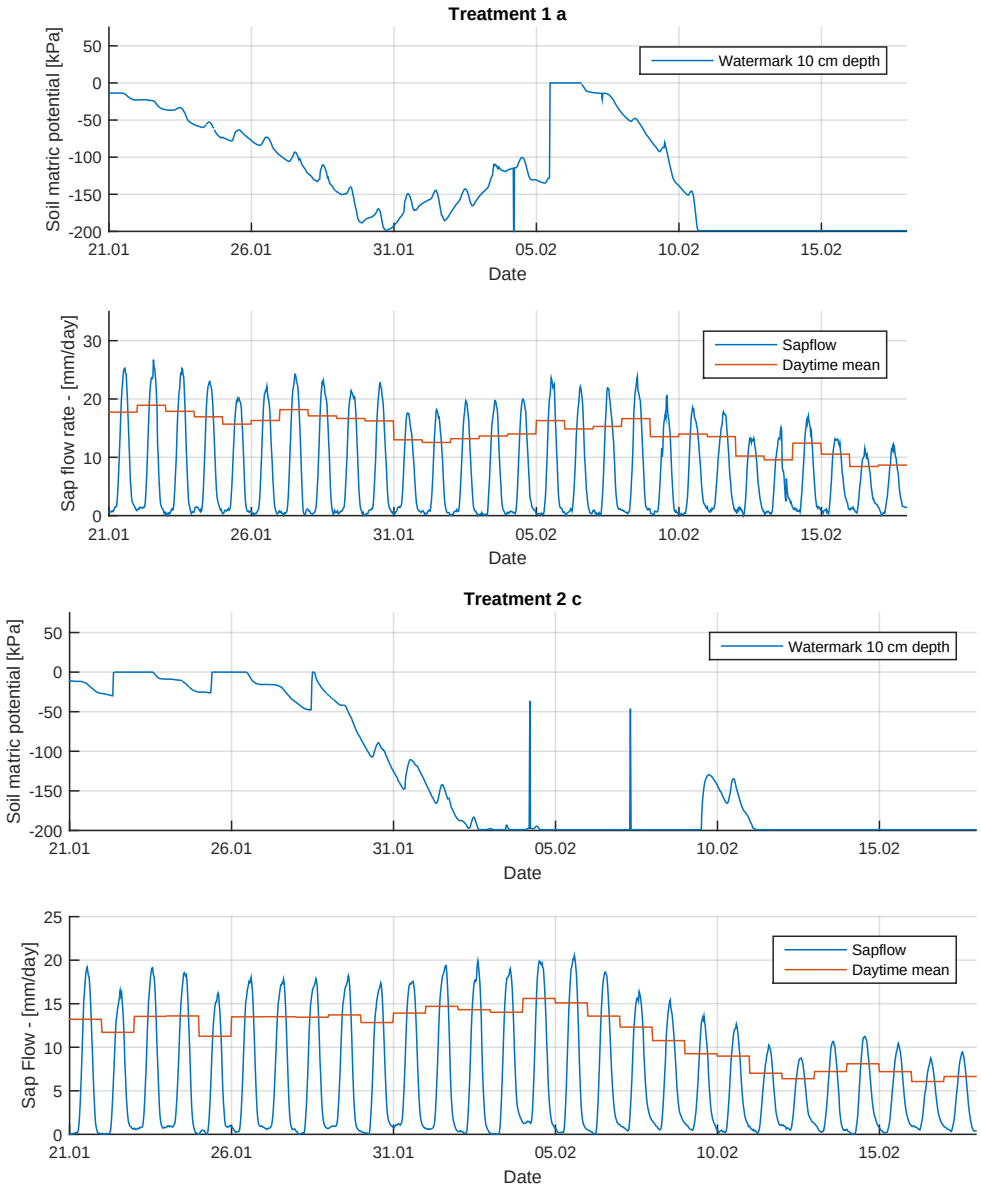

Figure A.5: Additional comparison between the soil matrix potential and the transformed sap flow rate for both treatments of the cabbage experiment during the late season. The blue sap flow curves represent the 30 minutes average, the blue Watermark curve the 15 minutes average and the red curves are the daytime means.

A.5 HYDRUS simulation

A.5.1 Results of the eggplant calibration

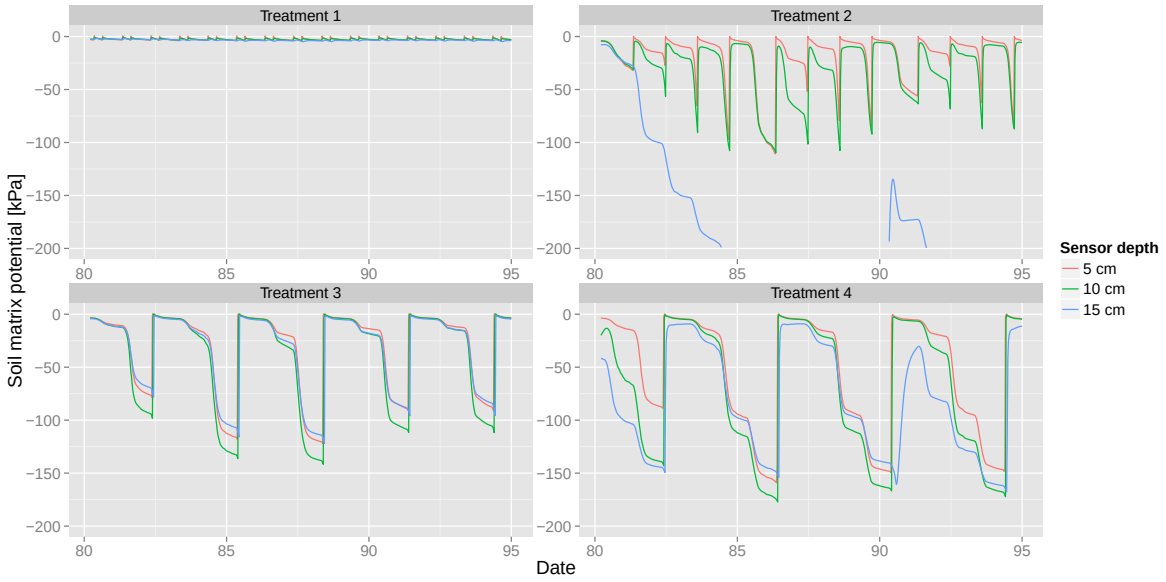

Figure A.6: Results of the HYDRUS simulations corresponding to the four treatments of the eggplant experiment at the beginning of the mid-season, 60 days after transplanting (February 3).

A.5.2 Early growth stage scenarios

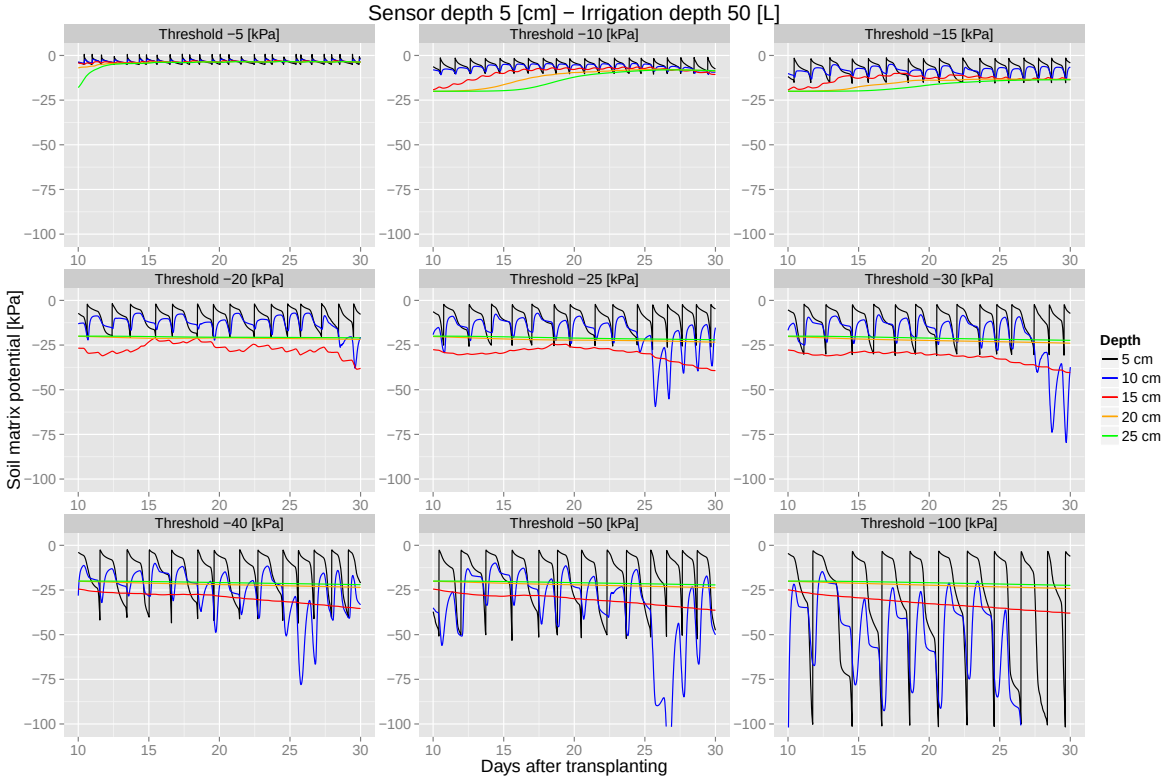

Figure A.7: Evolution of the simulated soil matrix potential at various depths for all scenarios during the early growth stage and using an irrigation depth of 50 liters.

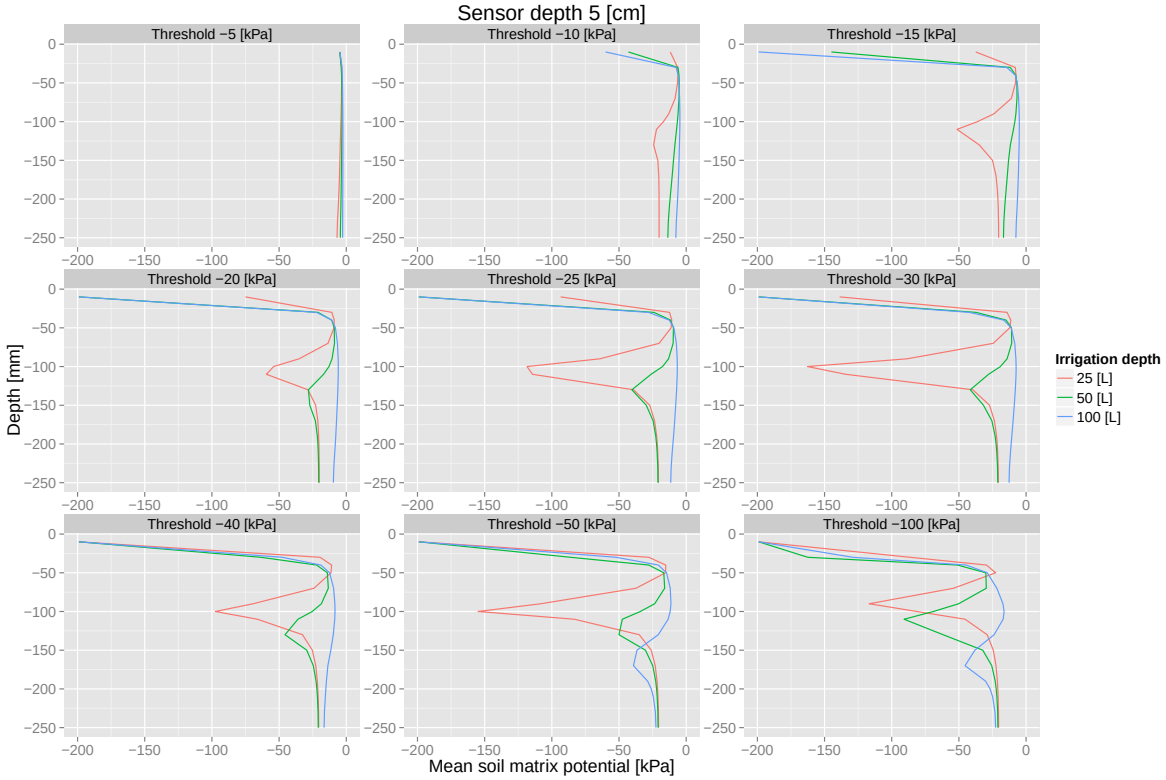

Figure A.8: Vertical profile of the mean soil matrix potential over time at 7.5 cm away from the dripper for all scenarios during the early growth stage

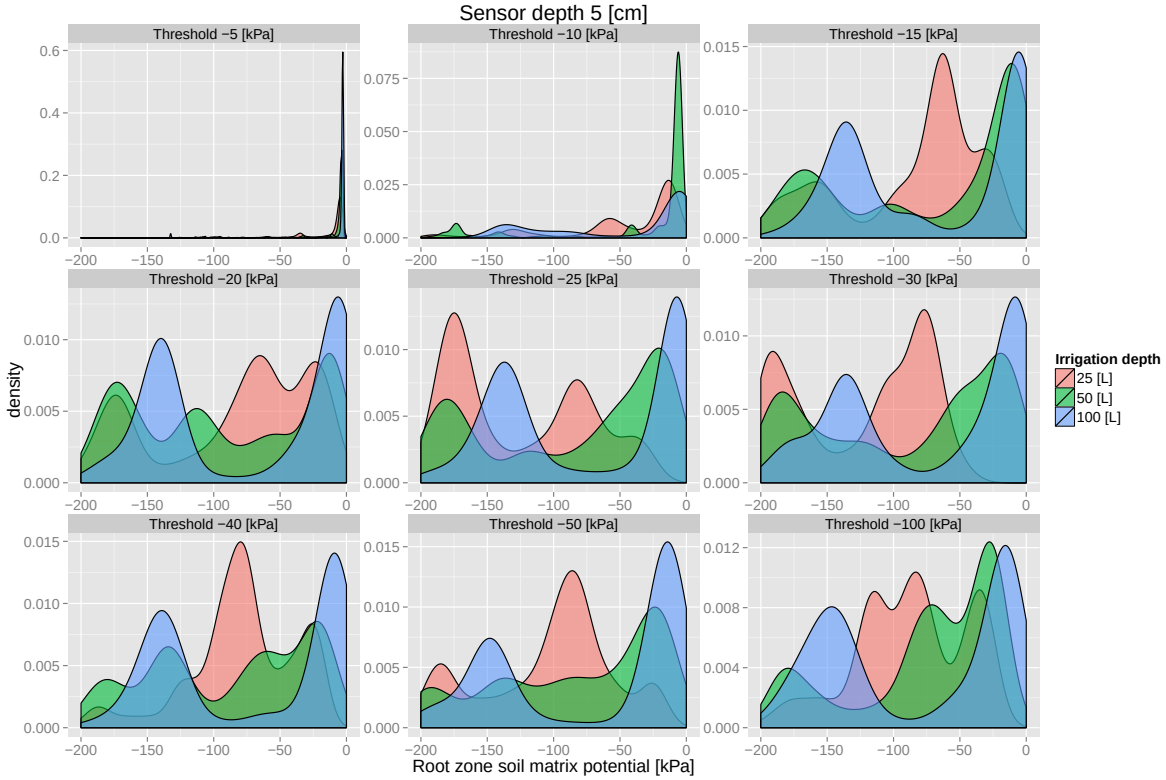

Figure A.9: Kernel probability density function of the soil matrix potential over time for the early growth stage and for all scenarios).

A.5.3 Mid-season growth stage scenarios

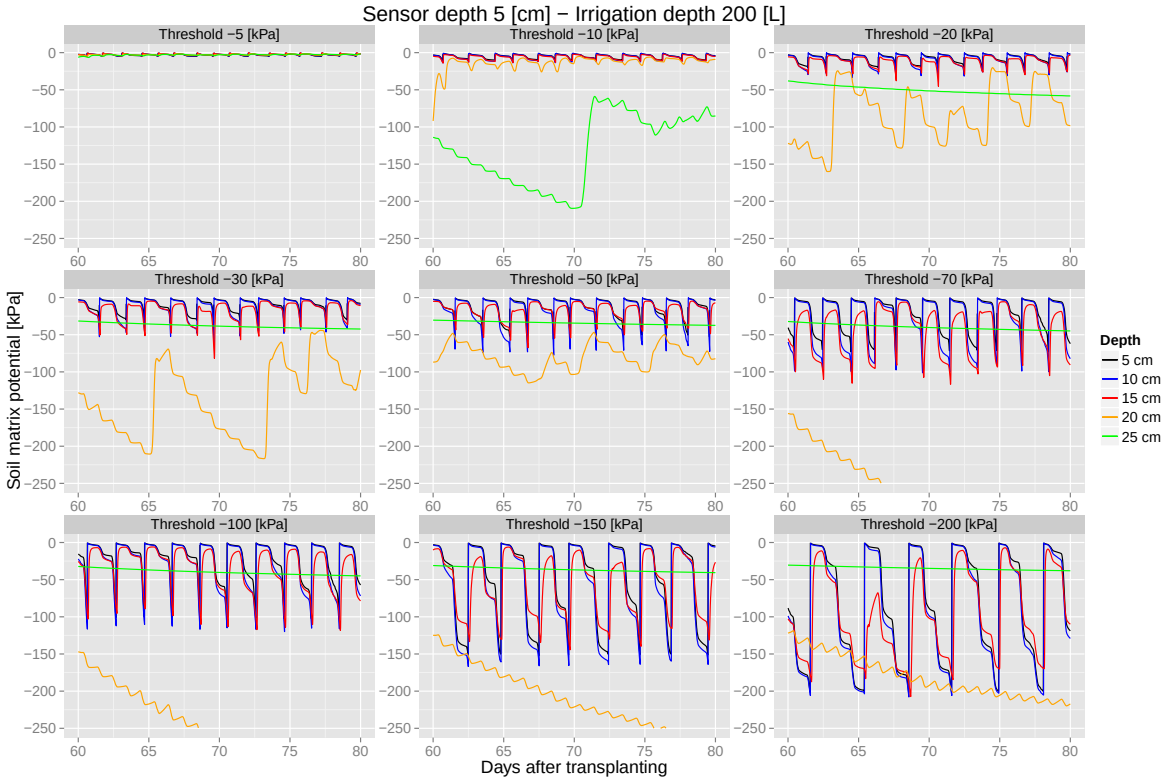

Figure A.10: Evolution of the simulated soil matrix potential at various depths for all scenarios during the mid-season stage and using an irrigation depth of 200 liters.

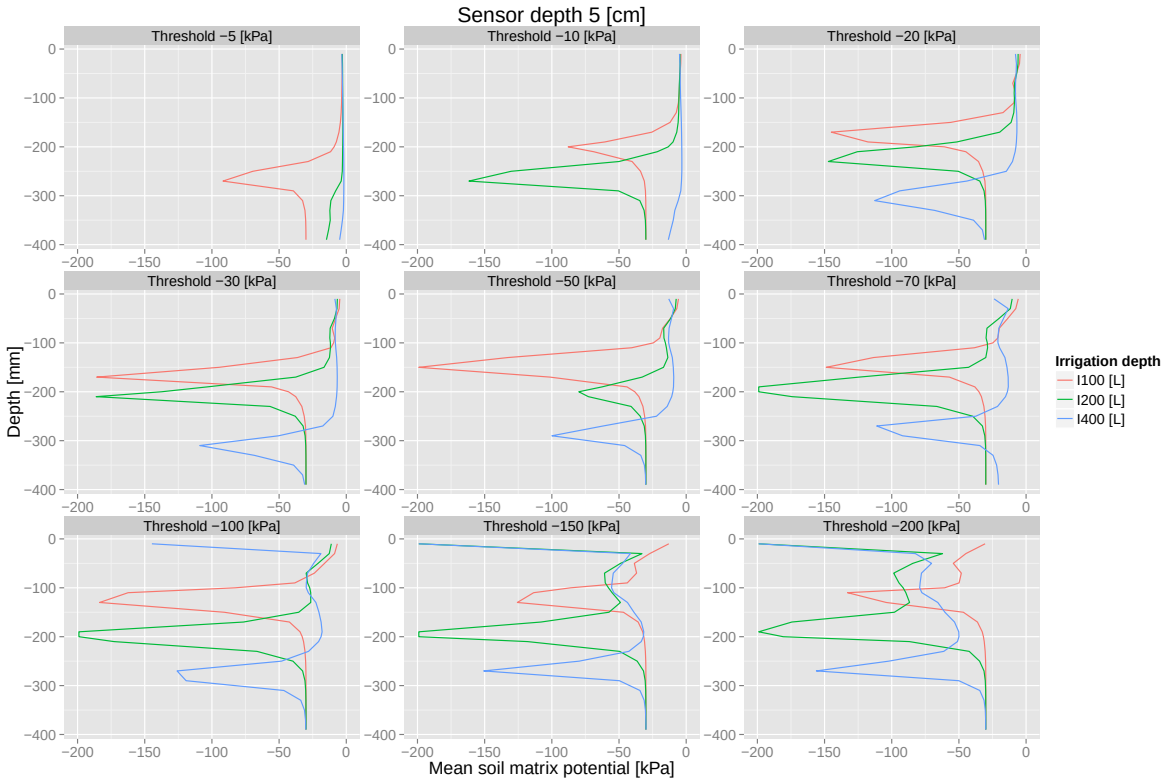

(a) -

Figure A.11: Vertical profile of the mean soil matrix potential over time at 7.5 cm away from the dripper for all scenarios during the mid-season stage

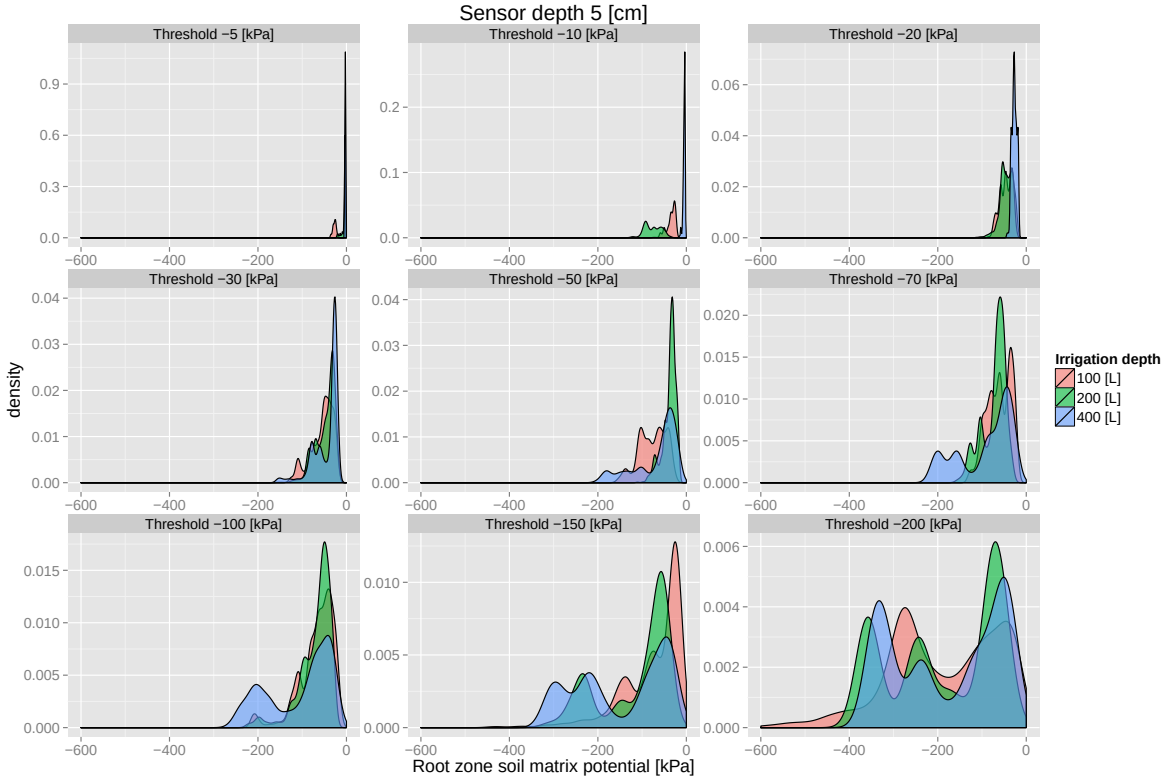

(a) -

Figure A.12: Kernel probability density function of the soil matrix potential over time for the mid-season stage and for all scenarios).

Bibliography

[1] Malik, K., United Nations Development Programme, and Human Development Report Office. *Sustaining Human Progress: Reducing Vulnerabilities and Building Resilience*. 2014.

[2] AQUASTAT. *FAO's Information System on Water and Agriculture - Burkina Faso*. 2014.

[3] Sonou, M. and Abric, S. "Capitalisation d'expériences sur le développement de la petite irrigation privée pour des productions à haute valeur ajoutée en Afrique de l'Ouest". In: *ARID, FAO, IWMI, BM, UE, FIDA, 139p* (2010).

[4] Tiercelin, J.-R. *Traité d'irrigation. : 2è édition*. Paris: Tec & Doc Lavoisier, Sept. 2006.

[5] Barrenetxea, G., Ingelrest, F., Schaefer, G., and Vetterli, M. "The hitchhiker's guide to successful wireless sensor network deployments". In: *Proceedings of the 6th ACM conference on Embedded network sensor systems*. ACM, 2008, pp. 43–56.

[6] *Atlas de l'Afrique – Burkina Faso*. Éditions du Jaguar. Jeune Afrique - Jaguar. 2005.

[7] Sanon, M. "Optimisation de l'irrigation à la parcelle par radiothermométrie. Application à une culture d'oignon (Allium cepa L.) en climat sahélien (Nord-Ouest du Burkina Faso)". In: *Science et changements planétaires / Sécheresse* 10.3 (Dec. 1999), pp. 228–228.

[8] Dembele, Y. and Some, L. "Propriétés hydrodynamiques des principaux types de sol du Burkina Faso". In: *Ouagadougou: INERA*. 1991.

[9] *USDA textural triangle*. URL: http://www.nrcs.usda.gov/wps/portal/nrcs/detail/soils/survey/?cid=nrcs142p2_054167 (visited on 07/04/2015).

[10] Raes, D., Steduto, P., Hsiao, T., and Fereres, E. *AquaCrop Version 4.0 - Reference Manual*. Rome: Food and Agriculture Organization of the United Nations, June 2012.

[11] Allen, R. G., Pereira, L. S., Raes, D., and Smith, M. "FAO Irrigation and drainage paper No. 56". In: *Rome: Food and Agriculture Organization of the United Nations* (1998), pp. 26–40.

[12] Rodríguez-Iturbe, I. and Porporato, A. *Ecohydrology of Water-Controlled Ecosystems: Soil Moisture and Plant Dynamics*. Cambridge University Press, Jan. 2005.

[13] Porporato, A., Laio, F., Ridolfi, L., and Rodriguez-Iturbe, I. "Plants in water-controlled ecosystems: active role in hydrologic processes and response to water stress: III. Vegetation water stress". In: *Advances in Water Resources* 24.7 (2001), pp. 725–744.

[14] Jones, H. G. "Irrigation scheduling: advantages and pitfalls of plant-based methods". In: *Journal of Experimental Botany* 55.407 (Sept. 2004), pp. 2427–2436.

[15] Steduto, P and Food and Agriculture Organization of the United Nations. *Crop yield response to water*. Rome: Food and Agriculture Organization of the United Nations, 2012.

[16] Taylor, S. A. *Physical edaphology: The physics of irrigated and nonirrigated soils*. Revised and Edited edition. San Francisco: W.H.Freeman & Co Ltd, Dec. 1972. 533 pp.

[17] Gupta, B. and Huang, B. "Mechanism of Salinity Tolerance in Plants: Physiological, Biochemical, and Molecular Characterization". In: *International Journal of Genomics* 2014 (2014), pp. 1–18.

[18] Shalhevet, J. "Using water of marginal quality for crop production: major issues". In: *Agricultural Water Management* 25.3 (1994), pp. 233–269.

[19] Assouline, S., Möller, M., Cohen, S., Ben-Hur, M., Grava, A., Narkis, K., and Silber, A. "Soil-Plant System Response to Pulsed Drip Irrigation and Salinity". In: *Soil Science Society of America Journal* 70.5 (2006), p. 1556.

[20] DECAGON. *Electrical Conductivity of Soil as a predictor of Plant Response*. DECAGON, 2007.

[21] Maas, E. V. "Testing crops for salinity tolerance". In: *Proc. Workshop on Adaptation of Plants to Soil Stresses. p.* Vol. 234. 1993, p. 247.

[22] *Crop salt tolerance data*. URL: http://www.fao.org/docrep/005/y4263e/y4263e0e.htm (visited on 07/04/2015).

[23] Vico, G. and Porporato, A. "From rainfed agriculture to stress-avoidance irrigation: II. Sustainability, crop yield, and profitability". In: *Advances in Water Resources* 34.2 (Feb. 2011), pp. 272–281.

[24] Vico, G. and Porporato, A. "From rainfed agriculture to stress-avoidance irrigation: I. A generalized irrigation scheme with stochastic soil moisture". In: *Advances in Water Resources* 34.2 (Feb. 2011), pp. 263–271.

[25] Twarakavi, N. K. C., Sakai, M., and Šimůnek, J. "An objective analysis of the dynamic nature of field capacity: DYNAMIC NATURE OF FIELD CAPACITY". In: *Water Resources Research* 45.10 (Oct. 2009), n/a–n/a.

[26] Rodriguez-Iturbe, I., Porporato, A., Ridolfi, L., Isham, V., and Coxi, D. R. "Probabilistic modelling of water balance at a point: the role of climate, soil and vegetation". In: *Proceedings of the Royal Society A: Mathematical, Physical and Engineering Sciences* 455.1990 (Oct. 8, 1999), pp. 3789–3805.

[27] Šimůnek, J., Šejna, M., Saito, H., Sakai, M., and Van Genuchten, M. T. *The HYDRUS-1D Software Package for Simulating the One-Dimensional Movement of Water, Heat, and Multiple Solutes in Variably-Saturated Media, Version 4.17.* Department of Environmental Sciences, University of California Riverside, Riverside, June 2013.

[28] Genuchten, M. T. van. "A Closed-form Equation for Predicting the Hydraulic Conductivity of Unsaturated Soils1". In: *Soil Science Society of America Journal* 44.5 (1980), p. 892.

[29] Carsel, R. F. and Parrish, R. S. "Developing joint probability distributions of soil water retention characteristics". In: *Water Resources Research* 24.5 (1988), pp. 755–769.

[30] Schaap, M. G., Leij, F. J., and Genuchten, M. T. van. "Rosetta: A computer program for estimating soil hydraulic parameters with hierarchical pedotransfer functions". In: *Journal of hydrology* 251.3 (2001), pp. 163–176.

[31] Feddes, R. A., Kowalik, P. J., and Zaradny, H. *Simulation of Field Water Use and Crop Yield.* Wiley, Jan. 1, 1978. 188 pp.

[32] Yadav, B. K., Mathur, S., and Siebel, M. A. "Soil moisture dynamics modeling considering the root compensation mechanism for water uptake by plants". In: *Journal of Hydrologic Engineering* 14.9 (2009), pp. 913–922.

[33] Genuchten, M. T. V. van and Laboratory, U. S. S. *A Numerical Model for Water and Solute Movement in and Below the Root Zone.* United States Department of Agriculture Agricultural Research Service U.S. Salinity Laboratory, 1987.

[34] Vrugt, J. A., Hopmans, J. W., and Šimunek, J. "Calibration of a two-dimensional root water uptake model". In: *Soil Science Society of America Journal* 65.4 (2001), pp. 1027–1037.

[35] Besharat, S., Nazemi, A. H., and Sadraddini, A. A. "Parametric modeling of root length density and root water uptake in unsaturated soil". In: *Turkish Journal of Agriculture and Forestry* 34.5 (2010), pp. 439–449.

[36] Coelho, E. F. and Or, D. "Root distribution and water uptake patterns of corn under surface and subsurface drip irrigation". In: *Plant and Soil* 206.2 (1999), pp. 123–136.

[37] Portas, C. A. M. "Development of root systems during the growth of some vegetable crops". In: *Plant and Soil* 39.3 (Dec. 1973), pp. 507–518.

[38] Bengough, A. G., McKenzie, B. M., Hallett, P. D., and Valentine, T. A. "Root elongation, water stress, and mechanical impedance: a review of limiting stresses and beneficial root tip traits". In: *Journal of Experimental Botany* 62.1 (Jan. 2011), pp. 59–68.

[39] Coelho, F. E. and Or, D. "A Parametric Model for Two-Dimensional Water Uptake Intensity by Corn Roots Under Drip Irrigation". In: *Agron. Abstracts* (1995), p. 189.

[40] Šimůnek, J. and Hopmans, J. W. "Modeling compensated root water and nutrient uptake". In: *Ecological Modelling* 220.4 (Feb. 2009), pp. 505–521.

[41] Thompson, R., Gallardo, M., Valdez, L., and Fernández, M. "Using plant water status to define threshold values for irrigation management of vegetable crops using soil moisture sensors". In: *Agricultural Water Management* 88.1 (Mar. 2007), pp. 147–158.

[42] Bower, C., Kratky, B., and Ikeda, N. "Growth of tomato on a tropical soil under plastic cover as influenced by irrigation practice and soil salinity". In: *Journal of the American Society for Horticultural Science* 100.5 (1975), pp. 519–521.

[43] Wang, Q., Klassen, W., Li, Y., Codallo, M., and Abdul-Baki, A. A. "Influence of cover crops and irrigation rates on tomato yields and quality in a subtropical region". In: *HortScience* 40.7 (2005), pp. 2125–2131.

[44] Smittle, D. A., Dickens, W. L., and Stansell, J. R. "Irrigation regimes affect yield and water use by bell pepper". In: *Journal of the American Society for Horticultural Science* 119.5 (1994), pp. 936–939.

[45] *Aubergines africaines*. URL: http://www.semagricmr.com/fr/notre-catalogue-de-semences/aubergines-africaines/auba07.php (visited on 04/07/2015).

[46] *East 30 Sensors Sap Flow Sensor - User's Manual*. East 30 Sensors.

[47] *Sensorscope | Capteurs*. URL: http://www.sensorscope.ch/fr/produits/capteurs (visited on 04/07/2015).

[48] *CLIMWAT 2.0 for CROPWAT*. URL: http://www.fao.org/NR/Water/infores_databases_climwat.html (visited on 07/04/2015).

[49] Irrometer. *Moisture Sensor Agricultural Irrigation Design Manual*. Irrometer, 2005.

[50] Mermoud, A., Tamini, T., and Yacouba, H. "Impacts of different irrigation schedules on the water balance components of an onion crop in a semi-arid zone". In: *Agricultural Water Management* 77.1 (Aug. 2005), pp. 282–295.

[51] Lv, G., Kang, Y., Li, L., and Wan, S. "Effect of irrigation methods on root development and profile soil water uptake in winter wheat". In: *Irrigation Science* 28.5 (July 2010), pp. 387–398.

[52] Deb, S. K., Shukla, M. K., and Mexal, J. G. "Numerical Modeling of Water Fluxes in the Root Zone of a Mature Pecan Orchard". In: *Soil Science Society of America Journal* 75.5 (2011), p. 1667.

[53] Beltrán, J. M. "Irrigation with saline water: benefits and environmental impact". In: *Agricultural water management* 40.2 (1999), pp. 183–194.

[54] Mmolawa, K. and Or, D. "Root zone solute dynamics under drip irrigation: A review". In: *Plant and soil* 222.1 (2000), pp. 163–190.

[55] Cardenas-Lailhacar, B. and Dukes, M. "Precision of soil moisture sensor irrigation controllers under field conditions". In: *Agricultural Water Management* 97.5 (May 2010), pp. 666–672.

[56] Verma, P., Loheide, S. P., Eamus, D., and Daly, E. "Root water compensation sustains transpiration rates in an Australian woodland". In: *Advances in Water Resources* 74 (Dec. 2014), pp. 91–101.